ADVANCES IN MODELING COHESIVE SEDIMENT DETACHMENT AND A PROCESS-BASED METHOD FOR STREAM RESTORATION TO DETERMINE SEDIMENT LOADS

By

KATE RIIS KLAVON

Bachelor of Science in Agricultural Engineering

Iowa State University

Ames, Iowa

2014

Submitted to the Faculty of the
Graduate College of the
Oklahoma State University
in partial fulfillment of
the requirements for
the Degree of
MASTER OF SCIENCE
May, 2016

ADVANCES IN MODELING COHESIVE SEDIMENT DETACHMENT AND A PROCESS-BASED METHOD FOR STREAM RESTORATION TO DETERMINE SEDIMENT LOADS

Thesis Approved:

Dr. Garey Fox

Thesis Adviser

Dr. Daniel Storm

Dr. Sherry Hunt

ACKNOWLEDGEMENTS

I would like to acknowledge the financial support of the USDA NIFA National Integrated Water Quality Program under project #2013-51130-21484. My committee members, Dr. Storm, Dr. Hunt, and Dr. Fox, have been extremely helpful throughout the project and my time at Oklahoma State University. I am particularly thankful for the support of my adviser, Dr. Garey Fox. His enthusiasm for learning, scientific curiosity, and drive have made him an outstanding mentor and have enabled me to reach a level of research I never would have imagined possible when I started working for him two years ago.

I am also appreciative of everyone who helped me in the field, lab, and office: Abigail Parnell, Dr. Abdul-Sahib Al-Madhhachi, Dr. Anish Khanal, Brad Rogers, Derek West, Dr. Erin Porter, Holly Enlow, John McMaine, Dr. Lucie Guertault, Michelle Melone, Mikayla Wanger, Rebecca Purvis, Dr. Ron Miller, Whitney Lisenbee, and Yan (Joey) Zhou.

Additionally, I would not be who I am or where I am today without my friends and entire family, especially Jennifer, Michael, and Marta Klavon. Finally, thanks to Adam Fricke for supporting my education and career goals and always bringing out the best in me.

Name: KATE RIIS KLAVON

Date of Degree: MAY, 2016

Title of Study: ADVANCES IN MODELING COHESIVE SEDIMENT DETACHMENT AND A PROCESS-BASED METHOD FOR STREAM RESTORATION TO DETERMINE SEDIMENT LOADS

Major Field: BIOSYSTEMS AND AGRICULTURAL ENGINEERING

Abstract: The majority of sediment loads to surface waters often originate from streambanks causing water quality issues in streams and reservoirs. Streambank erosion is a complex cyclical process involving subaerial processes, fluvial erosion, seepage erosion, and geotechnical failures and is driven by several soil properties that themselves are temporally and spatially variable. Therefore, it can be challenging to model streambank retreat. However, the ability to model streambank erosion has many important applications including the design of mitigation strategies for stream restoration practices. In order to account for the complicated nature of streambank retreat, process-based models that incorporate the forces and moments driving and resisting erosion are needed. However, several questions related to erosion processes still need to be researched in order for the models to be a more useful tool in the stream restoration community. The purpose of this research was to answer some of these lingering fundamental questions including: (i) are nonlinear mechanistic detachment models more appropriate than the traditional empirical approaches for quantifying sediment detachment due to fluvial forces and (ii) how can typical restoration practices be modeled in commonly used process-based models, such as the bank stability and toe erosion model (BSTEM), to estimate sediment load reductions to surface waters? Additionally, previous peer reviewed research utilizing BSTEM was analyzed to demonstrate current uses of the model and suggest further research needs.

TABLE OF CONTENTS

Chapter Page

LIST OF TABLES

Table Page

Table Page

LIST OF FIGURES

Figure Page

Figure Page

CHAPTER I

MODELING STREAMBANK RETREAT PROCESSES WITH THE BANK STABILITY AND TOE EROSION MODEL (BSTEM): A REVIEW

1.1 Abstract

The majority of watershed sediment loads to surface waters often originate from streambanks, causing impairment to water bodies. Streambank erosion is a complex cyclical process involving subaerial processes, fluvial erosion, seepage erosion, and geotechnical failures and is driven by several soil properties that themselves are temporally and spatially variable. Therefore, it can be extremely challenging to predict and model retreat. However, the ability to model streambank erosion has many important applications including the design of mitigation strategies for stream restoration practices. In order to highlight the current complexity required to model streambank erosion and suggest future research, this paper will review one of the most comprehensive streambank models available, the Bank Stability and Toe Erosion Model (BSTEM). The major areas of discussion will include (i) accounting for variability in geotechnical and fluvial soil parameters, (ii) what physical processes are still missing from the model, (iii) how the model can be used for stream restoration, and (iv) how the model has been improved in recent years. In addition, an overview of all peer reviewed studies up to the point of publication are included to guide those wishing to use BSTEM. This paper is not intended to criticize the model, but demonstrate that even one of the most advanced models still has shortcomings and needs to

continue to be developed so that process-based modeling can more easily be completed and incorporated into the stream restoration community.

1.2 Introduction

The Bank Stability and Toe Erosion Model (BSTEM) has been described by several to be one of the most advanced and commonly used tools for modeling streambank erosion processes (Heeren et al., 2012; Curran and Hession, 2013; Rinaldi and Nardi, 2013; Lai et al., 2015; Daly et al., 2015). Since its creation, the model has transformed from simply a stability model to a robust tool with the capability to predict fluvial erosion and geotechnical failures for streams with various geometries, soils, and flow conditions (Simon et al., 2000; Simon et al., 2011). The model has been used in a variety of studies related to the factors influencing the processes of streambank erosion, failure, and retreat. Although the model has proven highly useful in certain areas, its uses are limited and further research and development is needed in order for the model to continue to be used as a tool in predicting streambank erosion. The objectives of this paper are to (i) comprehensively review studies that have utilized BSTEM and report their findings, (ii) address the limitations of the model so that it can be used appropriately in its current form, and (iii) suggest directions of research that will help make the model a more useful tool in future applications.

1.3 Previous BSTEM Studies and Applications

A list of published, peer reviewed papers that used BSTEM as a part of their study and a summary of modeling objectives and findings are available in Table 1.1. To more thoroughly

Table 1.1. Summary of peer reviewed studies using the Bank Stability and Toe Erosion Model (BSTEM) as a component of the research.

Authors	Version of BSTEM	Location	Purpose	Validation of Results	Major Findings
Simon et al. (2000)	BSM	Goodwin Creek, MS	Show that a dynamic bank stability algorithm can be used in combination with specific field data to accurately represent the timing of bank failures	Compared known bank failure times to model predicted FoS	The bank stability algorithm sufficiently represented the timing of bank failures
Simon and Collison (2002)	BSM	Goodwin Creek, MS	Quantify mechanic and hydraulic effects of various riparian vegetative species from BSM predictions	Compared known bank failure timing under different riparian covers to predictions of FoS	The hydraulic and mechanical effects of riparian vegetation were both significant to bank stability
Simon and Thomas (2002)	BSM	Yalobusha River, MS	Assess the impact of debris plug removal on upstreambank stability	Not Reported	The rapid removal of the debris plug caused all upstream banks to be at risk of instability according to model predictions
Simon et al. (2002)	BSM	Missouri River, MT	Determine the effects of dam removal on stability, identify key factors impacting stability, and compare the BSM algorithm to another stability model	Not Reported	The key factors affecting bank stability were frequency and duration of flow events and both algorithms predicted similar stability for the same hydraulic conditions
Pollen and Simon (2005)	BSM	Fictitious Channel, MS	Assess two root failure models' (instantaneous and root bundle progressive model) impact on bank FoS	Compared both models' predicted increased shear strengths to direct shear tests completed on soils with and without roots	The root bundle progressive model improved estimates of root shearing resistance and therefore has the potential to improve estimation of streambank stability in BSM
Simon et al. (2006)	3.4	Upper Trucke River, CA	Quantify mechanical and hydrologic effects of two riparian vegetative species on streambank stability	Compared known bank failure timing under different riparian covers to model predictions of FoS	BSTEM showed the effect of different riparian species on the frequency of bank failures and delivery of sediment, Lemmon's Willow withstood steeper slopes and more saturated conditions
Wilson et al. (2007)	BSM	Little Topashaw Creek, MS	Evaluate model ability to account for streambank failure due to seepage erosion	Compared laboratory measured sediment loads to model predicted loads	The model simulated increased instability of banks due to seepage erosion, did not account for sediment loss due to sapping, and over predicted sediment loads
Cancienne et al. (2008)	4.1	Little Topashaw & Goodwin Creeks, MS	Determine importance of seepage undercutting relative to several parameters (bank shear strength, bank angle, soil pore water pressure, and root reinforcement)	BSTEM sensitivities matched previous studies for several parameters	BSTEM is most sensitive to pore water pressure distribution, small degrees of undercutting can counteract effects of root reinforcement, undercutting is most significant under unsaturated flow, and streambank stability models need to account for site-specific failure mechanisms

Parker et al. (2008)	-	Goodwin Creek, MS	Determine how variability in soil parameters within and between sites impacts BSTEM predictions and how to best incorporate uncertainty into modeling	Compared known bank failures to range in predicted FoS	Variability in soil parameters produced a significant range in FoS, the current addressing of uncertainty in BSTEM is not suitable, and a probabilistic approach is more appropriate than deterministic approaches
Lindow et al. (2009)	4.1	Fictitious Channel, NC	Analyze and model laboratory experiments to determine the effect of seepage, pore water pressure, and bank geometry on stability	Compared known bank failures to predicted FoS	The model could not predict the observed failures due to lateral seepage forces, therefore near bank groundwater flow processes should be incorporated into the model
Pollen-Bankhead and Simon (2009)	BSM	Fictitious Channels	Evaluate bank stability with variations of root density with depth to correctly apply RipRoot estimates to BSTEM layering	Not Reported	Combining Riproot and BSTEM models allowed for analysis of spatial and temporal variations on bank stability for various riparian vegetative species
Simon et al. (2009)	4.1	Upper Trucke River & Blackwood & Ward Creeks, CA	Evaluate effectiveness of three bank stability treatments (toe protection, top of bank vegetation, and decreased bed slope) by quantifying sediment load reductions	Not Reported	Toe protection reduced sediment loads by 69-100% and bank failures to a single episode, other stability treatments reduced loads by 42-54%, on average on un-treated banks 13.6% of sediment loads originated from hydraulic shear, results demonstrated importance of toe protection
Pollen-Bankhead and Simon (2010)	5.1	Ficticious Channels, MS	Incorporate effect of root permeated bank and toe material on soil erodibility and hydrologic effect of evapotranspiration into stability model	Effects of vegetation appeared to compare well to similar studies	The change in matric suction from evapotranspiration showed the greatest potential benefit to FoS but only in the summer. Root reinforcement was the most important contributor to FoS during the critical spring and winter months
Simon et al. (2011)	5.1	Goodwin Creek, MS	Determine bank stability conditions under a range of hydraulic and geotechnical conditions and erosion-control strategies, design sustainable bank stabilization measures	Simulations of existing conditions matched 10 years worth of observations at the site, post project monitoring	BSTEM was successfully used to design a stable bank with a constrained 1:1 slope requirement, type of vegetation required and rock toe protection were tested until a stable design was determined
Simon et al. (2011)	5.1	Lower Tombigbee River, AL	Use iterative modeling to quantify sediment loads of existing conditions and mitigation strategies	Known average 29 year retreat rate at the site for existing conditions	User should simulate at least a one year "worst case" flow hydrograph (including draw down conditions) in order to quantify sediment loads and load reductions, BSTEM can be used to calculate volumetric and retreat reductions from various mitigation strategies

Simon et al. (2011)	5.1	Upper Trucke River & Blackwood & Ward Creeks, CA	Use iterative modeling to quantify sediment loads of existing conditions and mitigation strategies	Not Reported	RGAs can be used to assess the percent of the banks considered highly or moderately erosive to estimate stream scale loads, load reductions and unit cost per ton of soil for implementing rock toe protection were calculated if various amounts of bank were treated along the reach. Load reductions to the lake and unit costs ranged from 33-87% and \$267-2500 t^{-1} respectively
Simon et al. (2011)	5.1	Big Souix River, SD	Determine average annual rates of streambank erosion and the effects of mitigation strategies	Results of spatially extrapolated loads were compared to suspended sediment loads from USGS gauge data	Loads were calculated for different percentile annual flows. Bank failures were typically only predicted during 90th percentile years. Loads for lower percentile flows were dominantly from fluvial erosion. Rock toe protection resulted in 85-100% reduction in load. Loads from streambanks contributed 10-25% of suspended sediment.
Midgley et al. (2012)[†]	5.2	Barren Fork Creek, OK	Evaluate BSTEM's ability to predict long term retreat and determine the importance of accurate geotechnical, fluvial, and near bank pore water pressure parameters	Compared observed bank retreat and failure timing to model retreat predictions for both default and measured fluvial and geotechnical properties	BSTEM was able to accurately predict the timing of bank failures when multiple hydrographs were executed iteratively, BSTEM under predicted retreat for both default and measured soil parameters, BSTEM predicted a more accurate retreat with measured soil parameters using the jet erosion test
Polvi et al. (2014)	-	North Joe Wright and Corral Creeks, CO	Use Riproot within BSTEM to determine the added cohesion due to roots for various sediment textures and plant species	Not Reported	Reported added root cohesion of four major vegetation types (tree, forb, graminoid, and shrub) on 6 different soil textures. The highest added cohesion was for Salix Geyeriana due to a large number of large roots for the species
Daly et al. (2015)[†]	-	Barren Fork Creek, OK	Assess model sensitivity to root cohesion and performance in predicting bank retreat. Evaluate a simple method for incorporating riparian practices into the model	Compared observed bank retreat and failure timing to model predictions, calibrate erodibility parameters based on aerial imagery	Calibration of erodibility parameters enabled the model to match both timing and amount of retreat for sites with and without vegetative cover. BSTEM was not sensitive to additional soil cohesion added due to roots
Gibson et al. (2015)	-	Goodwin Creek, MS	Integrate BSTEM with the sediment transport methods in HEC-RAS 5.0	Compared model predictions to historical bank migration times and magnitude of lateral retreat	Integration included BSTEM using HEC-RAS hydraulics to determine water surface profiles, HEC-RAS updating cross sections when failure was predicted by BSTEM, and HEC-RAS added failed bank material to the transport model. Location and shape of the final cross sections matched observed cross sections appropriately

Lai et al. (2015)	-	Goodwin Creek, MS	Develop a coupled flow, sediment transport, and bank stability model that includes a limit equilibrium geotechnical model, appropriately distributes failed bank material to the toe, can predict complex turbulent flow, simulates fluvial erosion, and simulates sediment transport.	Compared predicted retreat geometry to measured and previously modeled data	For five year modeling period the difference between predicted and modeled retreat was 0.2-5.2%, developed model shows the benefit of multidimensional models in streambank erosion, model was robust and easy to apply, future need for improving modeling of complex streams
Khanal et al. (2016)[†]	5.4	Barren Fork Creek, OK	Compare model performance for predicting fluvial erosion when a nonlinear-mechanistic model (the Wilson model) is used versus when alternate solution techniques for the Jet Erosion Test are used to solve the parameters of the linear excess shear stress equation	Compared observed bank retreat to model predictions for different fluvial erosion models and solution techniques	The nonlinear detachment model predicted retreat closest to the observed retreat. Linear models both over and under predicted retreat, depending on the solution technique used to evaluate Jet Erosion Test data
Konsoer et al. (2016)	-	Wabash River, IL	Evaluate the effect of lateral and vertical variability in resistance parameters of streambanks on the rates and mechanisms of retreat	Compared known retreat and failure mechanisms to BSTEM predictions, Riproot results were similar to previous studies	Erodibility coefficients derived from Jet Erosion Tests were up to 4 orders of magnitude higher than BSTEM default parameters; BSTEM predicted erroneous bank profiles with JET parameters; model simulations did not predict absolute rates of erosion; simulations did predict mechanisms of failure; default erodibility coefficients simulated reasonable long term erosion mechanisms; BSTEM retreat and failure mechanisms are highly sensitive to lateral and vertical variability in erosion resistance, geometry, and hydraulic conditions; BSTEM does not account for shear stress distributions due to meander bends and it should

*Several studies included more than BSTEM modeling. Only information related to BSTEM modeling is reported in the table.
**The Bank Stability Model (BSM) is the original form of BSTEM including only the bank stability algorithm.
*** [†] Designates that the device used to estimate fluvial erodibility parameters *in situ* was the "mini" jet erosion test (JET) not the original JET

understand previous studies involving BSTEM, a detailed review of several of the studies is presented by topic.

1.3.1 Quantifying Geotechnical Erodibility Parameters

Algorithms used to evaluate geotechnical stability within BSTEM calculate the ratio of driving forces to resisting forces, or a factor of safety (FoS). Failure is assumed to occur when the FoS is less than one. The FoS is calculated using several methods: horizontal layers, vertical slices, and cantilever shear failures. The model iteratively considers several failure planes and shear emergence elevations until the failure plane with the lowest FoS is determined. A complete explanation of current BSTEM stability calculations is available in several previous papers (Simon et al., 2009; Midgley et al. 2012; Daly et al., 2015).

The user input information necessary to evaluate geotechnical stability in BSTEM includes bank geometry; effective cohesion, c'; effective internal angle of friction, ϕ'; the angle that describes the relationship between matric suction and shear strength, ϕ^b; and parameters quantifying the dynamics of pore water pressure distributions. Geotechnical parameters, c' and ϕ', can be determined using four techniques: the Iowa Borehole Shear Tester (BST) for *in situ* measurements (Lohnes and Handy, 1968; Lutenegger and Halberg, 1981), direct shear tests (DST), triaxial shear tests (TST), or BSTEM default parameters.

Of the papers listed in Table 1.1 that reported methods for obtaining geotechnical parameters, approximately three quarters used the BST. Others used a combination of techniques for different soil layers (i.e. BST and DST, BST and TST, or BST and default parameters), some used solely default parameters, and a few did not state parameters or methods used for obtaining geotechnical parameters. Of those that used the BST to quantify geotechnical parameters, the number of BSTs per soil layer ranged from 1 to 16, with the vast majority not going into detail on the number of tests conducted. One study stated that at least duplicates were necessary for each soil layer (Daly et al., 2015), but no explanation was given for this requirement. BSTs are a time

intensive process, as one test includes hauling heavy equipment to the site, often through difficult terrain; manually auguring a hole to the desired depth; and finally executing the test. In addition, Simon et al. (1990) reported that results of up to fifty percent of BSTs completed *in situ* were unusable due to deriving negative parameters. More research is needed to determine the minimum amount of BSTs that should be conducted per soil layer, if the methods of parameter measurement (BST, TST, DST) are comparable, and an enhancement to the BST to make tests more reliable or an alternative method for deriving parameters *in situ*.

In addition to uncertainties on the most appropriate method of deriving geotechnical parameters, default parameters listed in Simon et al. (2011) are available for a very limited selection of soil types: gravel, sand and gravel, sand, loam, and clay. A sensitivity analysis of the stability algorithm in BSTEM by Parker et al. (2008) revealed that the FoS is highly sensitive to input geotechnical parameters and most sensitive to *c'*. The sensitivity analysis was performed for nine separate hydrological events on a single bank profile. Model FoS predictions were compared to known information on whether or not failure actually occurred at the bank for the given event. When mean geotechnical parameters were used, BSTEM predicted bank failures for three of the five banks known to be stable. Parameter means also predicted stable banks for all of the banks that had known failures. When the least and most resistant geotechnical parameters within a reasonable range were simulated for each bank, the range of FoS was from stable to unstable for all banks. This study highlights the effect on FoS within BSTEM due to variability in geotechnical parameters measured within the same bank layer (Parker et al., 2008).

Because geotechnical parameters can be highly variable and are also extremely important to determining bank stability, users should be aware of the implications of choosing default parameters. To demonstrate the effect of selecting default parameters, measured geotechnical parameters reported and information on soil texture was gathered from the studies listed in Table 1.1. The parameters were then separated by BSTEM soil default categories (sand, silt, and clay) and plotted in Figure 1.1. The plot reveals that users should measure parameters when possible

instead of relying on BSTEM default parameters for the most accurate representation of their study site.

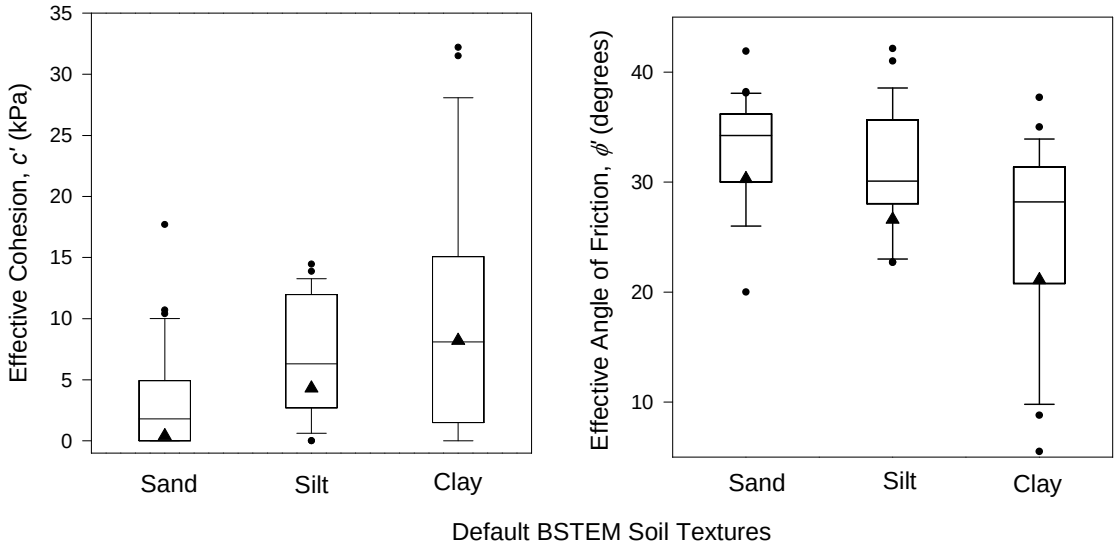

Figure 1.1. Box and whisker plots of measured geotechnical parameters of papers listed in Table 1.1 versus default BSTEM parameters (triangles). Information on soil texture provided by the paper was used to lump geotechnical parameters into sand, silt, and clay default categories.

1.3.2 Quantifying Fluvial Erodibility Parameters

In the later versions of BSTEM, predicting fluvial erosion was introduced to the model. Of the studies in Table 1.1, seven studies used the model to predict both fluvial erosion and geotechnical failures. The model typically uses the excess shear stress equation (Partheniades, 1965; Simon et al., 2000) to quantify the erosion rate, ε_r (m s^{-1}):

$$\varepsilon_r = k_d(\tau - \tau_c)^a \tag{1.1}$$

where τ is the average shear stress (Pa), k_d is the coefficient of erodibility (m^3 N^{-1} s^{-1}), and a is an exponent assumed to be unity.

Some studies suggest an empirical relationship between τ_c and the soil silt-clay content (Julian and Torres, 2006). However, Simon et al. (2011) suggests using the Jet Erosion Test (JET) or default parameters for cohesive soils and information from particle size distributions or default

parameters for non-cohesive soils when using BSTEM. Of the seven studies in Table 1.1 that incorporated the fluvial erosion prediction capabilities of BSTEM, all used JETs to quantify the erodibility of the cohesive soils. Figure 1.2 shows the range of JET results when categorized by BSTEM default soil textures for the studies in Table 1.1 that reported parameters used for fluvial erodibility. There was no consensus on the number of JETs needed to adequately quantify fluvial erodibility parameters. Simon et al. (2006) reported completing two JETs per bank layer, Daly et al. (2015) suggested at least triplicates, and Lai et al. (2015) completed 16 JETs on different soil layers and used the average for the BSTEM simulation. Konsoer et al. (2016) noted that JET predicted fluvial erodibility parameters were several orders of magnitude different than BSTEM default parameters, but that defaults were sufficient at predicting the style of failure over longer time periods. In contrast, Midgley et al. (2012) found that solutions from the JET were better at predicting retreat than the default parameters for long term simulations. Several authors suggested calibrating fluvial erodibility parameters. Lai et al. (2015) recommended calibrating k_d only, with justification that field measurements produce highly uncertain parameters. Several previous studies suggested calibrating fluvial erodibility parameters using a lumped α factor that modified equation 1.1 (Langendoen and Simon, 2008; Langendoen and Simon, 2009; Rousselot, 2009; Daly et al., 2015). The α was stated as accounting for spatial and temporal changes in soil resistance to fluvial forces due to several factors: roots, moisture content, and subaerial processes. In addition to α, Daly et al. (2015) also significantly reduced k_d in order to create calibrated model setups.

Additionally, fluvial erodibility parameters are suggested to be temporarily variable, dependent on subaerial processes, hydrologic events, and vegetation cover (Daly et al., 2015; Konsoer et al., 2016). None of the studies suggested an approach for adjusting fluvial erodibility parameters with time. One major research need is to study the temporal effects on fluvial erodibility parameters and incorporate the findings into the model.

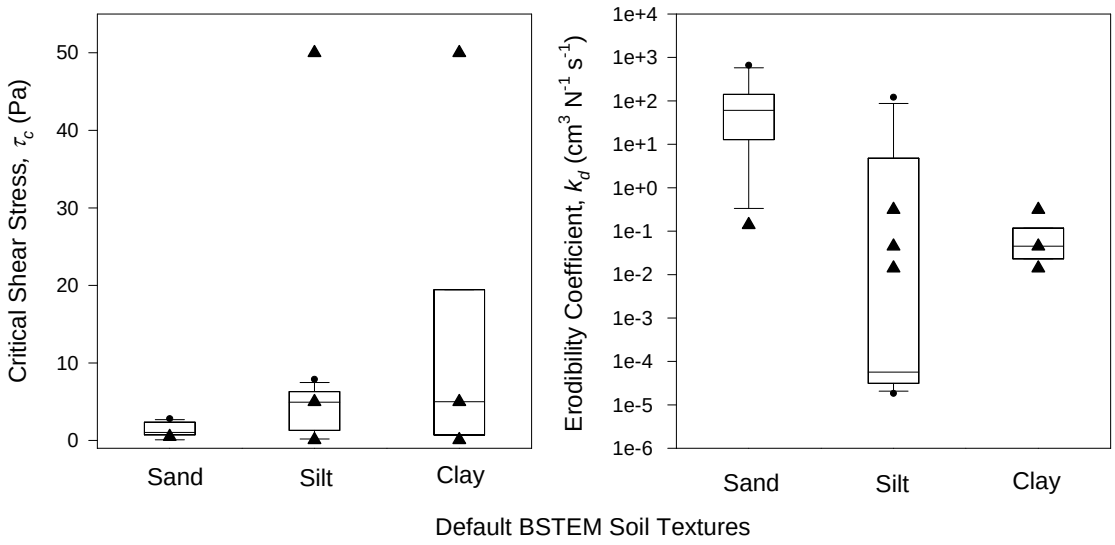

Figure 1.2. Box and whisker plots of measured fluvial erodibility parameters of papers listed in Table 1.1 versus default BSTEM parameters (triangles). Information on soil texture provided by the paper was used to lump parameters into sand, silt, and clay default categories. Note that BSTEM default parameters for silt and clay are selected as resistant, moderately erodible, or erodible.

Khanal et al. (2016) highlighted other issues with modeling fluvial erosion within BSTEM. The research incorporated an alternative to the excess shear stress equation, a non-linear, mechanistic model, into BSTEM to quantify the erosion rate (Wilson 1993a, 1993b). The model, referred to as the Wilson model, is based on the balance of all forces and moments driving and resisting detachment of a two-dimensional particle or aggregate:

$$\varepsilon_r = \frac{b_0\sqrt{\tau}}{\rho_b}\left[1-\exp\{-\exp(3-\frac{b_1}{\tau})\}\right] \tag{1.2}$$

where ρ_b is the bulk density of soil (g m^{-3}) and b_0 (g m^{-1} s^{-1} N$^{-0.5}$) and b_1 (Pa) are mechanistically defined parameters of the Wilson model. When the BSTEM predicted retreat for the Wilson model was compared to the predicted retreat for the traditional excess shear stress approach, the Wilson model more closely predicted actual retreat for the reach in consideration. Wilson parameters can be derived as easily as excess shear stress parameters using the JET (Al-Madhhachi et al., 2013b) and engineers should consider transitioning to the more mechanistic

model instead of the traditional empirical model. More studies on a variety of streambank conditions are needed to confirm the results of Khanal et al. (2016). Khanal et al. (2016) also demonstrated that the solution methodology used to analyze JET results for excess shear stress parameters significantly altered BSTEM predicted profiles, highlighting a need to determine which solution methodology should be used for deriving fluvial erodibility parameters.

1.3.3 Modeling the Effects of Vegetation

Extensive work has been done to model the effects of vegetation on soil geotechnical parameters and apply findings to integrate a user friendly sub-model within BSTEM called RipRoot (Simon and Collison, 2002; Pollen and Simon, 2005; Simon et al., 2006; Pollen-Bankhead and Simon, 2009; Pollen-Bankhead and Simon, 2010; Polvi et al., 2014). The sub-model predicts added cohesion due to roots for twenty-two different common riparian species and allows users to either estimate root distributions based on the age of the species or measured root diameter class data. Simon and Collison (2002) found that the hydraulic and mechanical effects of riparian vegetation were both significant to bank stability. The RipRoot sub-model was only designed and tested for top of bank vegetation, not vegetation covering an entire bank slope. Additionally, when applied to long term modeling, Daly et al. (2015) found that BSTEM was not sensitive to the minimal added cohesion due to roots and that adjusting fluvial parameters was a better approach when calibrating BSTEM input parameters for vegetation.

It is known that vegetation can affect shear stress distributions and therefore reduces the applied boundary shear stresses on a bank profile, reducing the impact of fluvial forces and decreasing the erosion rate. The lumped α suggested by Daly et al. (2015) is one potential method to account for the effects of vegetation on fluvial forces; however, significant research efforts are needed to mechanically estimate the reduction of applied shear stresses and incorporate the findings into the model, as was done for the effects of vegetation on soil strength parameters.

1.3.4 Modeling Seepage Erosion

Seepage erosion, or the erosion of unconsolidated sand above a more restrictive bank layer, is known to be an important erosion process in certain incised streams and can significantly contribute to bank failure (Wilson et al., 2007; Fox and Wilson, 2010). Two studies were completed to evaluate BSTEM's ability to account for erosion due to seepage (Wilson et al., 2007; Lindow et al., 2009). The studies highlighted the fact that BSTEM was missing capabilities to fully predict seepage erosion. The model could accurately predict failures of the typical seepage geometries, but needed to consider near bank groundwater flow in order to fully incorporate the seepage erosion process into the model (Wilson et al., 2007; Lindow et al., 2009). The model could be further developed to include an option for accounting for seepage erosion and other erosion processes that are dominant in the specific study area.

1.3.5 Applying BSTEM to Stream Restoration

In recent years, BSTEM has shown great potential for being an alternative to methods such as classification systems for stream restoration design (Simon et al., 2009; Simon et al., 2011). The appeal of BSTEM is that it is a process-based method, and therefore potentially can be used to predict actual stream response to various streambank mitigation strategies on varying stream reaches based on the forces and moments driving and resisting erosion and bank failure. As a tool, BSTEM is capable of aiding in design of site specific bank stabilization practices by determining minimum conditions for bank stability and quantifying retreat rates and sediment loads of various bank conditions, including conditions after restoration.

Simon et al. (2011) discussed BSTEM for streambank restoration by presenting a case study of uses of the model for such purposes. The following guidelines by Simon et al. (2011) were recommended for using the model in relation to restoration: (i) worst case conditions should be tested on existing conditions to first determine if restoration is even necessary; (ii) if restoration is necessary, BSTEM simulations can be completed with various mitigation strategies

for worst case conditions until a stable design is determined for the site specific characteristics; (iii) the model has been shown to simulate the effects of reducing bank slope by regrading, reducing bed slope (i.e., constructing a meander bend), covering the bank top with a variety of riparian vegetation species, and protecting the bank with rock; (iv) after a stable design is determined for worst case scenarios, long-term simulations should be performed to quantify retreat and sediment load reductions due to various mitigation strategies; and (v) BSTEM reductions can be combined with reach information to determine reach scale reductions to sediment loads.

On paper everything seems to be in order for BSTEM to be a great tool for stream restoration. However, BSTEM has yet to reliably quantify long-term sediment loads without significant calibration needed (Simon et al., 2009; Simon et al., 2011; Midgley et al., 2012; Daly et al., 2015). For example, Simon et al. (2011) completed a study on the Lower Tombigbee River in Alabama. Detailed site information was known as well as geotechnical parameters, fluvial parameters, stage, and retreat spanning back several years. The stream was reported to expect an average retreat of 1.2 m yr^{-1}. Stabilization practices, including combinations of rock toe and vegetation, were modeled and compared to simulations of no treatment over a one year simulation period. However, the no treatment simulation predicted a retreat of over 40 m during the simulation. This was not even close to the known average of 1.2 m yr^{-1}, and results were stated to not represent actual volumes of failures and only should be used to highlight relative differences between the existing, no treatment case and various restoration strategies. The model should be able to predict more reliable loads and retreat rates if it is to be used as a design tool by engineers and conservationists. From personal experience, the calibration process and model run-time for long term simulations is time intensive. In order to be a better tool for stream restoration the following research and development of the model is needed: (i) incorporation of more stabilization practices into the model, (ii) improving accuracy of predicted loads and retreats, (iii) the ability to run several stabilization practices at once, (iv) significantly decreasing simulation

run time, (v) an option to output stochastic retreats to account for uncertainty, and (vi) making the interface more user friendly and more easily modified. In addition, training courses may be necessary in order for agencies and private industries to learn how to use the tool correctly and understand model limitations.

Much work is also needed in order to extrapolate site specific BSTEM simulations to calculate entire stream-scale sediment loads and reductions to loads. To demonstrate the uncertainty in extrapolating results of BSTEM simulations, a Monte Carlo simulation was performed to determine the range of stream-scale sediment loads and reductions to loads for three different stabilization practices simulated in BSTEM on sites in the Fort Cobb Reservoir Watershed in southwest Oklahoma. A Monte Carlo simulation is a statistical method for determining sensitivity of a complex system to input parameters with uncertainty and variability (Dunn and Shultis, 2011). First, statistical distributions are determined for the independent parameter data. Statistical software can be used to determine distributions; this study used Minitab 16 (Minitab, 2009). Distributions should be chosen that are considered an acceptable fit, i.e., p-value is greater than 0.05, and have the lowest Anderson-Darling (AD) statistic. In addition, chosen distributions should always be checked against data to make sure the fit is appropriate. For example, data that are known to never be negative should have distributions assigned that reflect that quality. Once distributions are determined, probability density function (PFD) and cumulative density function (CFD) parameters can be obtained for the independent parameter data distributions. Simulation parameter data are then generated with a minimum of 1000 random numbers between 0 and 1 (Driels and Shin, 2004), setting the random number equal to the previously determined CFD, and back calculating the associated simulation parameter. Once all simulation parameters are determined, they can be used to calculate potential outcomes.

A ten year sediment load along two tributaries in the Fort Cobb Reservoir Watershed was calculated using two different approaches. The Fort Cobb Reservoir, located in southwest Oklahoma, provides public water supply, recreation, and wildlife habitat. Several conservation

practices have been implemented in the watershed in recent years including adoption of no-tillage management, conversion of cropland to grassland, cattle exclusion from streams, and various structural and water management practices. However, surface waters still do not meet water quality standards based on sediment. Streambank erosion from unstable streambanks in the watershed is one of the primary contributors of sediment loading to the reservoir. Four monitoring sites in the watershed were selected along two tributaries, Fivemile and Willow Creeks, to the reservoir from which the fluvial and geotechnical properties of the streambank were estimated. BSTEM was used to estimate sediment load reductions for three bank stabilization practices. The practices included rock toe protection, vegetation and grading only, and a combination rock toe protection, grading, and vegetation.

The first approach utilized aerial imagery to estimate the ten year load, L_{10yr} (kg):

$$L_{10yr} = BH \times \rho_b \times l_s \times l_r \tag{1.3}$$

where BH is the bank height (m), ρ_b is the average bank bulk density (kg m^{-3}), l_s is the length of the stream (m), and l_r is the average lateral bank retreat along the stream determined from aerial imagery (m). The BH and ρ_b are the independent variables and were generated using Monte Carlo methods. The other variables, l_s and l_r, are considered known averages and the same value was used for all simulations. The second approach utilized calibrated BSTEM simulations to calculate L_{10yr}:

$$L_{10yr} = L_{BSTEM} \times l_s \tag{1.4}$$

where L_{BSTEM} is the ten year sediment load per meter of bank predicted by calibrated BSTEM models on nine sites in the watershed (kg m^{-1}). The BSTEM predicted loads from five, 10 year simulations on Fivemile Creek and four, 10 year simulations on Willow Creek were used to generate L_{BSTEM} using the Monte Carlo methods. Stream length was again assumed known. Table 1.2 shows Monte Carlo distributions for the three independent Monte Carlo parameters: BH, ρ_b,

and L_{BSTEM} for both Willow and Fivemile Creeks used to calculate sediment loads for both methods.

Table 1.2. Minitab distributions and Monte Carlo inputs for Bank Height, *BH*; Bulk Density, ρ_b; and BSTEM predicted 10 year sediment loads, L_{BSTEM}, based on predictions from Chapter 3.

Variable	Creek	Distribution	Inputs for Monte Carlo*	p value	AD value
BH	Fivemile	Weibull	α = 4.67; β = 4.33	> 0.25	0.368
	Willow	Gamma	α = 57.88; β = 0.07	0.061	0.725
ρ_b	Fivemile	Loglogistic	β = 0.04 ; μ = 0.37	> 0.25	0.368
	Willow	3-Parameter Weibull	α = 5468.55; β = 527.89; γ = -526.47	0.383	0.340
L_{BSTEM}	Fivemile	Uniform	a = 128; b = 111919	-	-
	Willow	Uniform	a = 350; b = 25528	-	-

* α = shape; β = scale; γ = threshold; μ = location; a = minimum value; b = maximum value

Figure 1.3 shows the results of the Monte Carlo simulation for calculating sediment loads. The range of sediment loads was much smaller for the aerial imagery method (equation 1.3) for both creeks; however, average loads were within the same order of magnitude. To potentially decrease the range of predicted loads for the BSTEM method (equation 1.4), more sites would need to be modeled. For Fivemile creek, the BSTEM method (equation 1.4) predicted higher loads than the aerial imagery method (equation 1.3). For Willow Creek, the opposite was true. For all but the Fivemile Creek BSTEM method (equation 1.4), using average data nearly matched the Monte Carlo simulation averages.

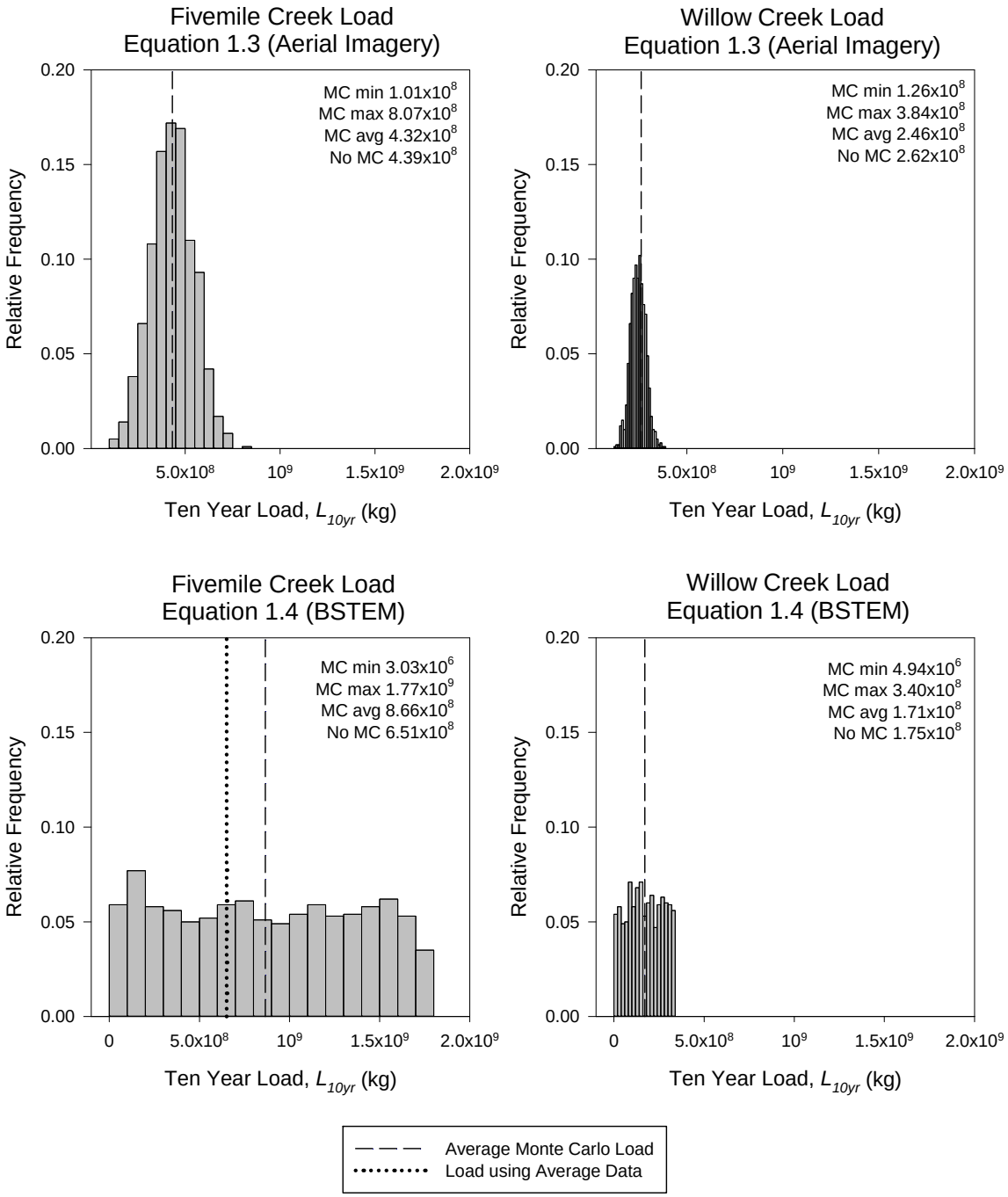

Figure 1.3 Histogram results of the Monte Carlo simulation to estimate total sediment loads to the reservoir over the ten year simulation. Note that MC stands for Monte Carlo and No MC is the load if averages were used to calculate loads.

After determining total sediment loads, the results from modeling three mitigation strategies (toe riprap, vegetation and grading only, and a combination of the two) in BSTEM at sites experiencing retreat were used to complete another Monte Carlo analysis for potential total

reduction loads. The following equation was used to calculate the maximum 10 year reduction to load, L_{R10yr} (kg), for each stream:

$$L_{R10yr} = BH \times \rho_b \times l_{sf} \times l_r \times R_{\%} \quad (1.5)$$

where l_{sf} is the length of stream without a forested riparian area (m) and $R_{\%}$ is the BSTEM simulated percent reduction to load for the different mitigation techniques. The $R_{\%}$ was an independent variable and was generated using Monte Carlo methods. Distributions for $R_{\%}$ are shown in Table 1.3. Because the amount of $R_{\%}$ data was small, simple distributions, triangular or uniform, were used. The assumption was made that mitigation practices would only be constructed where heavy riparian vegetation was not already present, therefore l_{sf} was determined using aerial imagery and was considered a known. The other parameters match those in equation 1.3.

Table 1.3 Minitab distributions and Monte Carlo inputs for Percent Reduction to Load, $R_{\%}$, for each of the stabilization practices modeled in Chapter 3.

Stabilization Practice	Distribution	Inputs for Monte Carlo*
Toe riprap only	Triangular	a = 53.9; b = 100; m = 100
Toe riprap + vegetation and grading	Triangular	a = 95.4; b = 100; m = 100
Vegetation and grading only	Uniform	a = 75.9; b = 99.9

*a = minimum value; b = maximum value; m = mode

The results of the Monte Carlo analysis for determining maximum load reductions are shown in Figure 1.4. The average load for all the Monte Carlo simulations was almost identical to the load reduction using solely averages. However, the ranges of load reduction were over an order of magnitude different, suggesting that stochastic methods should be considered when using BSTEM to predict reduction to sediment load for restoration practices. It is important to note that these simulations do not include the impact of stabilization practices on sediment transport capacity due to the one dimensional restraint of BSTEM.

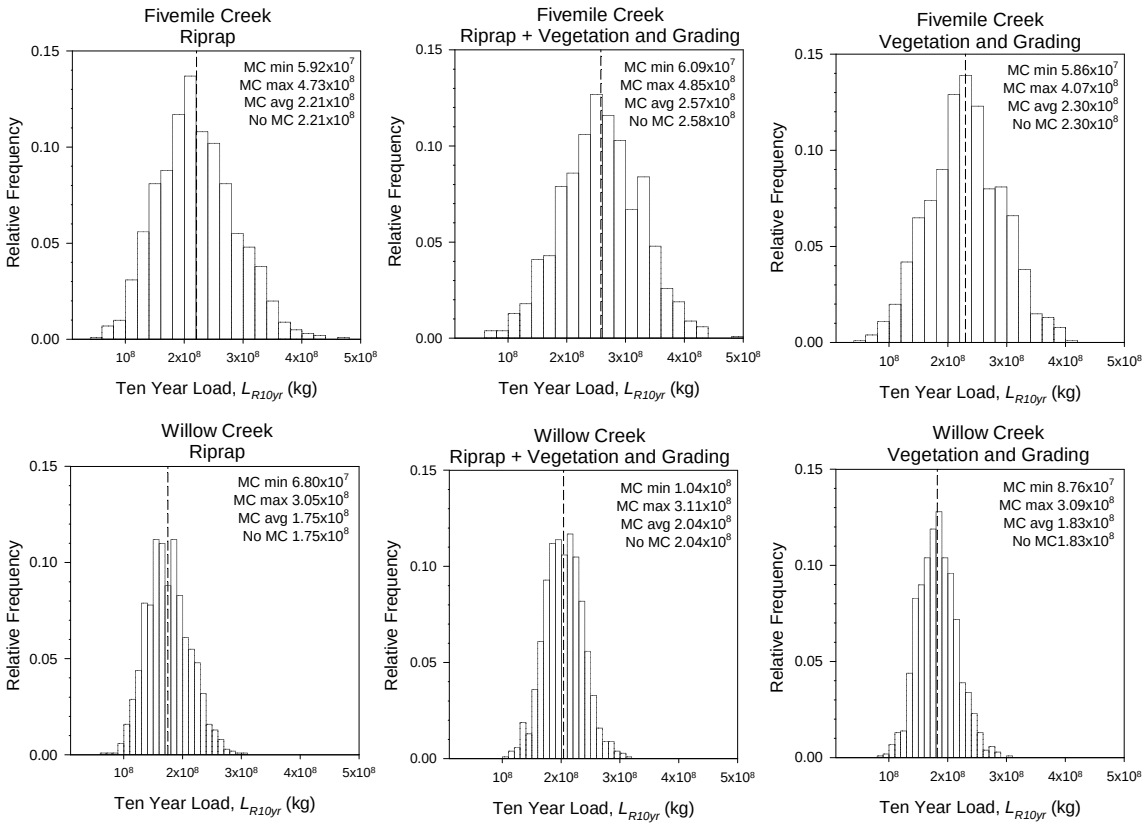

Figure 1.4 Histogram results of the Monte Carlo simulation to estimate the maximum sediment load reduction to the reservoir using the ten year BSTEM simulation. Note that MC stands for Monte Carlo and No MC is the load if averages were used to calculate loads.

1.3.6 Integrating BSTEM with Other Models

Some of the major issues with BSTEM are that the model does not account for the protection failed material may provide and does not account for complex turbulent flows, especially at a meander bend. In an attempt to combat some of these issues, BSTEM has been combined with two dimensional models to more appropriately model sediment transport, failed material as bank protection, and turbulent flow (Gibson et al., 2015; Lai et al., 20015). Lai et al. (2015) showed that BSTEM combined with a multidimensional model was beneficial. The study modeled Goodwin Creek in northern Mississippi, one of the most extensively monitored streams in the country, and was able to accurately represent long term retreat rates. Similarly, Gibson et al. (2015) found that when BSTEM 5.4 was integrated with HEC-RAS 5.0, the two models were

able to appropriately predict observed cross sections over a long term simulation. Integrated models showed good promise for resolving BSTEM's downfall of inaccurately quantifying long term sediment loads. However, future studies need to be completed with the integrated models on a variety of stream conditions in order to compare results and work out any issues with the integrated models.

1.4 Conclusions

Several studies have been completed using BSTEM, ranging from specifically bank stability modeling to evaluating the effects of vegetation and seepage to modeling for the purpose of streambank restoration and to integrating the model with multidimensional flow and sediment transport models to address some of the major issues. BSTEM is one of the most robust, comprehensively studied, and used process based models available for predicting streambank erosion and failure and yet still has several areas that need to be addressed so that the model can be more widely used and applicable. In review, the major issues with BSTEM that need to be addressed are accounting for spatial and temporal variability in geotechnical failure and fluvial erodibility parameters, incorporating seepage and other site specific processes into the model, researching the effects of riparian vegetation on bank shear stress distributions and erodibility parameters, decreasing BSTEM run-time for long term modeling, increasing the usability of the model for stream restoration, and confirming the preliminary results of the integrated multidimensional models. BSTEM is a useful tool and should be considered as an alternative to classification type stream restoration design. To make this possible more research and development of the model is required.

CHAPTER II

COMPARISON OF LINEAR AND NONLINEAR MODELS FOR COHESIVE SEDIMENT DETACHMENT: RILL EROSION AND HOLE EROSION TEST STUDIES

2.1 Abstract

Cohesive sediment detachment is typically modeled for channels, levees, spillways, earthen dams, and internal erosion using a linear excess shear stress approach. However, mechanistic nonlinear detachment models, such as the Wilson model, have recently been proposed in the literature. Questions exist as to the appropriateness of nonlinear relationships between applied shear stress and the erosion rate. Therefore, the objective of this research was to test the appropriateness of linear and nonlinear detachment models for cohesive sediment detachment using two data sets: (i) rill erodibility studies across a limited range of applied shear stress (0.9 to 21.4 Pa) and (ii) hole erosion tests (HETs) across a wide range of applied shear stress (12.6 to 62.0 Pa). The Wilson model was shown to be an appropriate particle detachment rate model from previously published data on rill erodibility and HETs. *In situ* and laboratory tests sometimes use a limited range of applied shear stress; therefore, users of these measurement techniques should be aware of the potential nonlinear behavior of cohesive sediment detachment especially at higher shear stress. Results suggest advantages for the nonlinear Wilson detachment model, but also identify the need for additional research to evaluate the various detachment models across a wider range of soil types.

2.2 Introduction

Many water management issues, including river channel degradation, bank stability, bridge scour, culvert scour, earthen spillway erosion, and levee and earthen dam overtopping, stem from excessive erosion of cohesive soils. Therefore, the ability to accurately predict cohesive soil erosion is a necessity for engineers worldwide. Prediction is a challenge due to numerous factors influencing soil erodibility such as soil texture, structure, unit weight, water content, swelling potential, clay mineralogy, and pore water chemistry (Utley and Wynn, 2008).

Typically, the erosion rate of a cohesive soil is predicted using a model that relates soil erodibility to a measure of hydraulic forces on the soil. The most common model is known as the excess shear stress equation (Partheniades, 1965). The model states that the erosion rate is proportional to the difference between the applied boundary shear stress and the critical shear stress:

$$\varepsilon_r = k_d(\tau - \tau_c)^a \tag{2.1}$$

where ε_r is the erosion rate (m s^{-1}), k_d is coefficient of erodibility (m^3 N^{-1} s^{-1}), τ is the applied shear stress (Pa), τ_c is the critical shear stress (Pa), and a is an exponent usually assumed to be unity (Partheniades, 1965). Typically the k_d is reported in units of cm^3 N^{-1} s^{-1}. The k_d and τ_c are collectively known as erodibility parameters. The τ_c is defined as the hydraulic stress at which particle detachment will initiate. The τ_c was originally defined for non-cohesive soils. There is no precise definition of τ_c for a cohesive soil as there is rarely a defining τ at which detachment of a cohesive soil particles start (Utley and Wynn, 2008).

2.2.1 Linear Detachment Rate Assumption

Linearization of the τ versus ε_r relationship is typically justified as a necessary condition to simplify the complex description of the detachment process (Zhu et al., 2001; Knapen et al.,

2007). However, whether or not the assumption of linearity holds over the entire range of possible τ in experiments still remains unanswered. In their comprehensive study of all available data relating soil erodibility and concentrated flow, Knapen et al. (2007) found that few authors attempted to search for the equation that best fit their experimental results. Some authors found that the linear relationship proved to fit well for a narrow range of τ (e.g., Ghebreiyessus et al., 1994; Prosser et al., 1995; Ghidey and Alberts, 1997; Van Klaveren and McCool, 1998); while other authors found a power relation better described ε_r (e.g., Hollick, 1976; Knisel, 1980; Vanliew and Saxton, 1983; Franti et al., 1999; Zhu et al., 2001). Most research has concluded that although the linear model has the advantage of being simple in application, it suffers from significant lack of fit when applied to experimental data encompassing a wide range of τ. Some authors (e.g., Lyle and Smerdon, 1965; Parker et al., 1995; Zhu et al., 1995, 2001) proposed using two different linear models by splitting the range into separate sections to overcome the deficiency of the linear model (Knapen et al., 2007). In summary, there is no consensus among researchers on the nature of the relation between ε_r and τ. Theoretical assumptions for linearity or nonlinearity have not been tested completely. Nevertheless, the type of relationship chosen has important consequences for the magnitude of erodibility parameters and estimation of ε_r (Knapen et al., 2007).

Wilson (1993a, 1993b) introduced an alternative to the excess shear stress model and Al-Madhhachi et al. (2014a, 2014b) modified the model to account for additional forces that influence detachment. The model, from this point forward referred to as the Wilson model, is based on the balance of all the forces and moments driving and resisting detachment of a two-dimensional particle or aggregate:

$$\varepsilon_r = \frac{b_0 \sqrt{\tau}}{\rho_b} \left[1 - \exp\{-\exp(3 - \frac{b_1}{\tau})\} \right] \tag{2.2}$$

where ρ_b is the bulk density of soil (g m^{-3}) and b_0 (g m^{-1} s^{-1} $N^{-0.5}$) and b_1 (Pa) are mechanistically defined parameters of the Wilson model. The parameters of the Wilson model (b_0 and b_1) require knowledge of several soil particle or aggregate parameters that are difficult to estimate.

According to the excess shear stress equation, once the threshold of τ_c is exceeded, ε_r increases linearly with applied τ. The Wilson model predicts no such critical threshold but does predict a similar increase in ε_r at lower applied τ. At higher τ, the ε_r increases with the square root of applied τ. This nonlinear shape of the Wilson model has proven to fit better than the linear excess shear stress equation with observed data from rill erosion studies (Wilson, 1993b).

2.2.2 Estimating Erodibility Parameters

Different techniques such as large flumes, small flumes, HETs, and JETs have been employed to obtain experimental data required for quantifying erodibility parameters. Flumes are the most traditional and frequently used technique for studying erosion characteristics of natural channels (Hanson, 1990a).

The HET is a laboratory test in which a soil sample is either obtained undisturbed in a tube or compacted into a standard proctor mold and internal erosion is induced through a hole created in the sample (Wan and Fell, 2004; Wahl et al., 2008). After drilling a 6-mm hole through the sample, the sample is placed in a device that allows water to flow through the hole under a constant hydraulic head. The head is increased in increments until erosion initiates. After erosion initiates, the head is held constant for up to 45 minutes while the hole diameter increases. Flow rates and head measurements at the inflow and outflow chambers are measured throughout the duration of the test. A final hole diameter is measured at the completion. Errors in measured hole diameters can exist when the hole created takes an irregular shape. Using the initial and final hole diameters and flow rates, friction factors for laminar and turbulent flow are calculated. The friction factors are assumed to vary linearly with time for the duration of the test. Using the

calculated friction factors, the flow rates and differential head measurements are used to calculate hole diameters at intermediate times. The difference in hole diameter is used to determine ε_r. Finally, applied shear is estimated using the following equation:

$$\tau = \rho g \frac{A}{O} I \tag{2.3}$$

where ρ is the density of water (kg/m^3), A is the wetted area (m^2), O is the wetted perimeter (m), and I is the hydraulic gradient along the length of the sample (m/m). The hydraulic gradient between the head measurements is assumed to be linear. Recent studies have questioned the accuracy of assuming a linear hydraulic gradient between head measurements due to the neglect of entrance and exit losses (Říha and Jandora, 2015). Further details of the test procedure and equations can be found in previous research (Wan and Fell, 2004; Wahl et al., 2008). Although there are some errors associated with the assumptions made to calculate τ and ε_r, the purpose of this study is to show the potential nonlinear behavior of cohesive soil detachment. Therefore the assumptions were deemed acceptable for the scope of this research.

The JET has proven to be among the most useful instruments because the test can be carried out *in situ*. JETs consist of a submerged jet of water impinging upon a soil surface creating a scour hole. The depth of scour hole is measured at different time intervals. Details of the apparatus and methods employed for JETs are described by Hanson (1990b). The experimental data obtained from the JETs can be analyzed using three different solution routines to derive the erodibility parameters of the linear excess shear stress model. The most popular method of analysis, referred to as Blaisdell's solution (Blaisdell et al., 1981), was developed by Hanson and Cook (1997, 2004). The solution method was based on principles of fluid diffusion presented by Stein and Nett (1997) and a hyperbolic-logarithmic function modeling the progression of the scour hole depth as developed by Blaisdell et al. (1981). This solution method first determines the τ_c based on the equilibrium depth of the scour hole. The equilibrium depth is

defined as the maximum depth beyond which the water jet cannot further erode the soil and is determined by using the hyperbolic curve fit to estimate the scour depth at time approaches infinity. The k_d is then iteratively solved for to minimize the error between the measured time and predicted time based on the basis of an integrated solution of the excess shear stress equation.

Two alternatives to the Blaisdell solution have been suggested recently: the iterative solution (Simon et al., 2010) and the scour depth solution (Daly et al., 2013). In contrast to the Blaisdell solution, the scour depth and iterative solutions solve for both τ_c and k_d simultaneously through iterations. The scour depth solution simultaneously solves for k_d and τ_c to minimize the error between the observed JET scour data and the predicted scour depth data following the solution of the excess shear stress equation (Daly et al., 2013). The iterative solution is initialized using the erodibility parameters determined by the Blaisdell solution (Simon et al., 2010). The scour hole is assumed to reach the equilibrium depth at the end of each test. An upper bound on τ_c is calculated using this equilibrium depth and is set as a constraint preventing the final estimated τ_c from exceeding this value. The final value of τ_c and k_d are then solved for simultaneously by minimizing the error between the measured time to reach the equilibrium scour depth and the time expected to reach equilibrium according to an integrated solution of the excess shear stress equation. Note that the parameters (b_0, b_1) of Wilson's model are also estimated from the JET data by minimizing the sum of squared error between the predicted scour depth data and observed data from the JET. The details of the procedure are described in Al-Madhhachi et al. (2013a).

Previous research has indicated that the Blaisdell solution estimates lower τ_c than the scour depth and iterative solutions (Simon et al., 2010; Daly et al., 2013). Because each method assumes that the τ-k_d relation is linear, the estimation of k_d by the Blaisdell solution is also lower than that estimated by scour depth and iterative solutions. At higher applied τ, ε_r predicted by the scour depth solution and the iterative solution are thus much higher due to their higher estimated

k_d. When used in stability models such as BSTEM, k_d is frequently used as a calibration parameter, and it has been observed that k_d estimated from JETs using the scour depth and iterative solutions requires significant scaling down to match the predicted and observed bank retreat (Daly et al., 2015). This necessity raises questions about the assumption of linearity between ε_r and τ.

2.2.3 Objectives

Building on previous research, it was hypothesized in this study that nonlinear detachment models are more appropriate across a wider range of applied τ compared to linear detachment models. The objective of this study was to compare linear and nonlinear models for cohesive sediment detachment across a range of studies: (i) field data from rill erodibility studies and (ii) laboratory data from hole erosion tests (HETs).

2.3 Methods and Materials

2.3.1 Field Rill Erosion Study

The rill erodibility studies of Elliot et al. (1990) were analyzed in this study. In the study, six rill erosion tests on 33 soil series from across the United States were conducted. Soil textures included clay, clay loam, loam, loamy sand, sand, sandy loam, silt loam, and silty clay. Rills of length 9 m, spaced every 4.6 m, and with slopes of 3 to 6% were tested in the experiments. Bulk density and soil moisture samples were collected. Each rill was tested in a three part series: (i) rainfall only until flow equilibrium was reached; (ii) rainfall plus flow added in increments at the head of each rill; and (iii) flow increments added at the head of each rill with no rainfall. Cross-sectional surveys were recorded for each flow increment, and used to determine hydraulic radius. The hydraulic radius, rill slope, and water density were used to calculate hydraulic shear stress (τ)

for each flow increment. Hydraulic shear stress (τ) was reported in Pa (range of 0.9 to 21.4 Pa with only 12 rills having shear stresses greater than 15 Pa) and rill detachment rate was reported in g s^{-1} m^{-2}. The detachment rates were converted from g s^{-1} m^{-2} to ε_r in cm s^{-1} using the bulk density measurements acquired during the original experiments and appropriate unit conversions. From the entire data set, only studies without rainfall were analyzed. In addition three of 180 rills were excluded from the analysis because ε_r were highly scattered relative to τ, which resulted in negative τ_c and k_d. Restraining the fit of these tests to positive τ_c and k_d resulted in negative R^2.

Wilson (1993b) analyzed this data, showing that the Wilson model fit as well as or better than a linear excess shear stress equation. Unique to this research, parameters for all three detachment models (linear and nonlinear excess shear stress equations and the Wilson model) were derived using the dynamic fit regression tool in SigmaPlot 12.5 (SigmaPlot, 2013) for each rill erodibility study. Also, the model fits were extrapolated outside the range of applied τ.

The fit of each detachment model to the observed data was quantified using a coefficient of determination, R^2, and the normalized objective function (NOF). The NOF is defined as the ratio of root mean squared difference of observed and predicted data and overall mean of the observed data:

$$NOF = \frac{\sqrt{\frac{\sum_{i=1}^{N}(x_i - y_i)^2}{N}}}{X_a} \tag{2.4}$$

where x_i and y_i are the observed data and prediction from fitted model, respectively, N is the number of observations and X_a is the mean of observed data. Smaller NOF values correspond to better fits of the model to the observed data (Fox et al., 2006; Al-Madhhachi et al., 2013a, 2014a,b).

The soils were then grouped by soil texture in order to compare the performance of the three detachment models relative to soil type. Also, two specific cases were analyzed as

representative examples in regard to model applicability of the rill erodibility data. One case was for Miami silt loam, rill #5; the other was for Nansene silt loam, rill #3. These specific cases were selected because one resulted in a nonlinear excess shear stress equation with $a>1$ and the other with $a<1$ in equation (1), demonstrating how slight differences in the collected data can produce considerable differences in the power term of the model which effects extrapolation at higher τ.

2.3.2 Laboratory Hole Erosion Test (HET) Study

Fourteen separate HET data sets from Wahl et al. (2008) were analyzed using the HET data analysis procedures of Wan and Fell (2004). The data sets consisted of three soils: soil 55T-160 (dispersive sandy lean clay) with 37% sand and 63% fines, soil MF (lean clay), and soil TE (lean clay to silt) with 16% sand and 84% fines. The tests utilized a range of τ between approximately 10 and 60 Pa. The three models (linear and nonlinear excess shear stress models and the Wilson model) were fit to the entire range of data in the same manner as was applied to the Elliot et al. (1990) data. Again, R^2 and NOF values were reported and compared to assess model performance.

In addition to fitting the three models to each of the data sets one data set, test #3 on soil 55T-160, was used to demonstrate the consequences of assuming a linear relationship between τ and ε_r when extrapolating fits from a small range of applied τ to a larger range of applied τ. Although it is not ideal, it is common practice in the field of cohesive sediment detachment to measure erodibility parameters on a limited range of τ and use the parameters in applications that contain considerably higher applied τ. The three models were fit to a limited range of τ of the data set (i.e. shear stresses ranging from 10Pa to 20Pa). The three model fits were then extrapolated to a higher range of applied shear stresses and plotted adjacent to the entire data set in order to visually compare the consequences of extrapolation on predicted ε_r.

2.4 Results and Discussion

2.4.1 Field Rill Erosion Study

An example of the model fits to two sets of rill erodibility data are shown in Figure 2.1 with summary statistics provided in Table 2.1. All three models performed similar in fitting the observed data with R^2 ranging between 0.93 and 0.96, and NOF from 0.13 to 0.14 (Table 2.1). Wilson (1993b) showed similar results in comparing the Wilson model to the linear excess shear stress equation. Note the restricted range in τ for these two data sets. In general, all the rill erodibility experiments were conducted with τ <15 Pa, with a few cases having data for τ >15 Pa. Extrapolating these fits to 50 Pa showed that the models that produced similar curve fits in the range of τ <15 Pa predicted significant deviations in ε_r at higher τ with the linear and nonlinear excess shear stress equations predicting much higher erosion rates (Figure 2.1).

Table 2.1. Parameters and fit statistics for the three detachment models for the two example rill erodibility data sets. Note that τ_c (Pa), k_d (cm^3 N^{-1} s^{-1}), b_1 (g m^{-1} s^{-1} N$^{-0.5}$), and b_0 (Pa).

	Nansene Rill #3				
	τ_c	k_d	a	R^2	NOF
Linear Excess Shear	3.3	8.5	1	0.94	0.13
Nonlinear Excess Shear	0	0.4	2.29	0.95	0.13
	b_1	b_0		R^2	NOF
Wilson Model	18.4	32.1		0.93	0.14
	Miami Rill #5				
	τ_c	k_d	a	R^2	NOF
Linear Excess Shear	4.1	13.3	1	0.96	0.13
Nonlinear Excess Shear	4.3	16	0.91	0.96	0.13
	b_1	b_0		R^2	NOF
Wilson Model	23.4	41.1		0.95	0.14

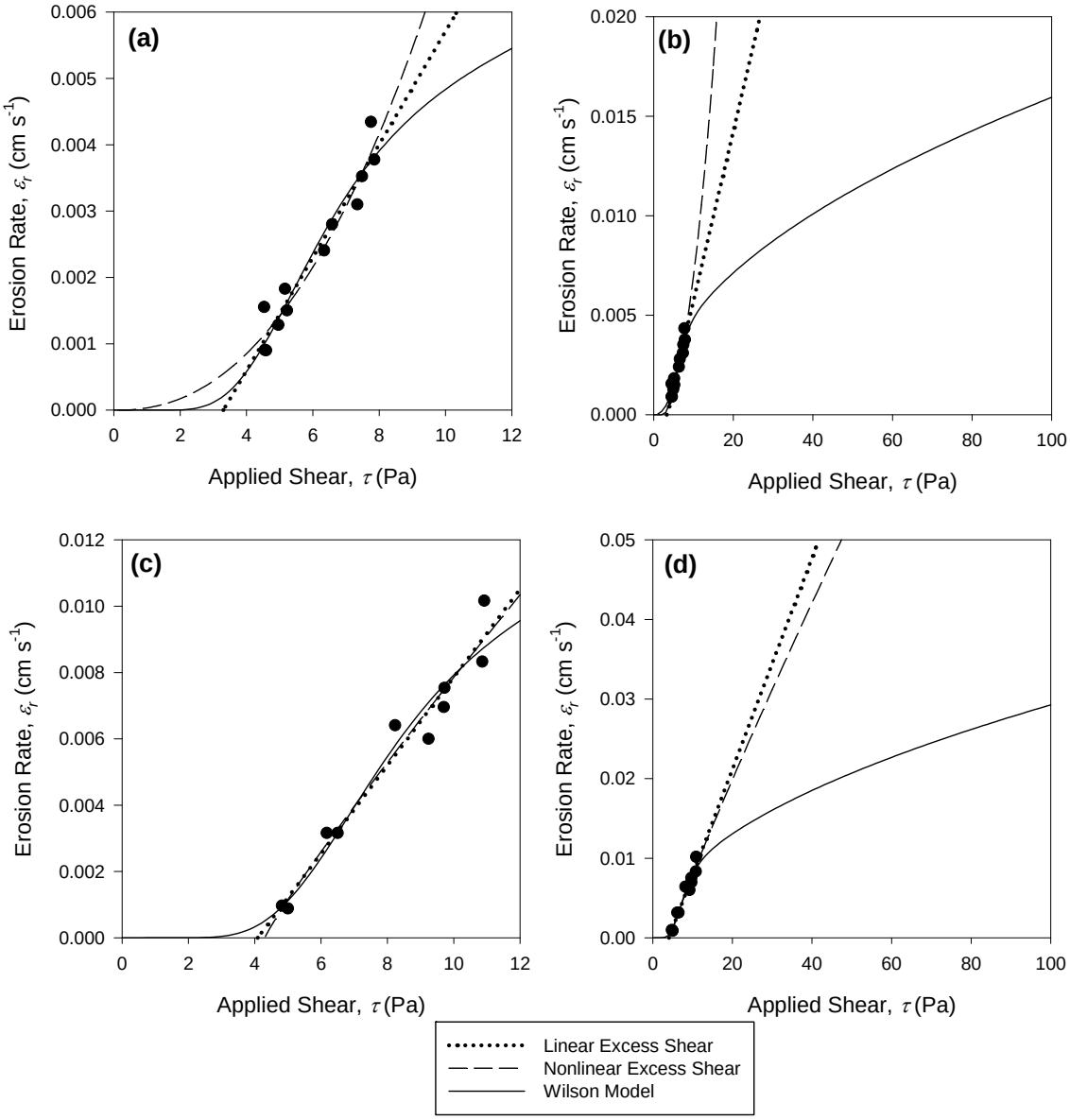

Figure 2.1. Example rill erodibility data: (a) and (b) Nansene soil series, rill #3; (c) and (d) Miami soil series, rill #5. (a) and (c) show fit to the linear excess shear stress equation, nonlinear excess shear stress equation, and the Wilson model. (b) and (d) are the extrapolation of the three models to shear stresses outside the measured range and corresponding predicted erosion rates for the expanded range. Note that for the nonlinear excess shear stress equation a>1 for (b) and a<1 for (d).

Across all the rill erodibility studies, the detachment models generally fit the data with R^2>0.5 and NOF<0.3 (Table 2.2). Also, no relationship was observed between model performance and soil texture, specifically the clay content. For example, all the detachment models fit most poorly to the silty clay soil texture with approximately equivalent performance for all other soil textures (Table 2.2). For some rills, there were samples in which ε_r declined at

higher τ, contrary to what is expected and theorized for cohesive soil detachment. Instead of removing these data sets from the analysis, they were included and in many cases resulted in nonlinear excess shear stress models with a approaching 0 as shown in Table 2.2.

Table 2.2 Average and range in parameters and model fit statistics for the rill erodibility studies (n = 177) reported in Elliot et al. (1990) and grouped by soil texture. Note that n_{type} is the number of rills within that soil texture and n_{rill} is the total number of rills tested.

Linear Excess Shear Stress												
			k_d		τ_c			R^2		NOF		
Soil Texture	n_{type}	n_{rill}	($cm^3N^{-1}s^{-1}$)		(Pa)							
Clay	1	6	2.8	1.4-4.3	0.4	0.0-0.9	0.55	0.09-0.86	0.21	0.15-0.31		
Clay Loam	3	18	3.4	1.2-7.6	4.3	0.0-9.0	0.73	0.43-0.94	0.30	0.10-0.59		
Loam	8	46	4.4	1.1-12.5	4.0	0.0-28.6	0.75	0.10-0.98	0.30	0.08-0.69		
Loamy Sand	1	6	9.6	4.6-16.4	1.0	0.1-1.7	0.56	0.16-0.84	0.31	0.21-0.51		
Sand	2	12	5.1	1.5-9.7	1.2	0.0-2.6	0.84	0.69-0.96	0.24	0.13-0.44		
Sandy Loam	6	35	4.1	1.0-8.5	1.4	0.0-3.2	0.79	0.08-0.98	0.20	0.07-0.64		
Silt Loam	7	42	5.2	1.2-13.2	3.3	0.0-8.0	0.79	0.43-0.97	0.24	0.08-0.48		
Silty Clay	2	12	4.7	0.9-12.9	3.1	0.0-4.9	0.45	0.08-0.81	0.77	0.27-1.33		
Nonlinear Excess Shear Stress												
			k_d		τ_c		a		R^2		NOF	
Soil Texture	n_{type}	n_{rill}	($cm^3N^{-1}s^{-1}$)		(Pa)							
Clay	1	6	6.3	2.0-12.7	1.7	0.0-3.0	0.63	0.18-1.20	0.61	0.26-0.86	0.2	0.16-0.31
Clay Loam	3	18	8.4	0.0-40.2	5.6	0.0-14.4	0.97	0.02-3.39	0.77	0.52-0.96	0.26	0.04-0.63
Loam	8	46	5.3	0.0-27.2	3.6	0.0-8.5	1.54	0.10-6.72	0.79	0.12-0.98	0.25	0.08-0.72
Loamy Sand	1	6	12.2	1.3-21.4	1.4	0.0-2.2	0.89	0.50-2.47	0.58	0.21-0.85	0.32	0.21-0.52
Sand	2	12	4.2	0.0-13.1	0.9	0.0-2.98	1.65	0.50-3.66	0.87	0.75-0.98	0.21	0.12-0.38
Sandy Loam	6	35	8.1	1.1-42.5	2.3	0.0-5.73	0.8	0.01-1.76	0.84	0.09-0.99	0.17	0.03-0.67
Silt Loam	7	42	8.0	0.0-30.6	3.4	0.0-13.2	1.11	0.00-3.16	0.81	0.43-0.99	0.23	0.05-0.51
Silty Clay	2	12	8.2	0.00-37.1	3.4	0.0-5.9	1.61	0.15-4.08	0.49	0.09-0.92	0.72	0.25-1.41
Wilson Model												
			b_0		b_1			R^2		NOF		
Soil Texture	n_{type}	n_{rill}	($g\ m^{-1}s^{-1}N^{-0.5}$)		(Pa)							
Clay	1	6	5.6	2.6-8.0	6.5	0.13-9.2	0.59	0.22-0.81	0.21	0.15-0.30		
Clay Loam	3	18	38.7	4.7-449.4	30.7	3.5-103.1	0.78	0.54-0.94	0.27	0.09-0.57		
Loam	8	46	35.2	3.09-665.0	26.6	10.2-50.3	0.79	0.13-0.97	0.26	0.09-0.68		
Loamy Sand	1	6	22.0	10.9-36.5	7.4	5.1-10.0	0.57	0.23-0.85	0.30	0.20-0.49		
Sand	2	12	13.6	7.8-21.1	9.6	4.0-19.8	0.85	0.76-0.94	0.24	0.17-0.35		
Sandy Loam	6	35	13.2	3.5-29.4	11.1	0.1-20.6	0.80	0.08-0.98	0.20	0.06-0.72		
Silt Loam	7	42	18.0	2.5-59.9	23.3	6.0-55.5	0.80	0.37-0.97	0.23	0.08-0.47		
Silty Clay	2	12	49.3	1.4-313.8	24.5	9.1-56.3	0.51	0.08-0.94	0.70	0.23-1.34		

In general, the Wilson model fit the rill erodibility data as well as or better than the linear or nonlinear excess shear stress equations. This data provides indication of the ability of nonlinear detachment models to result in similar but slightly improved predictions to linear models at lower ranges of τ. However, data where ε_r were measured across a wider range of τ was still needed to demonstrate suitability of the nonlinear models.

2.4.2 Laboratory Hole Erosion Test (HET) Study

One of the unique data sets available for ε_r versus τ was the HET experiments conducted by Wahl et al. (2008) primarily because of the extended range of τ. Model fits to four of the HET experiments is shown in Figures 2.2 and 2.3 and summarized in Table 2.3, where the nonlinear relationship between ε_r versus τ was clearly visible. Note that all detachment models fit the laboratory-controlled HET data better than the field rill erodibility studies (Tables 2.2 and 2.3). It can be deduced by extrapolating the observed HET data in Figure 2.2 that an appropriate estimation of τ_c was approximately 10 Pa. Attempting to fit the entire range of ε_r versus τ with a linear excess shear stress model resulted in an inappropriately derived τ_c of approximately 0.9 Pa (Table 2.3). More specifically, the linear excess shear stress model does not appropriately represent the known ε_r versus τ data at the lower range of τ when the model was fit to the entire data set (Figure 2.2b). Also, if applied τ was greater than 50 to 60 Pa, the linear excess shear stress equation with estimated k_d predicted a much higher ε_r than the nonlinear model. The nonlinear models (i.e., nonlinear excess shear stress model and Wilson model) seemed to provide a much more appropriate fit, with at least one of the nonlinear models having higher R^2 and lower NOF values for all of the HETs as compared to the linear model (Table 2.3).

Table 2.3. Parameters and fit statistics for the three detachment models for the HET data reported by Wahl et al. (2008). Note that *n* is the number of measurements within a specific HET.

		Linear Excess Shear Stress				Nonlinear Excess Shear Stress					Wilson Model			
HET	***n***	τ_c (Pa)	k_d ($cm^3N^{-1}s^{-1}$)	**NOF**	R^2	τ_c (Pa)	k_d ($cm^3N^{-1}s^{-1}$)	***a***	**NOF**	R^2	b_0 ($g\ cm^{-1}s^{-1}N^{-0.5}$) *x 10^{-2}*	b_1 (Pa)	**NOF**	R^2
55T-160-1	209	0.0	0.21	0.08	0.92	17.2	3.46	0.29	0.04	0.94	2.6	53.3	0.04	0.98
55T-160-2	268	0.0	0.18	0.07	0.97	11.6	1.32	0.50	0.02	0.99	2.1	49.6	0.05	0.98
55T-160-3*	222	0.9	0.24	0.09	0.96	13.8	2.00	0.47	0.08	0.96	2.8	50.7	0.06	0.98
55T-160-4	161	3.6	0.27	0.06	0.98	12.0	1.17	0.64	0.02	0.99	3.1	61.1	0.08	0.97
55T-160-7	83	12.0	0.47	0.05	0.98	0.0	0.01	1.9	0.04	0.99	3.6	72.8	0.08	0.95
55T-160-9†	121	10.8	0.23	0.10	0.96	22.1	1.69	0.50	0.03	0.99	2.5	89.6	0.05	0.99
55T-160-14	166	10.6	0.33	0.05	0.99	12.4	0.78	0.69	0.04	0.99	1.9	56.4	0.05	0.99
MF-5†	41	7.0	0.46	0.19	0.97	11.6	2.14	0.55	0.08	0.99	3.6	47.8	0.16	0.98
MF-6	45	5.7	0.38	0.15	0.97	8.8	1.33	0.61	0.06	0.99	2.7	41.3	0.11	0.98
MF-7	36	6.4	0.55	0.15	0.97	8.7	1.50	0.65	0.08	0.99	3.0	38.5	0.13	0.98
TE-1	8	5.5	1.23	0.04	0.99	2.8	0.53	1.23	0.04	0.99	8.0	42.5	0.11	0.95
TE-2	46	7.3	0.45	0.25	0.94	9.1	1.58	0.48	0.10	0.98	2.0	38.4	0.26	0.93
TE-3	14	6.6	2.01	0.24	0.95	8.3	6.16	0.38	0.05	0.99	8.0	35.5	0.34	0.90
TE-5†	26	4.2	0.68	0.15	0.93	8.0	3.35	0.44	0.05	0.99	3.9	31.4	0.08	0.98

*Figure 2.2 shows model performance for this test

† Figure 2.3 shows model performance for these tests

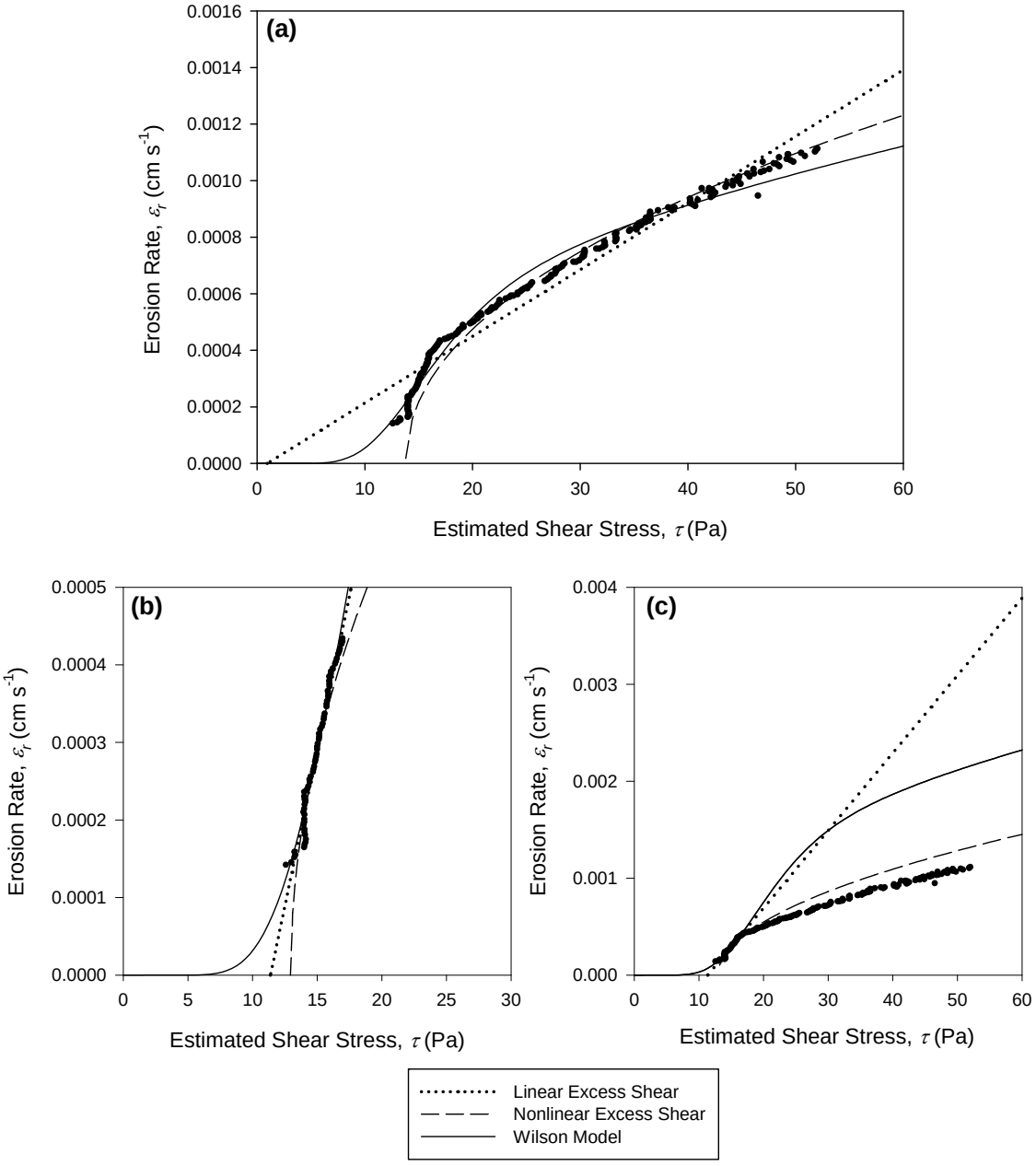

Figure 2.2. (a) Example hole erosion test (HET) data (test #3 on soil 55T-160 (dispersive sandy lean clay) with 37% sand and 63% fines) fit to the linear excess shear stress equation, nonlinear excess shear stress equation, and the Wilson model. (b) Model fits to a limited range of shear stress, as typically measured during *in situ* tests, and (c) extrapolation across the range of applied shear stress in the HET.

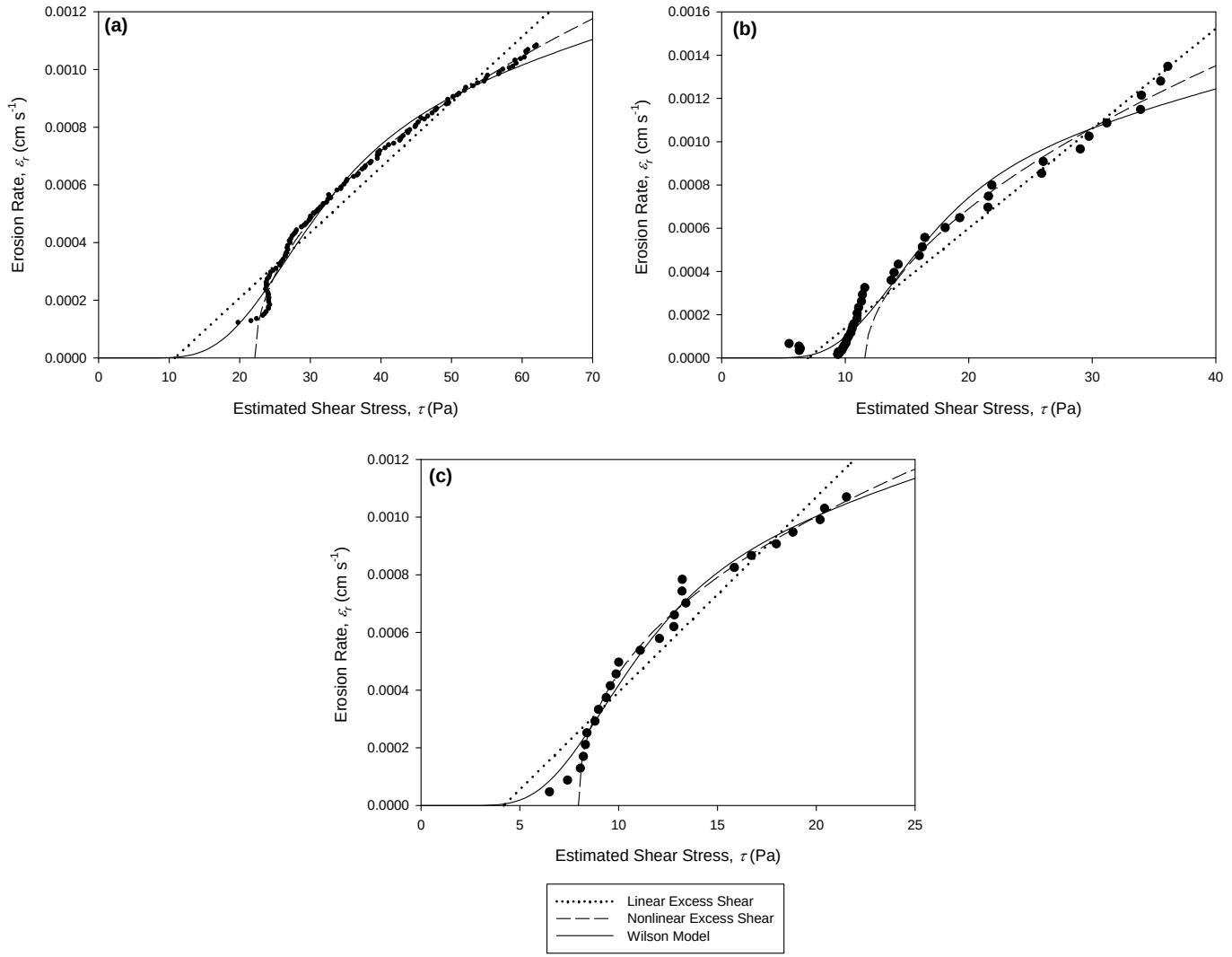

Figure 2.3.Example of hole erosion test (HET) data for tests (a) test #9 on soil 55T-160 (dispersive sandy lean clay with 37% sand and 63% fines), (b) test #5 on soil MF (lean clay), and (c) test #5 on soil TE (lean clay to silt with 16% sand and 84% fines) fit to the linear excess shear stress equation, nonlinear excess shear stress equation, and the Wilson model.

The estimation of τ_c appears to be improved when we focused our analysis on the lower range of applied τ (10 to 20 Pa, Figure 2.2b) as compared to when we used the entire range (Figure 2.2a). In fact, the estimated τ_c with a linear excess shear stress approach was approximately 11.0 Pa. While this appears more appropriate, the resulting $k_d = 0.75$ cm^3 N^{-1} s^{-1} was two to three times higher than the corresponding k_d given in Table 2.3 for the linear excess shear stress equation. This created a situation in which extrapolating to larger τ using these values derived from the linear portion of ε_r versus τ caused significant over estimation of the ε_r, as shown in Figures 2.2b and 2.2c.

Therefore, an improved τ_c estimate caused a higher estimated k_d because of the limited range of τ investigated in the analysis. We hypothesize that this scenario is also occurring in many cases for *in situ* JETs and relative to the three different solver routines. Daly et al. (2015) reported that the Blaisdell solution typically estimated a lower, conservative τ_c and therefore a lower k_d compared to other solution routines for the linear excess shear stress equation, similar to the linear excess shear stress fit shown in Figure 2.2a. The scour depth and iterative solutions estimate a better fitting τ_c (i.e., similar to the linear excess shear stress fit in Figure 2.2b and 2.2c) but a higher k_d. Therefore, when applied to predict erosion rates in simulation models, users are forced to reduce the k_d estimated from the scour depth and iterative solutions when the τ exceeds the range in τ used during soil testing in order to calibrate the model. This practice is not sound as it introduces additional uncertainties in the modeling procedure.

Furthermore, the linear model under predicted τ_c when the model was fit to a large range of applied τ (Figure 2.4). Assuming the nonlinear predictions of τ_c are closer to the true τ_c, based on the fact that the nonlinear model fit better for all HETs, the linear model under predicted τ_c for all but two of the fourteen tests.

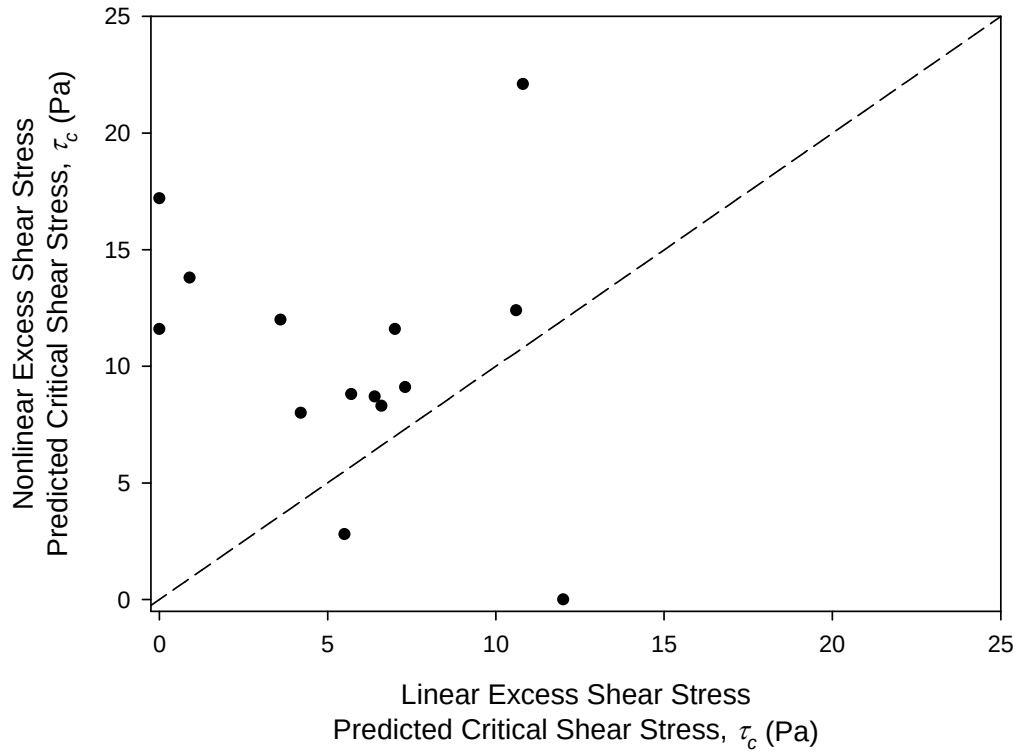

Figure 2.4. Comparison of τ_c predictions for the linear excess shear stress model and the nonlinear excess shear stress model for the HET data sets.

2.5 Conclusions

In many cases, erodibility tests are performed across a small range of applied shear stress in which a linear detachment model appears appropriate. Measurement techniques that utilize greater applied shear stress illustrate the nonlinear behavior of cohesive sediment detachment especially at higher applied shear stress. Erodibility parameters from these tests are typically used in erosion models that may simulate detachment under conditions of much greater applied stress. The Wilson model was shown to be an appropriate erosion rate model from previously published data on rill erodibility and hole erosion tests. The nonlinear excess shear stress model was also shown to adequately fit known ε_r versus τ data for a wide range of applied shear stress. However, it is important to note that it can be problematic to estimate erodibility parameters for this model due to the use of three parameters instead of two like the Wilson model. Such results suggest the

advantageous nature of the nonlinear Wilson detachment model, but also identify the need for additional research to evaluate the various detachment models for laboratory HETs and *in situ* JETs across a wider range of soil types. In addition, it would be extremely useful to compare how the detachment models perform in process based models containing estimations of cohesive soil erosion due to hydraulic shear forces. One such model in which this comparison would be particularly useful is one of the most commonly used and most advanced process based models available to evaluate streambank stability and fluvial erosion: The Bank Stability and Toe Erosion Model (BSTEM).

2.6 Acknowledgements

The author wishes to acknowledge the financial support of the Buchanan Family Trust through the Buchanan Endowed Chair and the Oklahoma Agricultural Experiment Station at Oklahoma State University. This project was also supported by Agriculture and Food Research Initiative Competitive Grant no. 2013-51130-21484 from the USDA National Institute of Food and Agriculture and through a FY 2012 US EPA 319(h) Special Project #C9-00F56701. In addition, this research would not have been possible without the support of Drs. Tony Wahl, Garey Fox, Erin Porter, and Anish Khanal.

CHAPTER III

PREDICTING THE IMPACT OF STREAMBANK STABILIZATION PRACTICES ON SEDIMENT LOADS USING A PROCESS-BASED BANK STABILITY AND TOE EROSION MODEL (BSTEM)

3.1 Abstract

Erosion from unstable streambanks is often a primary contributor of sediment loading within a watershed. The Bank Stability and Toe Erosion Model (BSTEM) is a process-based fluvial erosion and slope stability model that can be used to predict erosion and geotechnical failure for streams. The Fort Cobb Reservoir, located in southwest Oklahoma, provides public water supply, recreation, and wildlife habitat. Several conservation practices have been implemented in the watershed in recent years including adoption of no-tillage management, conversion of cropland to grassland, cattle exclusion from streams, and various structural and water management practices. However, surface waters still do not meet water quality standards based on sediment. Streambank erosion from unstable streambanks in the watershed is one of the primary contributors of sediment loading to the reservoir. Eight monitoring sites in the watershed were selected along two tributaries, Fivemile and Willow Creeks, to the reservoir from which the fluvial and geotechnical properties of the streambank were estimated. From 2003-2013, the average streambank retreat at these sites was as high as 1.2 m yr^{-1} as derived from aerial imagery. BSTEM was first applied using two different detachment models for fluvial erosion then calibrated to the observed retreat rates using excess shear stress parameters. Next, BSTEM was used to estimate sediment load

reductions for three bank stabilization practices. The practices included rock toe protection, vegetation and grading only, and a combination rock toe protection, grading, and vegetation, which reduced predicted loads by 54% to 100%, 76% to 99%, and 95% to 100%, respectively. Cost to sediment load reduction ratios were also determined for the streambank stabilization techniques and showed that considering costs in streambank restoration is important in selection of appropriate stabilization practices at the site scale. On average, vegetation and grading alone was the least expensive practice to install, $185 per meter of bank stabilized, and was also the most cost effective at reducing loads over the ten year simulation period, i.e., 414 kg reduction per meter of bank per dollar.

3.2 Introduction

Suspended sediment in surface water significantly reduces water quality and has been said to be the number one water quality problem in the United States. Excess sediment can destroy aquatic habitat, increase contaminant loads, and decrease water clarity (Simon and Darby, 1999). Typically a large percent, as much as 90%, of total sediment loads in surface waters originate from channel degradation or streambank erosion (Grissinger and Murphey, 1982; Walling et al., 1998; Simon and Klimetz, 2008; Purvis and Fox, 2016). In addition to the increase in surface water sediment loads, streambank erosion can cause further problems by destroying infrastructure and stream side property. Because of the known negative implications of streambank erosion, billions of dollars have been spent on stabilization projects to slow bank retreat (Lavendel, 2002; Bernhardt et al., 2005) along with several studies on restoration practices (Fischenich, 2001; Shields et al., 2003; Khosronejad et al., 2013). With such a large portion of streambank-derived material contributing to surface waters, estimating bank derived sediment loads and load reductions due to various stabilization scenarios is essential for restoration projects.

There are many processes that interact to contribute to streambank retreat. However, the two main processes are fluvial erosion and geotechnical failures (Darby et al., 2007; Rinaldi and Darby, 2007). Fluvial erosion, or the removal of soil material by the action of hydraulic forces, is typically estimated using excess shear stress equation with erodibility parameters (critical shear stress, τ_c in Pa, and the erodibility coefficient, k_d in $m^3\ N^{-1}\ s^{-1}$) of the bank material, but recently mechanistic models have been suggested as a more accurate representation of fluvial erosion. Geotechnical failure, or mass wasting, is controlled by the relationship of the forces resisting and driving failure of the bank, which is estimated using soil shear strength parameters typically derived from the Mohr-Coulomb theory. Both the erodibility and shear strength parameters (effective cohesion, *c'*, and internal angle of friction, ϕ') are functions of several soil properties including texture, weight, soil moisture conditions, structure of soil aggregates, compaction, clay mineralogy, pH, organic content, soil temperature, and freeze/thaw cycles (Knapen et al., 2007). These properties are often difficult to quantify, which further complicates the prediction of streambank retreat. Because of the complicated nature of predicting streambank retreat and the financial and environmental consequences of streambank restoration failure, it is essential that engineers develop and utilize models capable of completing process-based iterative calculations.

Process-based models, such as the Bank Stability and Toe Erosion Model (BSTEM) and the Conservational Channel Evolution and Pollutant Transport System (CONCEPTS), have been successfully used to model streambank retreat in previous studies (Midgley et al., 2012; Sutarto et al., 2014; Daly et al., 2015). However, little research has been done utilizing these models to analyze the effect of implementing various mitigation practices on reduction to sediment loads. Simon et al. (2009) conducted research in the Lake Tahoe Basin using BSTEM to estimate sediment loads and load reductions of certain mitigation practices based on hydrographs from separate storm events during 1995. The study emphasized the importance of bank toe protection from fluvial forces, stating that loads reduced by 69% to 100% when rock toe protection was

modeled. Other modeled mitigation strategies reduced loads by 42% to 54%. A cost to load reduction ratio was estimated for rock toe protection only (Simon et al., 2009). Additional, comprehensive studies are needed on streams with different characteristics. Little to no work has been published that develops a methodology for selecting streambank stabilization practices by considering reduced sediment loads and input costs to adopt a stabilization technique. Failure to use a process-based model to quantitatively analyze bank stabilization practices puts a design engineer at risk of the design failing or potentially increased costs due to an over-designed stabilization practice. In this study, BSTEM 5.4 Dynamic Version (BSTEM, 2016) was used as the process-based model to evaluate various stabilization practices on unstable streambanks in the Fort Cobb watershed in southwestern Oklahoma.

3.2.1 BSTEM Model Description

BSTEM was developed by the National Sedimentation Laboratory in Oxford, Mississippi, USA and has continually been updated since the original release (Simon et al. 2011). BSTEM is one of the most commonly used and most advanced process-based models available to evaluate streambank stability. The model uses inputs of soil erodibility and shear strength parameters; channel geometry of up to five horizontal soil layers; stream hydraulic characteristics including channel slope, Manning's *n*, reach length, radius of curvature; and a stream stage hydrograph.

The model steps through the hydrograph by first predicting fluvial erosion traditionally based on an excess shear stress equation (Partheniades, 1965; Simon et al., 2000). Erosion rate, ε_r (m s^{-1}), is calculated as:

$$\varepsilon_r = k_d(\tau - \tau_c)^a \tag{3.1}$$

where τ is the average shear stress (Pa) and a is an exponent usually assumed to be unity. Recently, the Wilson model (Wilson 1993a, 1993b; Al-Madhhachi 2014a, 2014b) was added to BSTEM as another option for calculating the erosion rate. The model was shown by Khanal et al. (2016) to better represent erosion rate data over a wider range of τ than the excess shear stress equation. The model is mechanistically defined and based on the balance of all the forces and moments driving and resisting detachment of a two dimensional particle or aggregate:

$$\varepsilon_r = \frac{b_0\sqrt{\tau}}{\rho_b}\left[1-\exp\{-\exp(3-\frac{b_1}{\tau})\}\right] \tag{3.2}$$

where ρ_b is the bulk density of soil (g m^{-3}) and b_0 (g m^{-1} s^{-1} $N^{-0.5}$) and b_1 (Pa) are mechanistically defined parameters of the Wilson model.

If fluvial erosion occurs, BSTEM determines if the new bank geometry is stable, based on the ratio of driving forces to resisting forces expressed as a factor of safety (FoS). Failure is assumed to occur when the driving forces exceed the resisting forces (i.e., FoS < 1). Various combinations of failure plane angle and shear emergence elevation on the bank face are considered within the model in order to determine the failure plane with the lowest FoS. Following the completion of the bank stability component of BSTEM, the model redraws the bank if failure has occurred and then moves to the next time step of the hydrograph (Simon et al., 2000; Cancienne et al., 2008; Simon et al., 2009; Midgley et al., 2012; Daly et al., 2015). It is important to note that BSTEM, and therefore simulation results, assume all eroded material is washed downstream as opposed to being deposited on the bank and that no additional bed degradation occurs.

3.2.2 Stabilization Practices

Simply speaking, a successful streambank stabilization technique will either reduce the driving forces acting on the bank or increase the forces resisting fluvial erosion or geotechnical

failure. One of the most common techniques used to slow the retreat of streambanks is to place large rocks along the bank to make it immobile. The rocks are sized to increase the force required to initiate streambank particle motion to a level essentially unreachable by the channel's flow. This technique is referred to as riprap and has shown to successfully stabilize banks, but questions still exist on the potential negative geomorphic and ecological consequences of implementation (Reid and Church, 2015). Riprap has traditionally been the preferred stabilization technique; however, in recent years bioengineering solutions have gained favor due to their positive ecological, economic, and aesthetic qualities, despite being considered less stable (Canada Dept. of Fisheries and Oceans et al., 2004). Examples of bioengineering techniques include vegetated gabions, brush mattresses, vegetated geogrids, and live stakes (Donat, 1995), but there has been limited research assessing the life span and stability of these emerging techniques (Canada Dept. of Fisheries and Oceans et al., 2004). In addition to bioengineering techniques, practices that redirect flow in order to reduce secondary currents and slow near bank velocities are also alternatives to the traditional riprap approach. Examples include submerged vanes (Odgaard and Kennedy, 1983) and bendway weirs (Derrick et al., 1994).

3.2.3 Objectives

Due to the complex nature of cohesive erosion and streambank failure and to successfully implement stream stabilization practices, engineers should focus their design efforts using process-based methods as opposed to more empirical approaches, such as analog or classification systems. The objective of this study was to demonstrate a process-based method for assessing the effectiveness of streambank stabilization practices by (i) quantifying sediment load reductions at the site scale using a process-based model to simulate various stabilization practices and (ii) conducting a comprehensive cost to benefit analysis of the stabilization practices.

3.3 Materials and Methods

3.3.1 Description of Field Sites

The Fort Cobb Reservoir Watershed, 786-km^2, contains mainly agricultural land and is located in the Central Great Plains ecoregion of southwestern Oklahoma. The watershed consists of streams ranging in order from first to fourth and contains four main sub-watersheds: Cobb Creek, 419-km^2; Lake Creek, 168-km^2; Fivemile Creek, 109-km^2; and Willow Creek, 73-km^2 (Franklin et al., 2013). All four creeks and the reservoir appeared on the 2014 Oklahoma 303(d) list of impaired waters. Resolving water quality issues is imperative as the reservoir provides public water supply, recreation, and wildlife habitat. For this reason, several upland conservation practices have been implemented in the watershed in recent years including adoption of no-tillage management, conversion of cropland to grassland, cattle exclusion from streams, and various structural and water management practices. However, surface waters still did not meet water quality standards based on sediment. Streambank erosion is considered a major contributor of sediment loading to the reservoir. Streambanks in this watershed consist of sand or sandy loam topsoil overlying a layer with higher clay content.

Five sites were selected at locations along Fivemile Creek, 19.7-km, designated FM1-FM5 and three sites were selected at locations along Willow Creek, 14.9-km, designated WC1-WC3 (Figure 3.1). The Fivemile and Willow Creek sub-watersheds consisted primarily of cropland and pasture with little urban and forested areas. Any forested areas were typically located along the creeks. At each site, at least one cross-sectional survey was conducted using an automatic level. Detailed notes were taken during surveying to record vegetation coverage and channel thalweg locations, since previous research has emphasized the importance of incorporating bank heterogeneity into process-based modeling (Sutarto, 2014). Therefore, bank layers, distinguished visually by color and apparent texture, were also thoroughly documented.

Figure 3.2 shows the bank profiles for each site along with soil layers and vegetation cover on the eroding bank or critical bank. In addition to cross-sectional surveys, stream slope at each reach was measured by surveying the elevation drop along the thalweg.

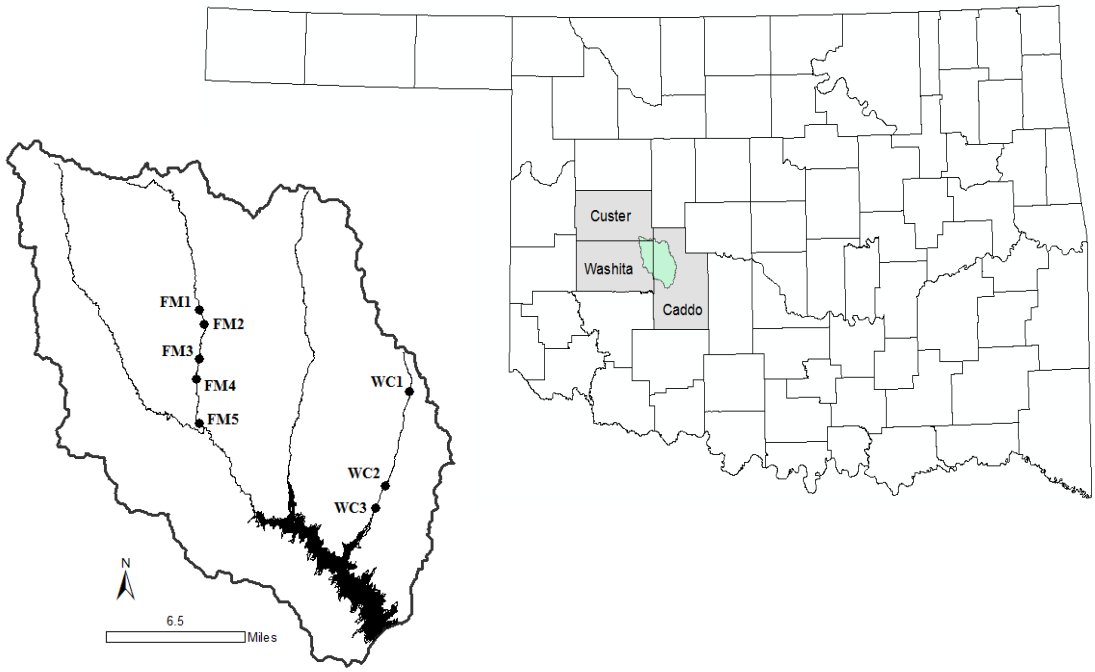

Figure 3.1. Fort Cobb Reservoir Watershed in southwest Oklahoma and locations of study sites along Fivemile (FM1-FM5) and Willow (WC1-WC3) Creeks.

3.3.2 Streambank Data Collection

An *in situ* submerged jet apparatus was used to quantify the resistance of the bank material to fluvial erosion. The apparatus, the "mini" Jet Erosion Test, is hence forth referred to as JET, and was selected due to its ability to conduct *in situ* measurements with minimal soil disturbance. To operate a JET, a submerged jet of water at a constant head impinges a soil bank face for increasing intervals of time until detachment stops. Scour depth versus time data were collected and used to determine erodibility parameters. A further description of the JET is presented by Al-Madhhachi et al. (2013a). At least two JETs were conducted

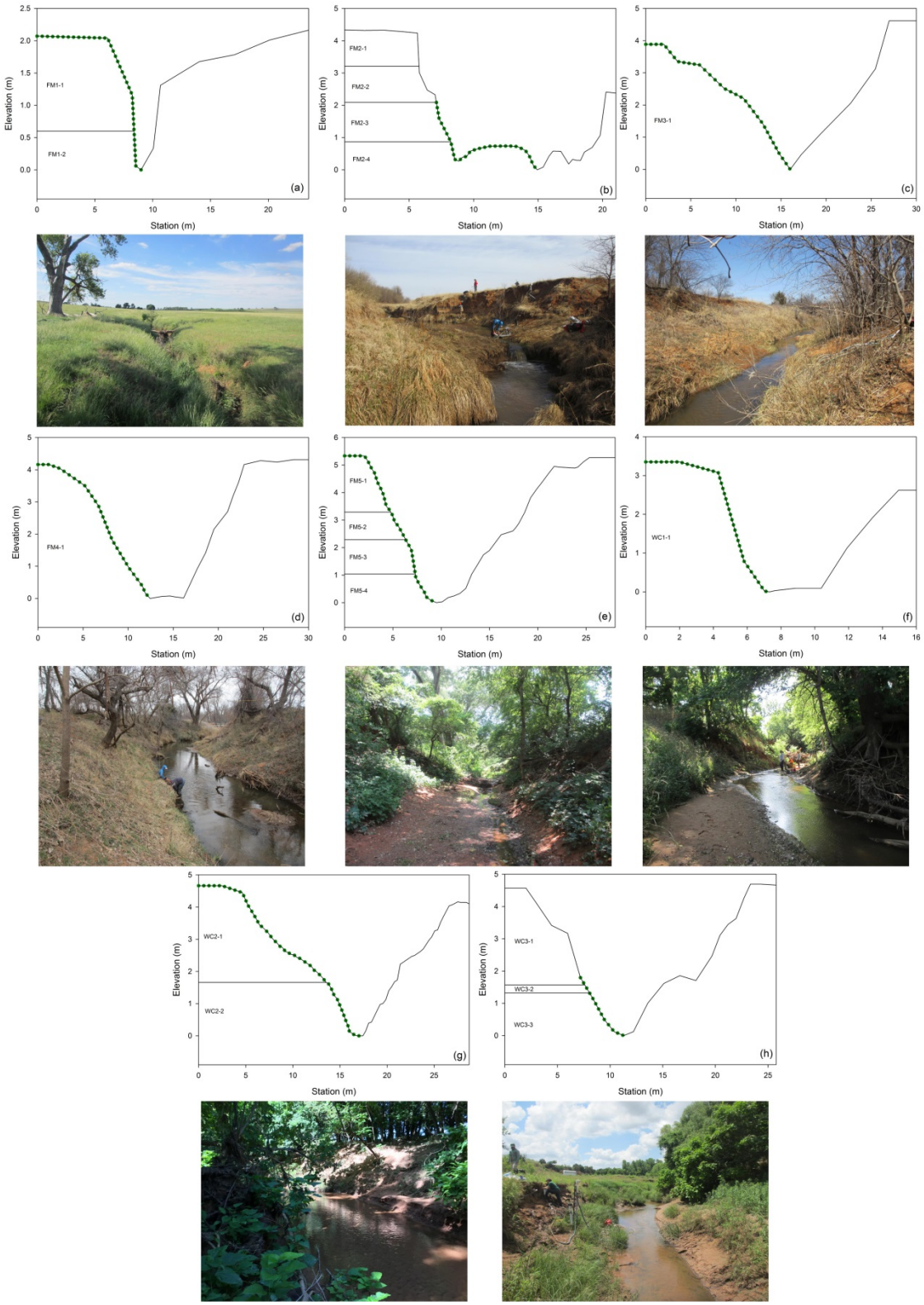

Figure 3.2. Cross-section geometry showing vegetation cover (dots) and soil layers on the critical bank with corresponding site picture below: (a-e) corresponds to Fivemile Creek sites (FM1-FM5) and (f-h) corresponds to Willow Creek sites (WC1-WC3) in the Fort Cobb Reservoir watershed. Soil layers are labeled in the *site name–soil layer* # format and match Table 3.1.

Table 3.1. Field data for each site and layer in the Fort Cobb Reservoir watershed. *Vegetation Height* refers to the height above the thalweg that vegetation is present. Soil layers where no JETs were completed report the selected representative monitored bank layer. Note that soil layers are listed in order from highest to lowest elevation and bank layers are labeled using the *site name - soil layer #* format used in Figure 3.2.

Bank Layer	Total Bank Height (m)	Vegetation Height (m)	Bed Slope ($m\ m^{-1}$)	Layer Thickness (m)	Soil Type	JETs[b] Completed	Average τ_c[c] (Pa)	Average k_d[c] ($cm^3\ N^{-1}\ s^{-1}$)	Average Bulk Density ($kg\ m^{-3}$)	Average b_0[d] ($g\ m^{-1}\ s^{-1}\ N^{-0.5}$)	Average b_1[d] (Pa)
FM1-1	2.07	2.07	0.003	1.47	Loamy Sand	2	0.055	34.65	1.45	75.79	3.46
FM1-2				0.60	FM2-2	0	FM2-2	FM2-4	FM2-4	FM2-2	FM2-2
FM2-1	4.34	2.09	0.004	1.13	Sandy Loam	2	0.14	17.8	1.75	68.21	10.81
FM2-2				1.12	Sandy Clay Loam	24	3.81	2.9	1.44	37.97	54.97
FM2-3				1.22	FM2-1	0	FM2-1	FM2-1	FM2-1	FM2-1	FM2-1
FM2-4				0.87	FM2-2	0	FM2-2	FM2-2	FM2-2	FM2-2	FM2-2
FM3-1	3.89	3.89	0.002	3.89	Loamy Sand	3	0.037	34.82	1.54	142.13	4.04
FM4-1	4.16	4.16	0.002	4.16	Sand	0	FM3-1	FM3-1	1.32	FM3-1	FM3-1
FM5-1	5.29	5.29	0.002	2.00	Sandy Loam	2	0.011	86.5	1.35	129.98	4.57
FM5-2				1.00	Clay Loam	2	0.225	5.36	1.38	44.41	13.28
FM5-3				1.25	FM5-1	0	FM5-1	FM5-1	FM5-1	FM5-1	FM5-1
FM5-4				1.04	FM5-2	0	FM5-2	FM5-2	FM5-2	FM5-2	FM5-2
WC1-1	3.35	3.35	0.007	3.35	Sandy Loam	2	0.0665	74.54	1.35	318.04	3.20
WC2-1	4.66	4.66	0.004	3.00	Loamy Sand	2	0.085	39.85	1.21	357.31	4.19
WC2-2[a]				1.66	Sandy Loam	3	2.637	1.72	1.35	29.78	3.25
WC3-1	4.57	3.07	0.002	3.00	Sandy Loam	2	0.0265	120.76	1.52	333.62	2.67
WC3-2				0.25	Loam	2	0.502	5.465	1.41	32.55	13.07
WC3-3				1.32	WC4-1	0	WC4-1	WC4-1	WC4-1	WC4-1	WC4-1

[a] Layer WC2-2 parameters were measured on a similar soil at a location just downstream as site conditions did not permit accurate JET measurements.
[b] JET = Jet Erosion Test
[c] τ_c and k_d are JET measured critical shear stress and erodibility coefficient, respectively, of the excess shear stress equation (Partheniades, 1965)
[d] b_0 and b_1 are JET measured parameters of the Wilson model (Wilson, 1993a)

on each bank layer at most of the eight sites. JETs were unable to be conducted on some of the layers due to the soil being too saturated. These data were analyzed to estimate τ_c and k_d using the Blaisdell's solution (Blaisdell et al., 1981) and b_0 and b_1 using methods described by Al-Madhhachi et al. (2013b). Soil samples were collected for each JET and analyzed for bulk density and soil texture (Table 3.1).

3.3.3 Aerial Imagery Analysis

As streams in the Fort Cobb Reservoir Watershed experience significant episodic retreat, aerial imagery was used to estimate bank retreat along Fivemile and Willow Creeks. Aerial images allow for a long term analysis of an entire watershed and specific sites within the watershed when field measurements are not available. Although aerial imagery may not be as accurate as field measurements, a major advantage exists in analyzing larger areas of interest with less time and costs. Aerial images of 1 m resolution of Caddo, Washita, and Custer Counties for 2003, 2008, and 2013 were obtained from the National Agricultural Imagery Program (NAIP). Each image was georeferenced in ArcMap (v10.2) and then used to estimate 10 year lateral bank retreat at each of the sites along Fivemile and Willow Creeks.

To estimate lateral retreat at each site, the critical streambank was digitized for the 2003 and 2013 images. The average distance between the polylines was then calculated and recorded as the estimated 10 year lateral bank retreat. For FM3, the 2013 image had dense vegetation cover which made identifying the streambank difficult. For this site, the 2008 image was used and retreat was estimated the same way. The retreat was then extrapolated to estimate the 10 year retreat rate. Site FM5 had dense vegetation cover for all images, thus the closest visible streambank was used to estimate retreat at the site.

3.3.4 Model Setup and Calibration

Several parameters were necessary to model the processes driving and resisting erosion at the eight monitoring sites. Default parameters, based on soil texture, for the soil strength parameters *c'* and ϕ' were used based on Simon et al. (2011). Effective cohesion of 2.4 kPa and 8.2 kPa were used for the sand to sandy loam and higher clay content layers, respectively. Note that typically *in situ* measurements of *c'* and ϕ' were preferred over default parameters. The Borehole Shear Test (BST, Handy Geotechnical Instruments, Inc., Madrid, IA) is an instrument used to measure soil strength parameters *in situ*. The texture of the soils and water table level in the Ft. Cobb Reservoir Watershed provided unreliable data from multiple BSTs, and thus defaults were deemed appropriate. Averages of the excess shear stress erodibility parameters, τ_c and k_d, and Wilson model parameters, b_0 and b_1, were calculated for each soil layer from all available JETs completed (Table 3.1).

A daily-average stream-flow hydrograph from a 2003-2013 calibrated Soil and Water Assessment Tool (SWAT) model for the watershed was used (Neitsch et al., 2011). Because fluvial erosion is sensitive to peak flows, for each site the daily average stream flow hydrograph was converted to an hourly triangular hydrograph. The hourly hydrograph's time to peak was set at nine hours based on the SCS triangular unit hydrograph (SCS, 1972) and started and ended at base flow. A base flow for each site was determined from the original flow hydrograph. Average daily flows less than the calculated base flow were set as the average flow in the generated hourly hydrograph. BSTEM required a stage hydrograph as opposed to the available SWAT generated flow hydrograph. Using the irregular channel module of the software program FlowMaster v8i (FlowMaster, 2009), flow stages were calculated for several flow rates for each site cross section with a range of Manning's *n* from 0.010 to 0.025 at an interval of 0.005. Rating curves of the generated flow-stage relationship for each of the sites were developed. A power equation was solved for using the regression tool of SigmaPlot 12.5 (SigmaPlot, 2013):

$$h(Q) = aQ^b \tag{3.3}$$

where Q is the flow (cms), h is the stage (m), and a and b are coefficients. The curves fit the data with coefficients of determination, R^2, greater than 0.96 and normalized objective function, NOF, less than 0.12 for all data sets (Table 3.2). The hourly flow hydrograph was then converted to an hourly stage hydrograph for each site and Manning's n combination using the power relationship. If an instantaneous or near instantaneous stage monitoring gauge was in place at a particular monitoring site, these data were preferred for a BSTEM simulation to reduce uncertainty. For this study, no such gauge was present at the selected monitoring sites.

Table 3.2. Coefficients, *a* and *b*, and curve fit statistics, R^2 and NOF, for the flow-stage relationship (equation 3.3) for each monitoring site in the Fort Cobb Reservoir watershed.

Monitoring Site	a[b]	b[b]	R^2	NOF[a]
FM1[c]	0.631	0.314	0.96	0.12
FM2	0.347	0.321	0.99	0.03
FM3	0.488	0.369	0.99	0.01
FM4	0.250	0.492	0.99	0.01
FM5	0.307	0.469	0.99	0.02
WC1	0.203	0.436	0.99	0.04
WC2	0.311	0.483	0.99	0.03
WC3	0.339	0.465	0.99	0.02

[a] Normalized Objective Function, $NOF = \frac{\sqrt{\frac{\sum_{i=1}^{N}(x_i - y_i)^2}{N}}}{X_a}$ where x_i and y_i are the observed data and prediction from fitted model, respectively, N is the number of observations, and X_a is the mean of the observed data. Note that smaller NOF values correspond to better fits of the model to observed data.

[b] Flow-stage relationship: $h(Q) = aQ^b$ where Q is the flow (cms), h is the stage (m), and a and b are coefficients.

[c] FM1-FM5 and WC1-WC3 are monitoring sites along Fivemile Creek and Willow Creek in the Fort Cobb Reservoir watershed, respectively

In order to determine if the Wilson model or excess shear stress equation was more appropriate for long term BSTEM simulations, a simulation was conducted using uncalibrated parameters for both models for all sites. All other parameters were kept constant and the predicted cross sections were compared.

Calibration was conducted for all sites and from this point forward, only excess shear stress parameters are discussed, as adjustment techniques already have been suggested in the literature (Daly et al., 2015). The main focus of the calibration process was on the adjustment of the erodibility parameters, τ_c and k_d, and effective cohesion, c', to account for the effects of vegetation, since roots enhance the mechanical shear strength of soils (Simon and Collison, 2002). Furthermore, added cohesion to soil due to vegetation has been linked to stream restoration in several previous studies (Abernethy and Rutherfurd, 1998; Shields and Knight, 2004). Polvi et al. (2014) completed a comprehensive study estimating added cohesion due to vegetation on several soil types for 14 common riparian species. Using the results from this study, a maximum effective cohesion for the sandy or sandy loam soil layers and the higher clay content soil layers were set at 5 kPa and 10 kPa, respectively. Vegetation can also reduce bank retreat by reducing the τ due to fluvial forces on the bank face (Gurnell, 2014). However, little quantitative information was known on the effect of vegetative protection on applied τ.

Previous studies suggested a method for adjusting τ_c and k_d parameters based on increases in applied τ due to secondary flows in a meander bend (Langendoen and Simon, 2008; Langendoen and Simon, 2009; Rousselot, 2009). Daly et al. (2015) reported that several other factors in addition to secondary meander bend flows that are not easily separable influence fluvial resistance to erosion including spatial and temporal changes in wetting and drying cycles, presence of vegetation, and moisture content. Therefore, a dimensionless adjustment factor, α, was used to modify equation 3.1 in order to account for several factors, including vegetation cover. The modified equation simplifies the hydraulics so that parameters, τ_c and k_d, can easily be adjusted in model calibration:

$$\varepsilon_r = k_d(\alpha\tau - \tau_c) = \alpha k_d(\tau - \frac{\tau_c}{\alpha}) \tag{3.4}$$

where α is directly proportional to k_d and indirectly proportional to τ_c, which produces a decreased k_d and increased τ_c when applied τ is decreased (i.e., α is less than one). BSTEM simulations were performed for each site with the various stage hydrographs corresponding to the range of Manning's *n* and with both default and vegetation adjusted effective cohesion, *c'*, on the soil layers covered with vegetation. Finally, various α values, ranging from 0.01 to 0.99 at an interval of 0.01, were used on both the default and added effective cohesion simulations on the vegetation layers. The model with parameters that closest matched the known bank retreat, derived from aerial imagery, was chosen as the calibrated model for each site. Results of the calibration are presented in Table 3.3.

Table 3.3. Comparison of known retreat from 2003-2013 derived from aerial imagery analysis to BSTEM calibrated model retreat along with parameter adjustments due to vegetation, *α* and *c'*, and uncertainty in flow to stage calculations, Manning's *n*.

Monitoring Site	Aerial Retreat (m)	BSTEM Retreat (m)	α	c'	Manning's *n*
FM1	0.0	0.0	0.01	Default	0.010
FM2	5.0	6.7	0.18	Default	0.010
FM3	12.0[a]	15.6	0.04	Adjusted	0.010
FM4	0.0	0.0	0.05	Adjusted	0.010
FM5	11.3[b]	11.6	0.08	Adjusted	0.010
WC1	0.0	2.0	0.02	Adjusted	0.010
WC2	0.0	0.0	0.20	Default	0.010
WC3	8.6	3.2	0.01	Adjusted	0.010

[a] Extrapolated from 2003 & 2008 images
[b]Retreat from near-by bank due to thick vegetation

3.3.5 Sediment Load Reductions from Modeling Stabilization Practices

Three common stabilization practices were modeled on the sites that experienced retreat over the simulation period: FM2, FM3, FM5, and WC3. The first stabilization practice involved placing rock protection on the toe only, which will hence be referred to as toe riprap. The second stabilization practice involved vegetating and grading the entire bank face. Various gradation ratios were simulated for each site ranging from 3:1 to 4:1 at an increment of 0.5:1. The final

stabilization practice involved a combination of the first two methods: toe riprap and grading (3:1) and establishing vegetation on the portion of the bank above the toe.

Stabilization practices were modeled in BSTEM over the same simulation period as the calibration. If the stabilization practice involved changing the geometry of the channel, rating curves were created using the Manning's *n* determined from calibration. The hourly flow hydrograph was converted to a stage hydrograph using the rating curve generated power function in the same manner as in the calibration. Vegetation was modeled using the calibrated k_d, τ_c, and *c'* parameters. Note that this is a conservative estimate, as established riparian vegetation on stable slopes might have more of an effect on soil parameters than current, minimal vegetation. Riprap was sized for a 100 year return flow event at each of the four sites according to the factor of safety procedure developed at Colorado State University (Stevens et al., 1976). The 100 year flow for each site was determined by completing regional flood frequency analysis described in Dalrymple (1960) using data from four USGS gage stations in the watershed and USGS PeakFQ v7.1 (PeakFQ, 2014) software. Riprap d_{50} calculations were used to estimate τ_c using the Shields-Yalin diagram for incipient motion (Shields, 1936). The k_d was estimated according to Hanson and Simon's (2001) equation that relates k_d to τ_c:

$$k_d = 0.2{\tau_c}^{-0.5} \tag{3.5}$$

where k_d and τ_c are in units of $cm^3\ N^{-1}\ s^{-1}$ and Pa, respectively. Riprap design calculations are presented in Table 3.4. After each stabilization practice was modeled in BSTEM, eroded area for each soil layer was calculated. The area was multiplied by the bulk density of the layer (Table 3.1) to estimate a volume contributing to sediment loads per meter of bank for each layer. The volumes were summed for each site to estimate a total sediment load for the site.

Table 3.4. Riprap sizing (d_{50}) for a 100 year design flow (Q_{100}) along with corresponding BSTEM input parameters τ_c and k_d.

Monitoring Site	Q_{100} (cms)	Riprap d_{50} (cm)	τ_c (Pa)	k_d ($cm^3\ N^{-1}\ s^{-1}$)
FM2[a]	211	9.9	80	0.022
FM3	257	9.9	80	0.022
FM5	287	17.1	139	0.017
WC3	212	9.5	77	0.023

[a] FM2, FM3, and FM5 and WC3 are monitoring sites on Fivemile and Willow creeks, respectively, that experienced retreat over the 10 year period as calculated from historical aerial imagery.

3.3.6 Cost Analysis

Mean construction cost data from Means (2016) were used to estimate stabilization practices' costs at each of the monitoring sites where stabilization was modeled. Riprap costs were determined by calculating the volume of riprap necessary to cover the toe. Riprap depth was determined using the standard 1.5 d_{50} design calculation from Table 3.4. Riprap volume for a support trench at the bed of the channel was also calculated using a depth, d_s (cm), and width, d_w (cm), according to USGS and Federal Highway Administration design guide (Blodgett and McConaughy, 1986):

$$d_s = 6.5{d_{50}}^{-0.115} \tag{3.6}$$

$$d_w = 1.5d_s \tag{3.7}$$

where d_{50} (cm) is the median diameter of the riprap rocks designed for a 100 year design flow. Excavation costs for channel grading and riprap were estimated by calculating volume of sediment removed based on channel geometry and by choosing the appropriate excavation equipment. Vegetation costs were estimated by calculating the number of tree cuttings required to cover the surface of each bank with 10 tree cuttings per square meter of bank area used. Fescue seed, geotextile material, and surveying and engineering costs were also determined. Equipment

and vegetation spacing was kept consistent at each of the sites. Total costs were calculated on a per meter of bank restored basis.

3.4 Results and Discussion

3.4.1 Wilson Model and Excess Shear Stress Equation Model Performance

When parameters were held constant within BSTEM, except for the method of fluvial erosion prediction, the Wilson model retreat predictions matched observed data better than the traditional excess shear stress equation compared to observed data using uncalibrated average parameters for all sites. Retreat ranged from 0.0 m to 47.5 m over the ten year period for the Wilson model simulations (Figure 3.3 and 3.4). The pre-calibration excess shear stress equation simulations over predicted retreat for all sites. Most retreats were over 500 m (Figure 3.3). The extreme over prediction of retreat for the excess shear stress parameters is most likely due to the linear restraint of the equation, i.e., not accounting for nonlinear behavior at higher applied shear stresses. These results were similar to findings of Kanal et al. (2016) that when the Wilson model was used to predict fluvial erosion in BSTEM retreat for cohesive soils better matched actual retreat compared to the excess shear stress equation..

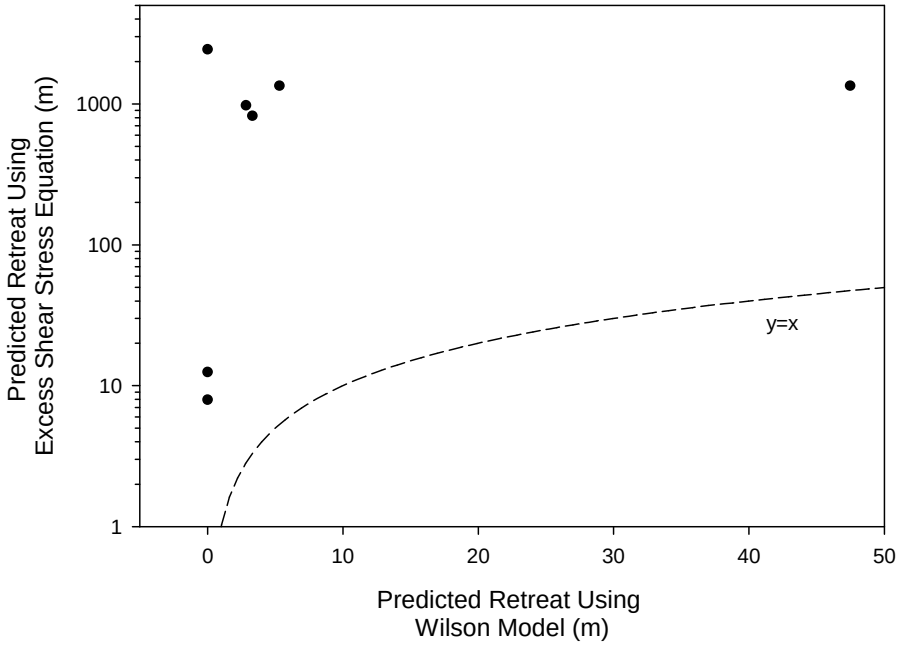

Figure 3.3. Comparison of BSTEM predicted retreat using uncalibrated parameters when two different methods were used for modeling fluvial erosion: The Wilson model and Excess Shear Stress Equation.

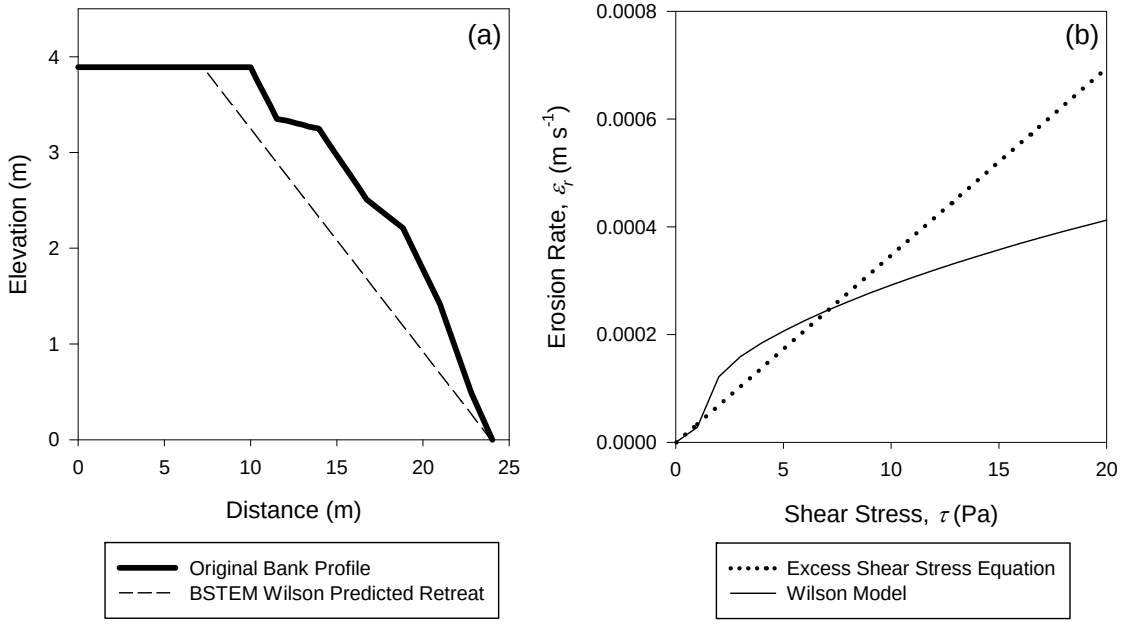

Figure 3.4. (a) BSTEM retreat predictions using uncalibrated Wilson model parameters for site FM3 (note that excess shear stress parameters predicted a retreat of approximately 1000 m at this site) and (b) detachment rates for a range of applied shear stress for the Wilson model and excess shear stress equation using parameters from Table 3.1.

3.4.2 Sediment Load Reductions from Modeling Stabilization Practices

Predictions for BSTEM of channel cross sections for the calibration and three stabilization practice simulations, as shown in Figure 3.5, were used to calculate eroded area over the 10 year simulation period. Using field measured bulk density of the soil layers multiplied by the eroded area of the bank soil layer, sediment loads were estimated for the baseline and stabilization practice simulations at each site (Figure 3.6a). Additionally, percentage reduction from the calibrated load was calculated for each stabilization practice (Figure 3.6b).

For all sites, stabilization practices reduced the eroded sediment load to the stream (Figure 3.6). Methods for modeling toe riprap in BSTEM appeared to be appropriate as no erosion occurred where riprap was placed in all of the simulations. For sites FM2, FM3, and WC3 toe riprap was enough to completely eliminate bank retreat. This result was similar to the findings of Simon et al. (2011). For most sites, vegetation and grading alone was less effective at reducing erosion than toe riprap. Interestingly, one site, FM5, did not match this trend (Figures 3.5 and 3.6). This result may inform engineers that if chosen, riprap should be placed higher up on the bank than in the simulation to be a more effective stabilization technique. In addition, this contradiction shows that techniques used to model vegetation on the bank face in process-based models needs to be further developed, with a particular focus on how vegetation reduces τ. In all simulations, toe riprap combined with vegetation and grading the upper portion of the bank contributed less sediment loads than riprap alone, as expected.

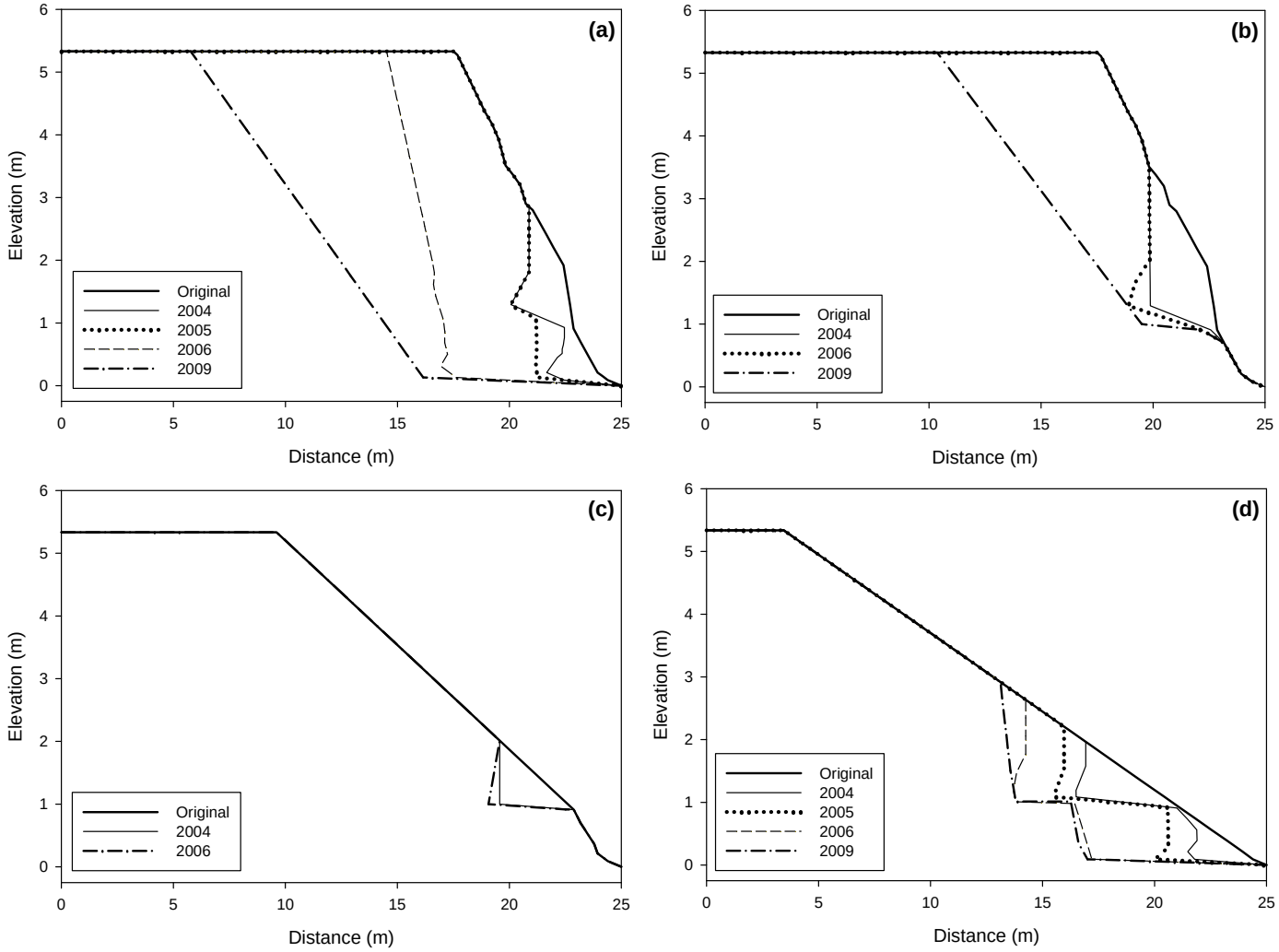

Figure 3.5. Example BSTEM predictions of modeled stabilization practices for stream reach FM5: (a) no practice or calibration; (b) toe riprap; (c) toe riprap with grading and vegetation above the toe; and (d) vegetation and grading only.

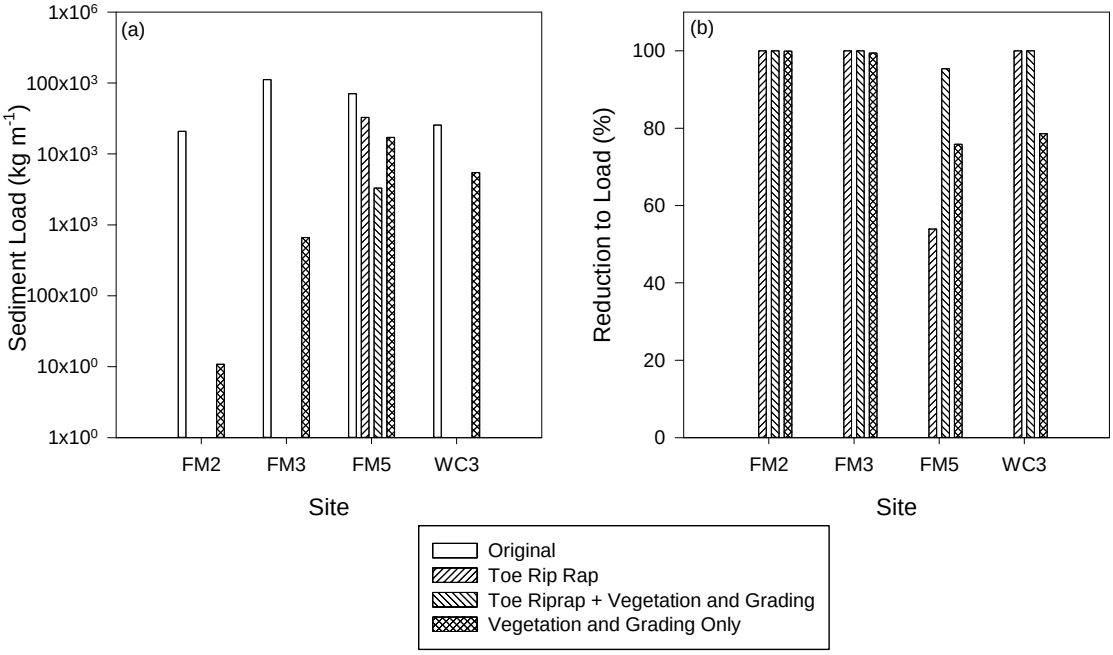

Figure 3.6. Load reductions of stabilization practices presented as (a) total load reduction to the stream in kg per meter of critical bank and (b) percent reduction of original load.

3.4.3 BSTEM Factor of Safety

In addition to final cross sections, BSTEM provides several predictions useful to engineers, including the Factor of Safety (FoS) at each time step of the hydrograph. This indicates when geotechnical failures occurred during the simulation and provides information on how stable the practice was overall in comparison to other practices or no practice. Graphics similar to those shown in Figure 3.7 were analyzed for all simulations. For all sites, stabilization practices with toe riprap had less geotechnical failures compared to the no-practice calibration simulation. Also, simulations with toe riprap, vegetation, and grading had higher average FoS over the simulation period compared to toe riprap alone. FoS for simulations involving vegetation were not as consistent. For some sites, vegetation and grading FoS never fell below one and were higher during the simulation period than stabilization practices with toe riprap. This indicated erosion was purely from fluvial forces on vegetation and grading simulations. Other sites had

vegetation and grading simulations with more bank failures, i.e., FoS below 1, compared to the no practice simulation (Figure 3.7). However, the sediment load was still less for the vegetation and grading. Also, predictions of cross sections over time at these sites (Figure 3.5) indicated that although BSTEM reported a FoS less than one, no change in the profile occurred. This does not fit expected results and reveals potential issues with BSTEM calculations and vegetation modeling methods.

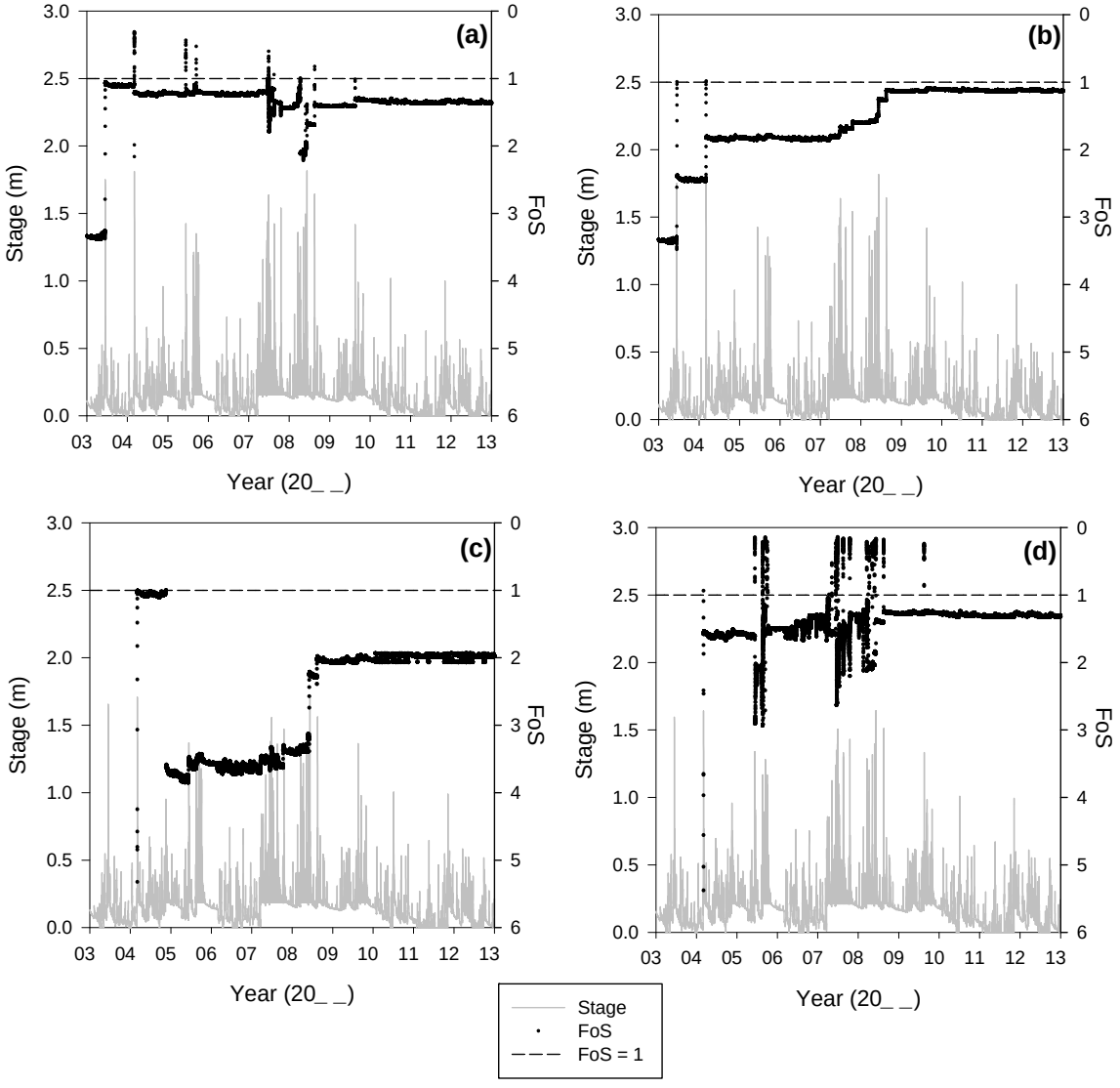

Figure 3.7. Example BSTEM FoS predictions for FM5 (site with more bank failures on vegetation and grading simulation than no practice) of modeled stabilization practices: (a) no practice/calibration; (b) toe riprap; (c) toe riprap with grading and vegetation above the toe; and (d) vegetation and grading only.

3.4.4 Insights from Calibration Alpha Factors

Only one site (FM1) was identified as having grasses covering the entire bank during field investigations. The corresponding α from calibration was 0.01. One site (FM3) was identified as mixed grasses and trees covering the entire bank with an α slightly higher at 0.04. Four sites (FM4, FM5, WC1, and WC2) were identified as forested covering the entire bank face. The α at these sites ranged from 0.01 to 0.20 with an average of 0.08. If the α was significantly related to vegetation cover, i.e., vegetation had the most impact on applied shear stresses, these results indicated that there may be a way to predict α based on vegetation cover. Figure 3.8 demonstrates this potential relationship. Previous studies using the α □revi□ □revious for□calibration used an α ranging from 1.0 to 3.7 for all sites to account for the increased shear stresses at a meander bend (Daly et al., 2015). This contradiction supports a research need for better calibration methods, especially to predict the impact of vegetation on fluvial erodibility parameters and shear stress distributions in order to better model vegetation in process-based models, such as BSTEM.

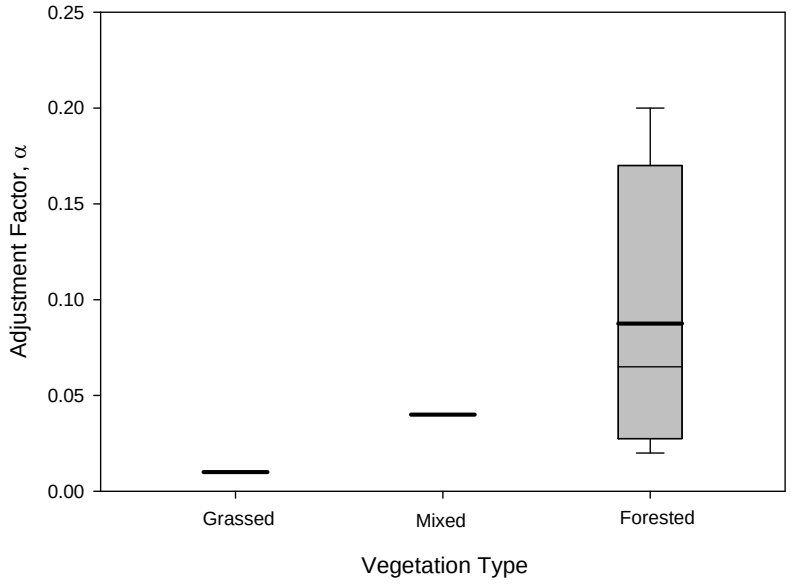

Figure 3.8. Box and whisker plots of calibration alpha factor results on sites FM1, FM3, FM4, FM5, WC1, and WC2 in the Fort Cobb Reservoir Watershed for different vegetation coverage type. Only calibration alpha factors from sites with vegetation covering the entire bank are shown.

3.4.5 Cost Analysis

Cost analysis showed expected results; per meter of bank restored, the least expensive practice was grading and vegetating the bank, followed by toe riprap, and the combination practice was the most expensive on average (Table 3.5). Site FM5 broke this trend as the amount of sediment needing to be excavated was considerably more and thus more expensive for the grading and vegetation only stabilization practice. Table 3.5 provides useful information to engineers when considering design alternatives. For example, at all sites grading and vegetation was the design that achieved the most reduction per dollar spent. However, if cost is the most important design consideration, the table provides information on which stabilization practice should be used at each site based on the lowest cost per meter of bank. If cost is not the most important factor, the table can be used to determine which stabilization practice most reduced sediment loads. Furthermore, at several sites there were multiple stabilization practices that reduced similar amounts of sediment (FM2, FM3, WC3). In this case, the table can be used to determine the least expensive option when sediment load reductions are similar.

Table 3.5. Ten-year sediment load reductions, cost of stabilization practice, and sediment load reduction per dollar per meter of streambank and respective average and standard deviation.

Stabilization Practice	Monitoring Site	Sediment Load Reduction (kg m^{-1} x10^4)	Cost per m of bank ($ m^{-1})	Reduction per dollar (kg $\$^{-1}$)
Toe Riprap	FM2	2.1	326	64
	FM3	11.2	337	332
	FM5	3.8	227	169
	WC4	2.6	240	106
	Average (±σ[a])	*4.9 (4.2)*	*283 (57)*	*168 (118)*
Toe Riprap + Vegetation and Grading	FM2	2.1	456	46
	FM3	11.2	381	294
	FM5	6.8	407	166
	WC4	2.6	327	78
	Average (± σ)	*5.7 (4.3)*	*393 (54)*	*146 (111)*
Grading and Vegetation	FM2	2.1	206	101
	FM3	11.1	90	1241
	FM5	5.4	270	199
	WC4	2.0	175	115
	Average (± σ)	*5.2 (4.3)*	*185 (75)*	*414 (553)*

[a] σ is the standard deviation

3.5 Conclusions

The process-based method was successful at predicting sediment loads and overall stability of various stabilization practices at the site scale. The practices included rock toe protection, vegetation and grading only, and a combination rock toe protection, grading, and vegetation, which reduced predicted loads by 54% to 100%, 76% to 99%, and 95% to 100%, respectively. Extensive calibration was needed to predict a reasonable retreat at all sites. In order for process-based models to continue be useful to the stream restoration community, reasonable sediment loads should be able to be predicted with little calibration required. This study highlights several areas where future research is necessary for such advancements of process-based models. For instance, when the Wilson model was used to predict fluvial erosion, as compared to the traditional excess shear stress equation approach, the Wilson model was better at predicting long term retreat. This is most likely due to the nonlinear behavior of cohesive soil

detachment as shown in previous studies and further supports the use of the mechanistic, nonlinear model for long-term retreat modeling within BSTEM. However, no adjustment method is available for the Wilson model parameters and therefore the Wilson model cannot be calibrated or used to model stabilization practices at this point in time. Additionally, future work is needed to improve methods for modeling the hydraulic effects of vegetation, whether that is improving the alpha factor method or implementation of an alternative method, such as integrating BSTEM with two-dimensional flow models. Finally, results show the usefulness of combining cost estimates with sediment load estimates. Cost estimates can be difficult to obtain, with little available public data. However, a tool to estimate costs for various stream restoration designs would be highly beneficial to land owners that are considering implementation of various stabilization practices.

3.6 Acknowledgements

The author wishes to acknowledge the financial support of the Buchanan Family Trust through the Buchanan Endowed Chair and the Oklahoma Agricultural Experiment Station at Oklahoma State University. This project was also supported by National Integrated Water Quality Program Project Grant no. 2013-51130-21484 from the USDA National Institute of Food and Agriculture. In addition, this research would not have been possible without the support Dr. Eddy Langendoen.

CHAPTER IV

SUMMARY AND CONCLUSIONS

4.1 Summary and Conclusions

The majority of sediment loads to surface waters often originate from streambanks causing water quality issues in streams and reservoirs. Streambank erosion is a complex cyclical process involving subaerial processes, fluvial erosion, seepage erosion, and geotechnical failures and is driven by several soil properties that themselves are temporally and spatially variable. Therefore, it can be challenging to model retreat. However, the ability to model streambank erosion has many important applications including the design of mitigation strategies for stream restoration practices. In order to account for the complicated nature of streambank retreat, process-based models, that incorporate the forces and moments driving and resisting erosion, are needed, however several questions still need to be answered in order for them to be a more useful and widely used tool in the stream restoration community. The purpose of this research was to answer some of these lingering fundamental questions including: (i) if nonlinear mechanistic detachment models are more appropriate than the traditional empirical approaches for quantifying sediment detachment due to fluvial forces and (ii) how typical restoration practices can be modeled in one of the most commonly used process-based bank stability and toe erosion model (BSTEM) to estimate sediment load reductions to lakes and reservoirs. Additionally, previous peer reviewed work completed utilizing BSTEM was analyzed to demonstrate current uses of the model to

suggest further research needs.

For the first objective, cohesive sediment detachment is typically modeled for channels using a linear excess shear stress approach. However, mechanistic nonlinear detachment models, such as the Wilson model, have recently been proposed in the literature. Questions exist as to the appropriateness of nonlinear relationships between applied shear stress and the erosion rate. Therefore, the objective was to test the appropriateness of linear and nonlinear detachment models for cohesive sediment detachment using two data sets: (i) rill erodibility studies across a limited range of applied shear stress (0.9 to 21.4 Pa) and (ii) hole erosion tests (HETs) across a wide range of applied shear stress (12.6 to 62.0 Pa).

Nearly 200 rill erodibility data sets of Elliot et al. (1990), consisting of erosion rate versus a small range of applied shear stress and 14 HET data sets from Wahl et al. (2008), consisting of erosion rate versus a larger range of applied shear stress, were analyzed. Parameters were derived for three detachment models: linear excess shear stress equation, nonlinear excess shear stress equation, and the Wilson model. The fit of each detachment model to the observed data were quantified using a coefficient of determination, R^2, and the normalized objective function (NOF).

The nonlinear, mechanistic detachment model was shown to be a more appropriate erosion rate model from previously published data on rill erodibility and hole erosion tests. The nonlinear excess shear stress model was also shown to adequately fit known erosion rate versus applied shear stress data for a wide range of applied shear stress. However, it is important to note that it can be problematic to estimate erodibility parameters for this model due to the use of three parameters instead of two like the Wilson model. Such results suggest the advantageous nature of the nonlinear, mechanistic detachment model and challenge existing theoretical approaches to modeling sediment detachment, but also identify the need for additional research to evaluate the

various detachment models for laboratory HETs and *in situ* JETs across a wider range of soil types.

For the second objective, the Fort Cobb Reservoir, located in southwest Oklahoma, provides public water supply, recreation, and wildlife habitat. Several conservation practices have been implemented in the watershed in recent years including adoption of no-tillage management, conversion of cropland to grassland, and cattle exclusion from streams. However, the watershed still does not meet water quality standards based on sediment. Streambank erosion is hypothesized to be one of the primary contributors of sediment loading to the reservoir. The objective was to use BSTEM to quantify sediment load reductions of three bank stabilization practices: toe riprap; vegetation and grading only; and a combination toe riprap, grading, and vegetation.

Eight monitoring sites were selected at locations along two tributaries to the Fort Cobb Reservoir. At each site, at least one cross sectional survey was taken using an auto level. Detailed notes were taken during surveying to record vegetation cover, the channel thalweg locations, and bank soil layers. An *in situ* submerged jet apparatus was used to quantify the resistance of the bank material to fluvial erosion and to derive parameters for the excess shear stress equation and Wilson model. The model was calibrated at each site using retreat measurements derived from aerial imagery over a ten year period. Next, three common stabilization practices were modeled on the sites that experienced retreat over the simulation period. The first stabilization practice involved placing toe riprap. The second stabilization practice involved vegetating and grading the entire bank face. The final stabilization practice involved a combination of the first two methods: toe riprap and grading and establishing vegetation on the portion of the bank above the toe. Sediment load reductions were determined and the cost of each stabilization practice was estimated using 2015 mean construction costs. Cost to load reduction ratios were then determined for each of the stabilization practices modeled.

Extensive calibration was necessary to predict reasonable retreats when the excess shear stress equation was used to quantify fluvial erodibility. In contrast, the uncalibrated Wilson model predicted a more reasonable retreat. However, no methods currently exist to adjust Wilson model parameters in order to model restoration practices. This highlights a need for future research in this area. Stabilization practices reduced sediment loads from 54% to 100%, 76% to 99%, and 95% to 100% for toe riprap, vegetation and grading only, and the combination of toe riprap and vegetation and grading, respectively. When reduction rates were compared with cost of practice to calculate a cost to load reduction rate, grading and vegetation achieved the most reduction per dollar spent for all sites. Analyzing calibration results and factor of safety predictions of the model revealed a need for better methods to adjust fluvial erosion parameters to account for reduction of applied shear stress due to vegetative cover.

The final objective was to highlight future research needs for BSTEM by discussing need to consider variability in geotechnical and fluvial soil parameters, what physical processes are still missing from the model, how the model can be used for stream restoration, and how the model has been improved in recent years. Twenty-one peer reviewed articles utilizing BSTEM were analyzed to demonstrate that even one of the most advanced models still has shortcomings and needs to continue to be developed so that process-based modeling can more easily be completed and more widely used by the stream restoration community.

Major issues with BSTEM that need to be addressed include accounting for spatial and temporal variability in geotechnical failure and fluvial erodibility parameters, incorporating seepage processes into the model, predicting the impact of riparian vegetation on applied shear stress, decreasing BSTEM run-time for long term modeling, increasing the usability of the model for stream restoration, and confirming the preliminary positive results of the integrated multidimensional models.

Results of this study are highly beneficial to the field of stream restoration and modeling cohesive erosion and detachment. Because of the huge financial and environmental costs

associated with stream restoration design failure, which unfortunately does happen with current restoration techniques, it is essential that the community involved with the design and implementation of stream restoration move towards incorporating process-based modeling into their work. Process-based modeling allows a complete analysis whether a design will be stable for a variety of conditions. This research supports a new theory for sediment detachment and is unique to any publications to date. The nonlinear, mechanistic detachment model was shown to be better suited to quantify erosion rates over a larger range of applied shear stress. Often times, detachment parameters are measured using devices that operate at low applied shear stress. When results are extrapolated to higher shear stresses observed in nature, such as during a storm event, it is critical that an appropriate detachment model be applied. Secondly, this research demonstrated that the Wilson model was more accurate than the excess shear stress equation when used in process-based models, such as BSTEM, to predict retreat. However, no procedures exist for modifying Wilson model parameters to simulate streambank stabilization; therefore, modelers are forced to use a less accurate model for the purpose of stream restoration design. Also this research highlights the need for researchers, engineers, and land owners to be able to easily estimate cost of a stabilization practice in order to determine what is best for their specific needs. Finally, this research will be extremely important moving forward with the development of process-based models, as several areas needing future research were explicitly highlighted.

REFERENCES

Abernethy, B., & Rutherfurd, I. D. (1998). Where along a river's length will vegetation most effectively stabilise stream banks? *Geomorphology, 23*(1), 55-75. doi:10.1016/s0169-555x(97)00089-5.

Al-Madhhachi, A. T., Fox, G. A., & Hanson, G. J. (2014a). Quantifying the erodibility of streambanks and hillslopes due to surface and subsurface forces. *Transactions of the ASABE, 57*(4), 1057-1069.

Al-Madhhachi, A. T., Fox, G. A., Hanson, G. J., Tyagi, A. K., & Bulut, R. (2014b). Mechanistic detachment rate model to predict soil erodibility due to fluvial and seepage forces. *Journal of Hydraulic Engineering, 140*(5). doi:10.1061/(ASCE)hy.1943-7900.0000836.

Al-Madhhachi, A. T., Hanson, G. J., Fox, G. A., Tyagi, A. K., & Bulut, R. (2013a). Measuring soil erodibility using a laboratory "mini" jet. *Transactions of the ASABE, 56*(3), 901-910.

Al-Madhhachi, A. T., Hanson, G. J., Fox, G. A., Tyagi, A. K., & Bulut, R. (2013b). Deriving parameters of a fundamental detachment model for cohesive soils from flume and jet erosion tests. *Transactions of the ASABE, 56*(2), 489-504.

Bernhardt, E. S., Palmer, M., Allan, J. D., Alexander, G., Barnas, K., Brooks, S., . . . Follstad-Shah, J. (2005). Synthesizing U. S. river restoration efforts. *Science, 308*(5722), 636-637.

Blaisdell, F. W., Anderson, C. L., & Hebaus, G. G. (1981). Ultimate dimensions of local scour. *Journal of the Hydraulics Division-ASCE, 107*(3), 327-337.

Blodgett, J. C., & McConaughy, C. E. (1986). *Rock riprap design for protection of stream channels near highway structures; Volume 2, Evaluation of riprap design procedures*.

BSTEM. (2016). *Bank Stability and Toe Erosion Model*. Ver. 5.4 Dynamic. Oxford, Mississippi. USDA Agricultural Research Service National Sedimentation Laboratory.

Canada Dept. of Fisheries and Oceans, Habitat and Enhancement Branch, and Quigley, J.T. (2004). Streambank protection with rip-rap: an evaluation on the effects on fish and fish habitat. Fisheries and Oceans Canada.

Cancienne, R. M., Fox, G. A., & Simon, A. (2008). Influence of seepage undercutting on the stability of root-reinforced streambanks. *Earth Surface Processes and Landforms, 33*(11), 1769-1786. doi:10.1002/esp.1657.

Curran, J. C., & Hession, W. C. (2013). Vegetative impacts on hydraulics and sediment processes across the fluvial system. *Journal of Hydrology, 505*, 364-376. doi:10.1016/j.jhydrol.2013.10.013.

Dalrymple, T. (1960). *Flood-frequency analyses, manual of hydrology: Part 3*.

Daly, E. R., Fox, G. A., Al-Madhhachi, A. T., & Miller, R. B. (2013). A scour depth approach for deriving erodibility parameters from jet erosion tests. *Transactions of the ASABE, 56*(6), 1343-1351.

Daly, E. R., Miller, R. B., & Fox, G. A. (2015). Modeling streambank erosion and failure along protected and unprotected composite streambanks. *Advances in Water Resources, 81*, 114-127. doi:10.1016/j.advwatres.2015.01.004.

Darby, S. E., Rinaldi, M., & Dapporto, S. (2007). Coupled simulations of fluvial erosion and mass wasting for cohesive river banks. *Journal of Geophysical Research-Earth Surface, 112*(F3), 15. doi:10.1029/2006jf000722.

Derrick, D. L., Pokrefke Jr, T. J., Boyd, M. B., Crutchfield, J. P., & Henderson, R. R. (1994). *Design and development of bendway weirs for the dogtooth bend reach, Mississippi River*.

Donat, M. (1995). Bioengineering techniques for streambank restoration. *A Review of Central European Practices. Vancouver, BC, Canada: Watershed Restoration Program. Ministry of Environment, Lands and Parks, and Ministry of Forests*.

Driels, M.R., and Shin, Y.S. (2004). Determining the number of iterations for Monte Carlo simulations of weapon effectiveness. No. NPS-MAE-04-005. Naval Postgraduate School Department of Mechanical and Astronautical Engineering. Monterey, CA.

Dunn, W. L., & Shultis, J. K. (2011). *Exploring monte carlo methods*: Elsevier.

Elliot, W. J. (1990). Compendium of soil erodibility data from WEPP cropland soil field erodibility experiments 1987 & 88.

Fischenich, C. (2001). *Stability thresholds for stream restoration materials*.

FlowMaster. (2009). *FlowMaster Hydraulic Calculator Software*. Ver. 8i. Santa Rosa, California. Bentley Systems, Inc.

Fox, G. A., Sabbagh, G. J., Chen, W. L., & Russell, M. H. (2006). Uncalibrated modelling of conservative tracer and pesticide leaching to groundwater: comparison of potential Tier II exposure assessment models. *Pest Management Science, 62*(6), 537-550. doi:10.1002/ps.1211.

Fox, G. A., & Wilson, G. V. (2010). The role of subsurface flow in hillslope and stream bank erosion: A review. *Soil Science Society of America Journal, 74*(3), 717-733. doi:10.2136/sssaj2009.0319.

Franklin, D. H., Steiner, J. L., Duke, S. E., Moriasi, D. N., & Starks, P. J. (2013). Spatial considerations in wet and dry periods for phosphorus in streams of the fort cobb

watershed, united states. *Journal of the American Water Resources Association, 49*(4), 908-922. doi:10.1111/jawr.12048.

Franti, T. G., Laflen, J. M., & Watson, D. A. (1999). Predicting soil detachment from high-discharge concentrated flow. *Transactions of the ASAE, 42*(2), 329-335.

Ghebreiyessus, Y. T., Gantzer, C. J., & Alberts, E. E. (1994). Soil-erosion by concentrated flow - shear-stress and bulk-density. *Transactions of the ASAE, 37*(6), 1791-1797.

Ghidey, F., & Alberts, E. E. (1997). Plant root effects on soil erodibility, splash detachment, soil strength, and aggregate stability. *Transactions of the ASAE, 40*(1), 129-135.

Gibson, S., Simon, A., Langendoen, E., Bankhead, N., & Shelley, J. (2015). *A physically-based channel-modeling framework integrating HEC-RAS sediment transport capabilities and the USDA-ARS bank-stability and toe-erosion model (BSTEM).* Paper presented at the Federal Interagency Sediment Conference, SedHyd Proceedings.

Grissinger, E. H., & Murphey, J. B. (1982). Present problem of stream channel instability in the bluff area of northern Mississippi. *Journal of the Mississippi Academy of Sciences (USA)*.

Gurnell, A. (2014). Plants as river system engineers. *Earth Surface Processes and Landforms, 39*(1), 4-25. doi:10.1002/esp.3397.

Hanson, G. J. (1990a). Surface erodibility of earthen channels at high stresses. I open channel testing. *Transactions of the ASAE, 33*(1), 127-131.

Hanson, G. J. (1990b). Surface Erodibility of Earthen Channels at High Stresses. II developing an In Situ Testing Device. *Transactions of the ASAE, 33*(1), 132-0137.

Hanson, G. J., & Cook, K. R. (1997). Development of excess shear stress parameters for circular jet testing, American Society of Agricultural Engineers Paper No. 97-2227. *American Society of Agricultural Engineers: St. Joseph*.

Hanson, G. J., & Cook, K. R. (2004). Apparatus, test procedures, and analytical methods to measure soil erodibility in situ. *Applied engineering in agriculture, 20*(4), 455.

Hanson, G. J., & Simon, A. (2001). Erodibility of cohesive streambeds in the loess area of the midwestern USA. *Hydrological processes, 15*(1), 23-38.

Heeren, D. M., Mittelstet, A. R., Fox, G. A., Storm, D. E., Al-Madhhachi, A. T., Midgley, T. L., . . . Tejral, R. D. (2012). Using rapid geomorphic assessments to assess streambank stability in oklahoma ozark streams. *Transactions of the ASABE, 55*(3), 957-968.

Hollick, M. (1976). Towards a routine test for the assessment of the critical tractive forces of cohesive soils. *Transactions of the ASAE, 19*(6), 1076-1081.

Julian, J. P., & Torres, R. (2006). Hydraulic erosion of cohesive riverbanks. *Geomorphology, 76*(1-2), 193-206. doi:10.1016/j.geomorph.2005.11.003.

Khanal, A., Klavon, K. R., Fox, G. A., & Daly, E. R. (2016). Comparison of linear and nonlinear models for cohesive sediment detachment: Rill erosion, hole erosion test, and streambank erosion studies. *Journal of Hydraulic Engineering*.

Khosronejad, A., Hill, C., Kang, S., & Sotiropoulos, F. (2013). Computational and experimental investigation of scour past laboratory models of stream restoration rock structures. *Advances in Water Resources, 54*, 191-207. doi:10.1016/j.advwatres.2013.01.008.

Knapen, A., Poesen, J., Govers, G., Gyssels, G., & Nachtergaele, J. (2007). Resistance of soils to concentrated flow erosion: A review. *Earth-Science Reviews, 80*(1-2), 75-109. doi:10.1016/j.earscirev.2006.08.001.

Knisel, W. G. (1980). CREAMS: a field scale model for Chemicals, Runoff, and Erosion from Agricultural Management Systems [USA]. *United States. Dept. of Agriculture. Conservation research report (USA).*

Konsoer, K. M., Rhoads, B. L., Langendoen, E. J., Best, J. L., Ursic, M. E., Abad, J. D., & Garcia, M. H. (2016). Spatial variability in bank resistance to erosion on a large meandering, mixed bedrock-alluvial river. *Geomorphology, 252*, 80-97. doi:10.1016/j.geomorph.2015.08.002.

Lai, Y. G., Thomas, R. E., Ozeren, Y., Simon, A., Greimann, B. P., & Wu, K. W. (2015). Modeling of multilayer cohesive bank erosion with a coupled bank stability and mobile-bed model. *Geomorphology, 243*, 116-129. doi:10.1016/j.geomorph.2014.07.017.

Langendoen, E. J., & Simon, A. (2008). Modeling the evolution of incised streams. II: Streambank erosion. *Journal of Hydraulic Engineering-ASCE, 134*(7), 905-915. doi:10.1061/(ASCE)0733-9429(2008)134:7(905).

Langendoen, E. J., & Simon, A. (2009). Closure to "Modeling the Evolution of Incised Streams. II: Streambank Erosion" by Eddy J. Langendoen and Andrew Simon. *Journal of Hydraulic Engineering-ASCE, 135*(12), 1107-1108.

Lavendel, B. (2002). The business of ecological restoration. *Ecological Restoration, 20*(3), 173-178.

Lindow, N., Fox, G. A., & Evans, R. O. (2009). Seepage erosion in layered stream bank material. *Earth Surface Processes and Landforms, 34*(12), 1693-1701. doi:10.1002/esp.1874.

Lohnes, R. A., & Handy, R. L. (1968). Slope angles in friable loess. *Journal of Geology, 76*(3), 247-258.

Lutenegger, A. J., & Hallberg, G. R. (1981). Borehole shear test in geotechnical investigations *Laboratory shear strength of soil*: ASTM International.

Lyle, W. M., & Smerdon, E. T. (1965). Relation of compaction and other soil properties to erosion resistance of soils. *Transactions of the ASAE, 8*(3), 419-0422.

Means, R. S. (2016). *Facilities construction cost data* (Vol. 31): RS Means Company.

Midgley, T. L., Fox, G. A., & Heeren, D. M. (2012). Evaluation of the bank stability and toe erosion model (BSTEM) for predicting lateral retreat on composite streambanks. *Geomorphology, 145*, 107-114. doi:10.1016/j.geomorph.2011.12.044.

Minitab. (2009) *Minitab Statistical Software*. Ver. 16. State College, Pennsylvania. Minitab, Inc.

Neitsch, S. L., Arnold, J. G., Kiniry, J. R., & Williams, J. R. (2011). *Soil and water assessment tool theoretical documentation version 2009*.

Odgaard, A. J., & Kennedy, J. F. (1983). River-bend bank protection by submerged vanes. *Journal of Hydraulic Engineering-ASCE, 109*(8), 1161-1173.

Parker, C., Simon, A., & Thorne, C. R. (2008). The effects of variability in bank material properties on riverbank stability: Goodwin Creek, Mississippi. *Geomorphology, 101*(4), 533-543. doi:10.1016/j.geomorph.2008.02.007.

Parker, D. B., Michel, T. G., & Smith, J. L. (1995). Compaction and water velocity effects on soil-erosion in shallow flow. *Journal of Irrigation and Drainage Engineering-ASCE, 121*(2), 170-178. doi:10.1061/(ASCE)0733-9437(1995)121:2(170).

Partheniades, E. (1965). Erosion and deposition of cohesive soils. *Journal of the Hydraulics Division, 91*(1), 105-139.

PeakFQ. (2014) *PeakFQ Flood Frequency Software*. Ver. 7.1. Reston, Virginia. U.S. Geological Survey.

Pollen, N., & Simon, A. (2005). Estimating the mechanical effects of riparian vegetation on stream bank stability using a fiber bundle model. *Water Resources Research, 41*(7), 11. doi:10.1029/2004wr003801.

Pollen-Bankhead, N., & Simon, A. (2009). Enhanced application of root-reinforcement algorithms for bank-stability modeling. *Earth Surface Processes and Landforms, 34*(4), 471-480. doi:10.1002/esp.1690.

Pollen-Bankhead, N., & Simon, A. (2010). Hydrologic and hydraulic effects of riparian root networks on streambank stability: Is mechanical root-reinforcement the whole story? *Geomorphology, 116*(3-4), 353-362. doi:10.1016/j.geomorph.2009.11.013.

Polvi, L. E., Wohl, E., & Merritt, D. M. (2014). Modeling the functional influence of vegetation type on streambank cohesion. *Earth Surface Processes and Landforms, 39*(9), 1245-1258. doi:10.1002/esp.3577.

Prosser, I. P., Dietrich, W. E., & Stevenson, J. (1995). Flow resistance and sediment transport by concentrated overland-flow in a grassland valley. *Geomorphology, 13*(1-4), 71-86. doi:10.1016/0169-555x(95)00020-6.

Purvis, R. A., and Fox, G. A. (2016). Streambank sediment loading rates at the watershed scale and the benefit of riparian protection. *Earth Surf. Process. Landforms, doi:* 10.1002/esp.3901.

Reid, D., & Church, M. (2015). Geomorphic and ecological eonsequences of riprap placement in river systems. *Journal of the American Water Resources Association, 51*(4), 1043-1059. doi:10.1111/jawr.12279.

Říha, J., & Jandora, J. (2015). Pressure conditions in the hole erosion test. *Canadian Geotechnical Journal, 52*(1), 114-119. doi:10.1139/cgj-2013-0474.

Rinaldi, M., & Darby, S. E. (2007). 9 Modelling river-bank-erosion processes and mass failure mechanisms: progress towards fully coupled simulations. *Developments in Earth Surface Processes, 11*, 213-239.

Rinaldi, M., & Nardi, L. (2013). Modeling interactions between riverbank hydrology and mass failures. *Journal of Hydrologic Engineering, 18*(10), 1231-1240. doi:10.1061/(ASCE)he.1943-5584.0000716.

Rousselot, P. (2009). Discussion of "Modeling the evolution of incised streams. II: streambank erosion" by Eddy J. Langendoen and Andrew Simon. *Journal of Hydraulic Engineering-ASCE, 135*(12), 1107-1107.

Shields, A. (1936). *Application of similarity principles and turbulence research to bed-load movement*.

Shields Jr, F. D., Copeland, R. R., Klingeman, P. C., Doyle, M. W., & Simon, A. (2003). Design for stream restoration. *Journal of Hydraulic Engineering, 129*(8), 575-584.

Shields Jr, F. D., & Knight, S. (2004). *Ten years after: stream habitat restoration project in retrospect.* Paper presented at the Proc., World Water & Environmental Resources Congress.

SigmaPlot. (2013). *SigmaPlot Statistical Software*. Ver. 12.5. San Jose, California. Systat Software, Inc.

Simon, A., & Collison, A. J. C. (2002). Quantifying the mechanical and hydrologic effects of riparian vegetation on streambank stability. *Earth Surface Processes and Landforms, 27*(5), 527-546. doi:10.1002/esp.325.

Simon, A., Curini, A., Darby, S. E., & Langendoen, E. J. (2000). Bank and near-bank processes in an incised channel. *Geomorphology, 35*(3-4), 193-217. doi:10.1016/s0169-555x(00)00036-2.

Simon, A., & Darby, S. E. (1999). The nature and significance of incised river channels. *Incised River Channels: Processes, Forms, Engineering and Management. John Wiley & Sons, Chichester*, 3-18.

Simon, A., & Klimetz, L. (2008). Relative magnitudes and sources of sediment in benchmark watersheds of the Conservation Effects Assessment Project. *Journal of Soil and Water Conservation, 63*(6), 504-522. doi:10.2489/jswc.63.6.504.

Simon, A., Larsen, M. C., & Hupp, C. R. (1990). The role of soil processes in determining mechanisms of slope failure and hillslope development in a humid-tropical forest eastern Puerto Rico. *Geomorphology, 3*(3), 263-286.

Simon, A., Pollen, N., & Langendoen, E. (2006). Influence of two woody riparian species on critical conditions for streambank stability: Upper Truckee River, California: Wiley Online Library.

Simon, A., Pollen-Bankhead, N., Mahacek, V., & Langendoen, E. (2009). Quantifying reductions of mass-failure frequency and sediment loadings from streambanks using toe protection and other means: Lake Tahoe, United States. *Journal of the American Water Resources Association, 45*(1), 170-186. doi:10.1111/j.1752-1688.2008.00268.x

Simon, A., Pollen-Bankhead, N., & Thomas, R. E. (2011). Development and application of a deterministic bank stability and toe erosion model for stream restoration. *Stream Restoration in Dynamic Fluvial Systems*, 453-474.

Simon, A., & Thomas, R. E. (2002). Processes and forms of an unstable alluvial system with resistant, cohesive streambeds. *Earth Surface Processes and Landforms, 27*(7), 699-718. doi:10.1002/esp.347.

Simon, A., Thomas, R. E., Curini, A., & Shields, F. D. (2002). Case study: Channel stability of the Missouri River, eastern Montana. *Journal of Hydraulic Engineering-ASCE, 128*(10), 880-890. doi:10.1061/(ASCE)0733-9429(2002)128:10(880).

Simon, A., Thomas, R. E., & Klimetz, L. (2010). *Comparison and experiences with field techniques to measure critical shear stress and erodibility of cohesive deposits.* Paper presented at the 2nd Joint Federal Interagency Conference, Las Vegas, NV.

Soil Conservation Service. (1972). "Hydrology," Sect. 4, Soil Conservation Service National Engineering Handbook. U.S. Department of Agriculture, Washington, D.C.

Stein, O. R., & Nett, D. D. (1997). Impinging jet calibration of excess shear sediment detachment parameters. *Transactions of the ASCE, 40*(6), 1573-1580.

Stevens, M. A., Lewis, G. L., & Simons, D. B. (1976). Safety factors for riprap protection. *Journal of the Hydraulics Division, 102*(5), 637-655.

Sutarto, T., Papanicolaou, A. N., Wilson, C. G., & Langendoen, E. J. (2014). Stability Analysis of Semicohesive Streambanks with CONCEPTS: Coupling Field and Laboratory Investigations to Quantify the Onset of Fluvial Erosion and Mass Failure. *Journal of Hydraulic Engineering, 140*(9), 19. doi:10.1061/(ASCE)hy.1943-7900.0000899

Utley, B., & Wynn, T. M. (2008). *Cohesive soil erosion: Theory and practice.* Paper presented at the World Environmental and Water Resources Congress.

Van Klaveren, R. W., & McCool, D. K. (1998). Erodibility and critical shear of a previously frozen soil. *Transactions of the ASAE, 41*(5), 1315-1321.

Vanliew, M. W., & Saxton, K. E. (1983). Slope steepness and incorporated residue effects on rill erosion. *Transactions of the ASAE, 26*(6), 1738-1743.

Wahl, T. L., Regazzoni, P.L., & Erdogan, Z. (2008). *Determining erosion indices of cohesive soils with the hole erosion test and jet erosion test*: US Department of Interior, Bureau of Reclamation, Technical Service Center.

Walling, D. E., Owens, P. N., & Leeks, G. J. L. (1998). The role of channel and floodplain storage in the suspended sediment budget of the River Ouse, Yorkshire, UK. *Geomorphology, 22*(3-4), 225-242. doi:10.1016/s0169-555x(97)00086-x.

Wan, C. F., & Fell, R. (2004). Laboratory tests on the rate of piping erosion of soils in embankment dams. *Geotechnical Testing Journal, 27*(3), 295-303.

Wilson, B. N. (1993a). Development of a fundamentally based detachment model. *Transactions of the ASAE, 36*(4), 1105-1114.

Wilson, B. (1993b). Evaluation of a fundamentally based detachment model. *Transactions of the ASAE, 36*(4), 1115-1122.

Wilson, G. V., Perketi, R. K., Fox, G. A., Dabney, S. M., Shields, F. D., & Cullum, R. F. (2007). Soil properties controlling seepage erosion contributions to streambank failure. *Earth Surface Processes and Landforms, 32*(3), 447-459. doi:10.1002/esp.1405.

Zhu, J. C., Gantzer, C. J., Anderson, S. H., Peyton, R. L., & Alberts, E. E. (2001). Comparison of concentrated-flow detachment equations for low shear stress. *Soil & Tillage Research, 61*(3-4), 203-212. doi:10.1016/s0167-1987(01)00207-0.

Zhu, J. C., Gantzer, C. J., Peyton, R. L., Alberts, E. E., & Anderson, S. H. (1995). Simulated small-channel bed scour and head cut erosion rates compared. *Soil Science Society of America Journal, 59*(1), 211-218.

APPENDICES

Monte Carlo Analysis: Fivemile Creek collected bank height (*BH*) data: (a) histogram and Weibull probability density function distribution plot and (b) probability plot (Minitab, 2009)

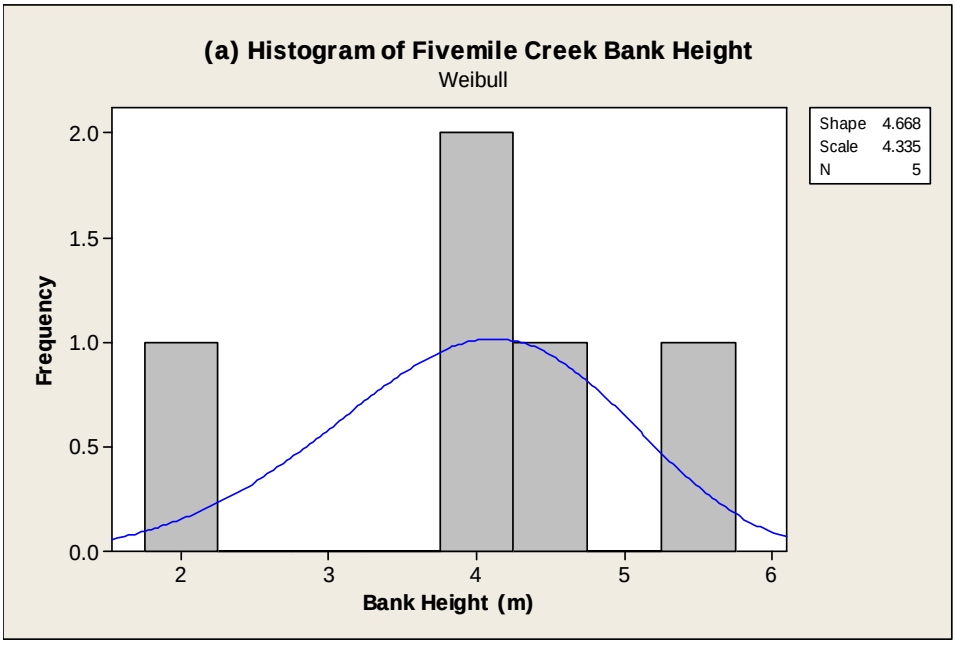

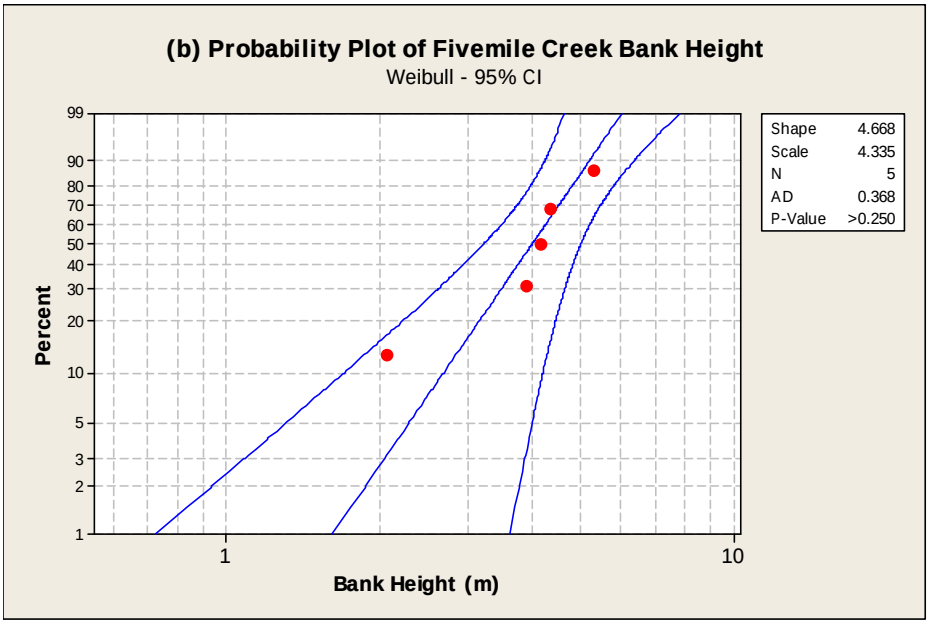
(b) Probability Plot of Fivemile Creek Bank Height
Weibull - 95% CI
Percent
99
90
80
70
60
50
40
30
20
10
5
3
2
1
1
10
Bank Height (m)
Shape 4.668
Scale 4.335
N 5
AD 0.368
P-Value >0.250

Monte Carlo Analysis: Willow Creek collected bank height (*BH*) data: (a) histogram and Gamma probability density function distribution plot and (b) probability plot (Minitab, 2009)

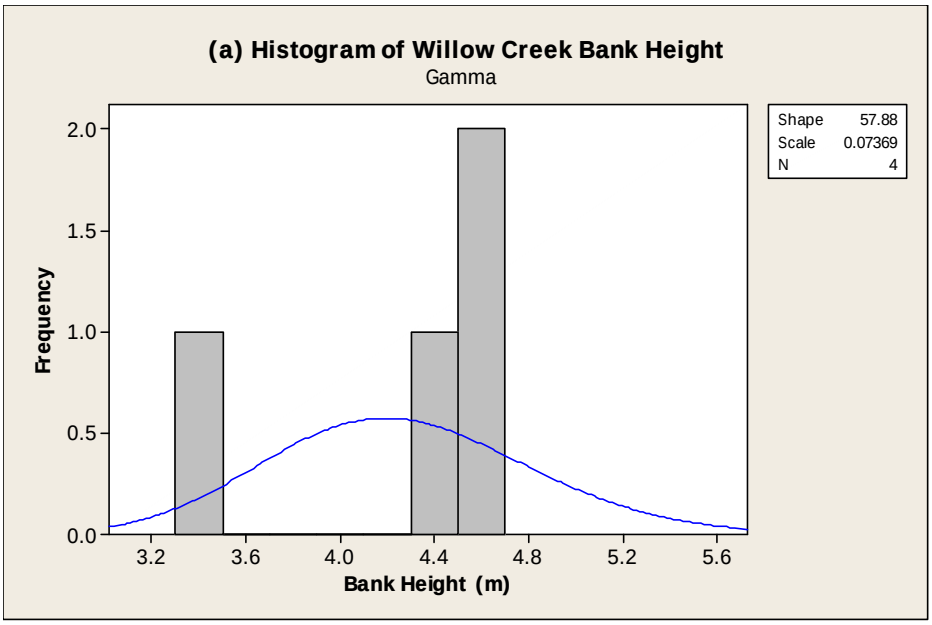

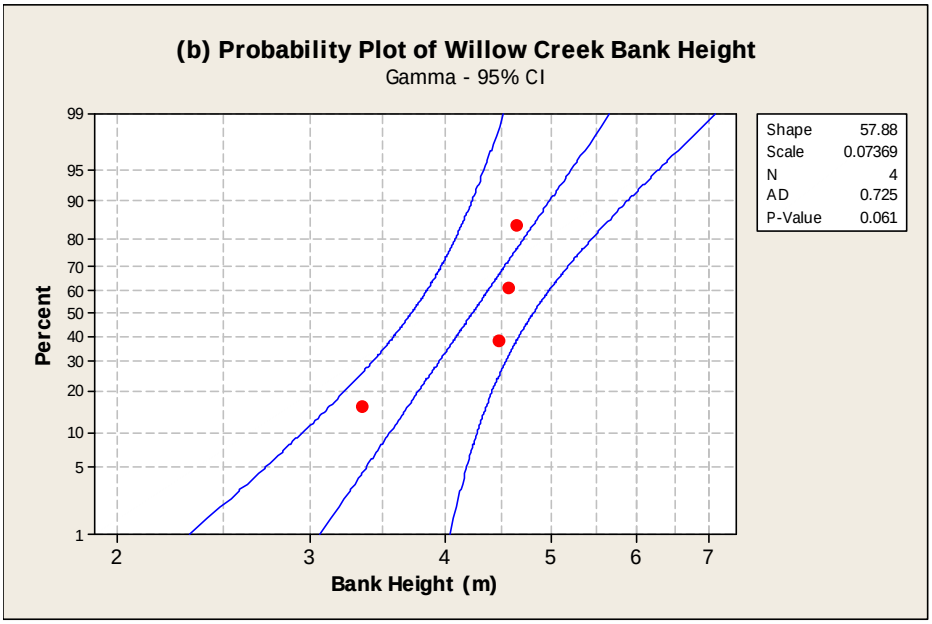

Monte Carlo Analysis: Fivemile Creek collected bulk density (ρ_b) data: (a) histogram and Loglogistic probability density function distribution plot and (b) probability plot (Minitab, 2009)

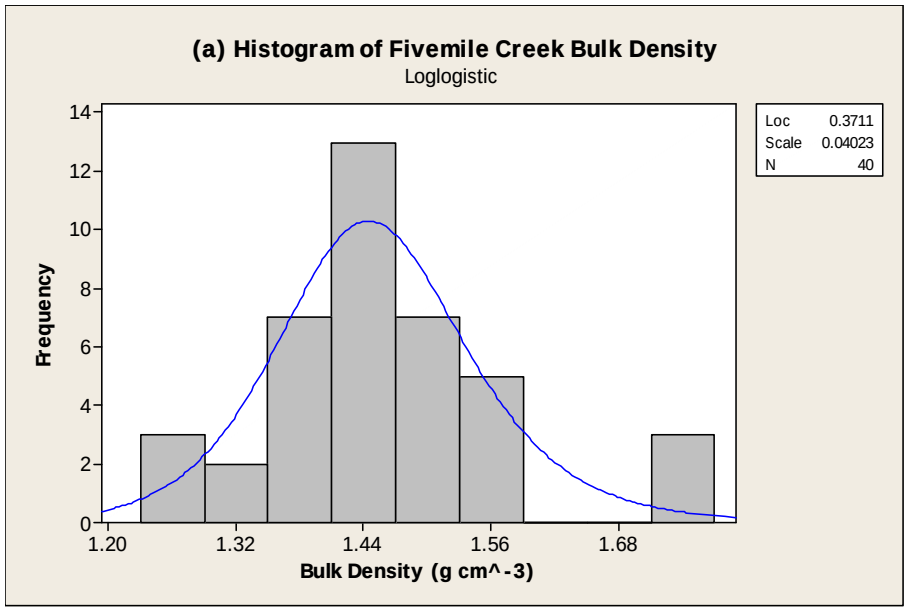

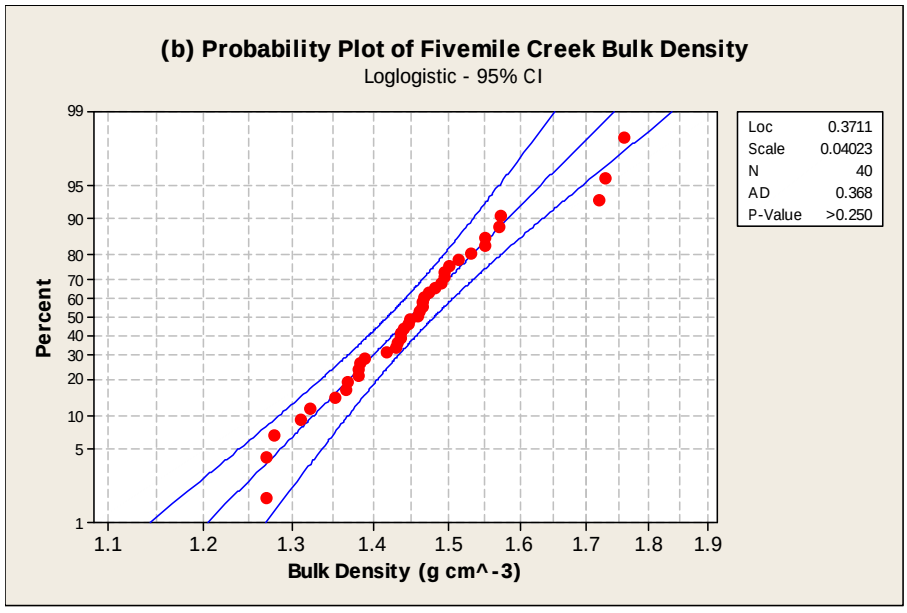

Monte Carlo Analysis: Willow Creek collected bulk density (ρ_b) data: (a) histogram and 3-parameter Weibull probability density function distribution plot and (b) probability plot (Minitab, 2009)

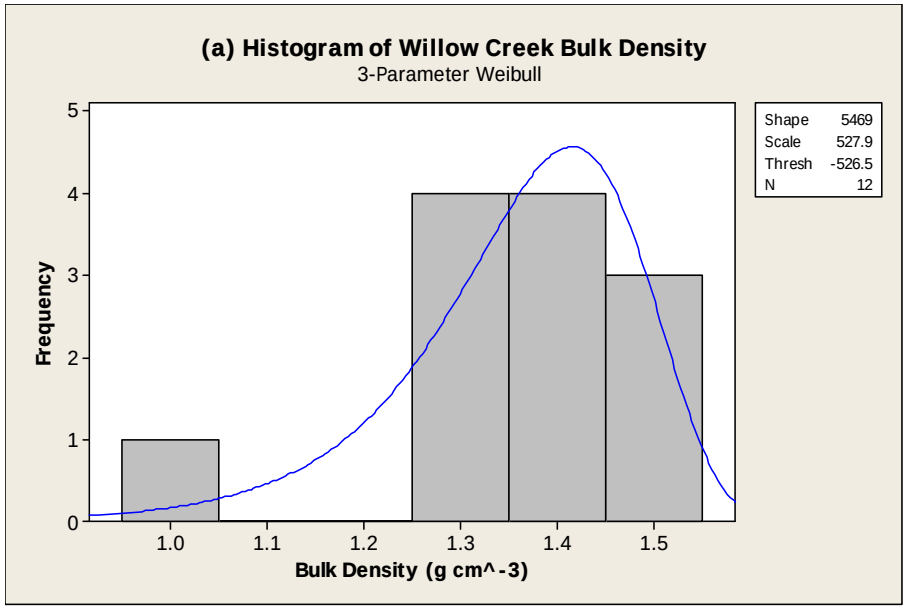

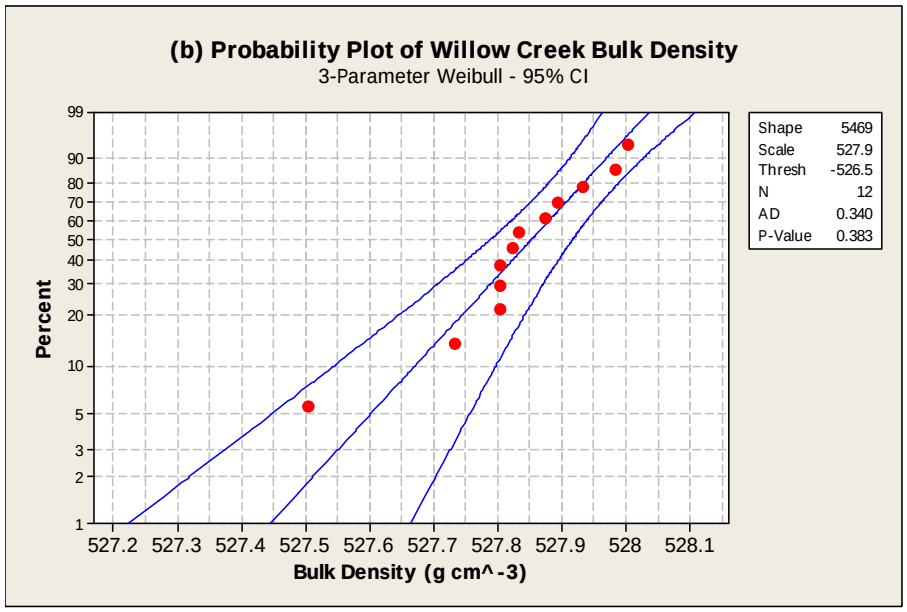

Monte Carlo Analysis: Fivemile Creek 10 year BSTEM retreat (L_{BSTEM}) data: (a) histogram (Minitab, 2009)

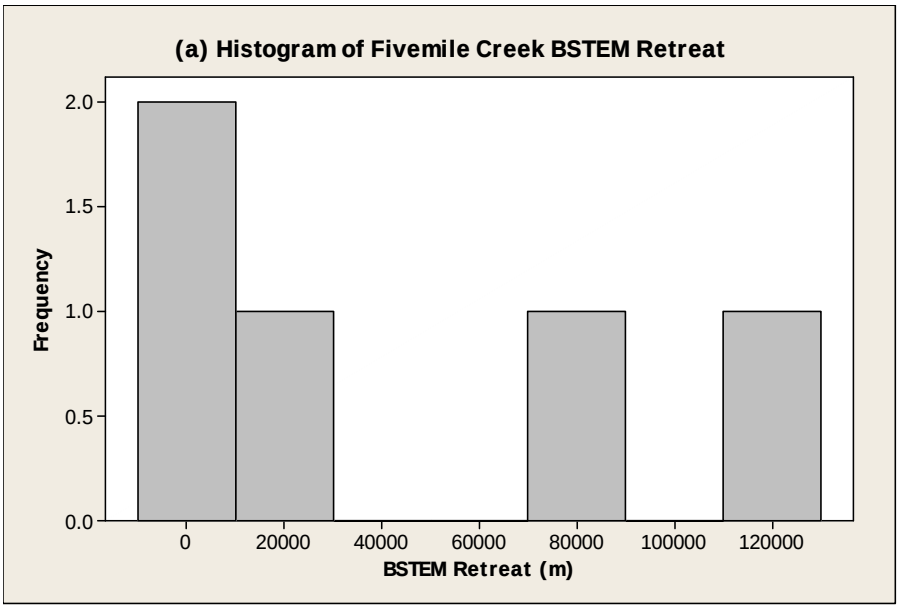

Monte Carlo Analysis: Willow Creek 10 year BSTEM retreat (L_{BSTEM}) data: (a) histogram (Minitab, 2009)

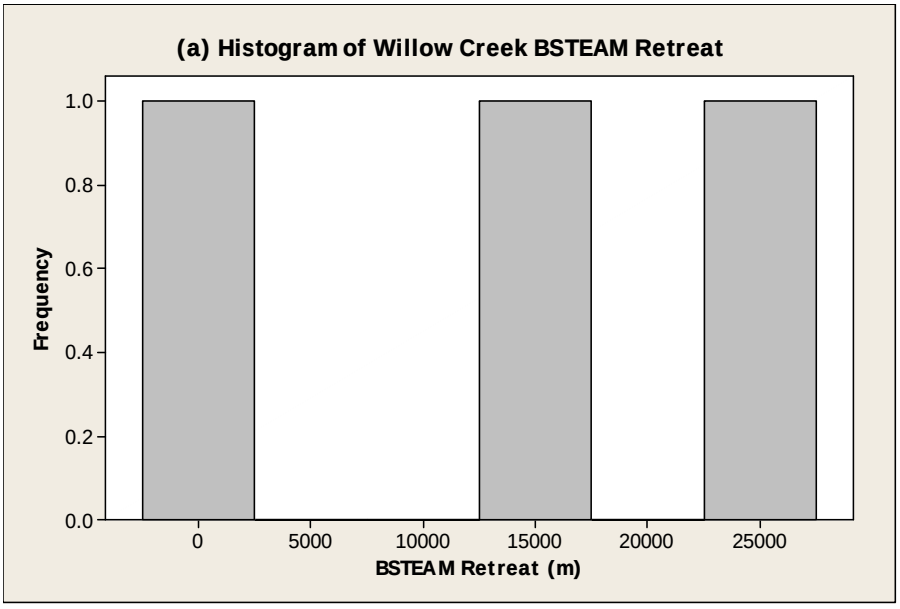

Monte Carlo Analysis: Histograms for percent reduction to load ($R_{\%}$) for each of the stabilization practices: (a) riprap toe only, (b) riprap toe + vegetation and grading, (c) vegetation and grading only

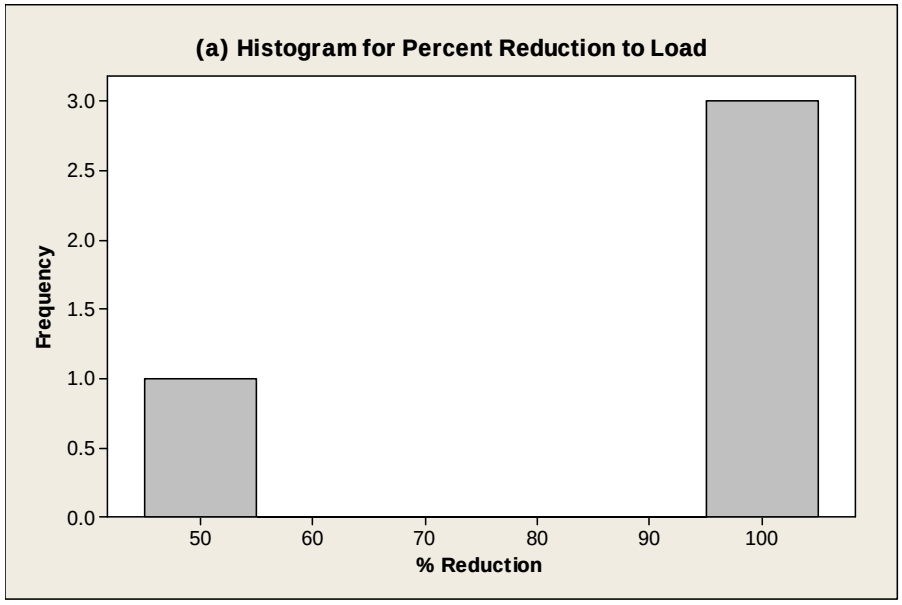

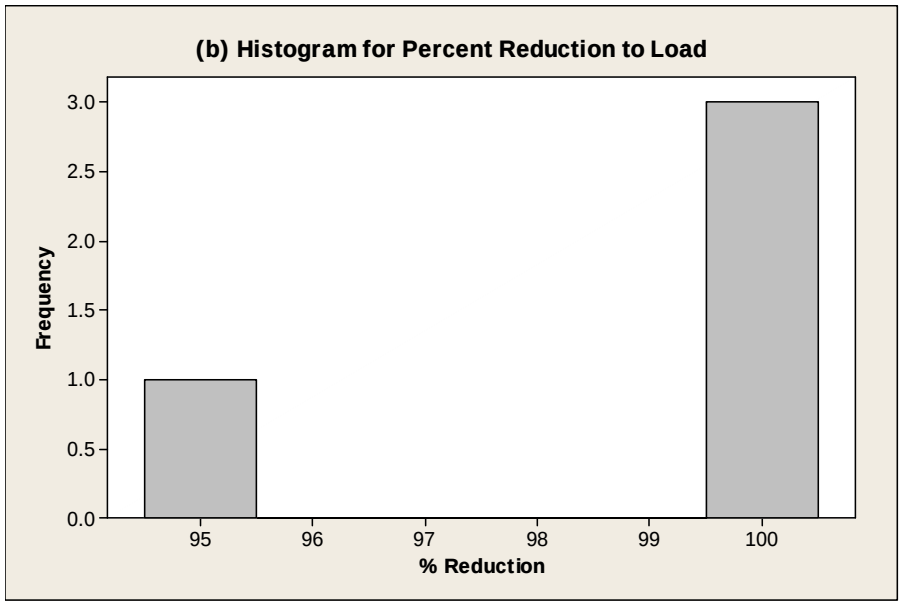

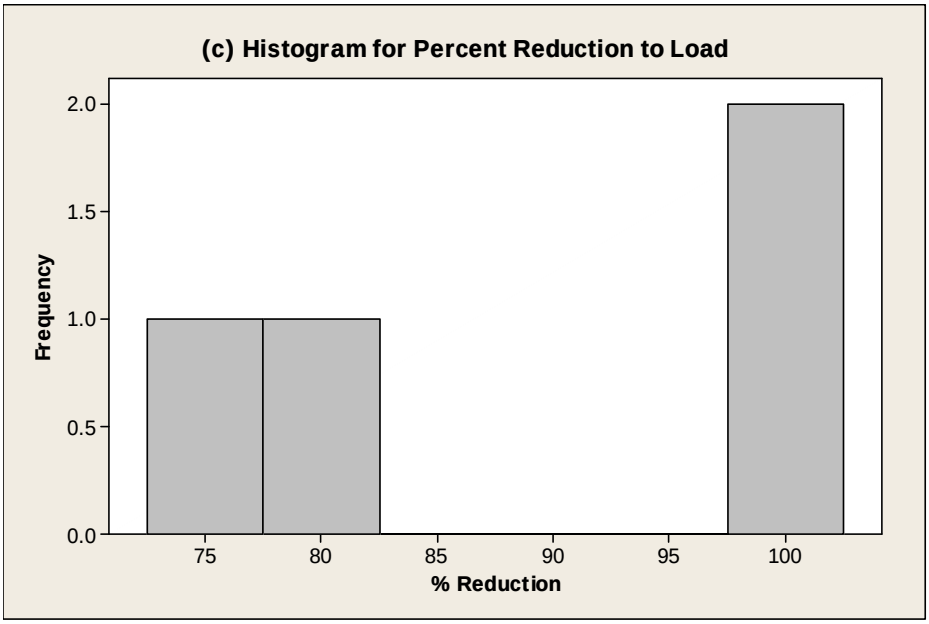
(c) Histogram for Percent Reduction to Load
Frequency
2.0
1.5
1.0
0.5
0.0
75
80
85
90
95
100
% Reduction

Flood Frequency Analysis: USGS gage station information used. Gage stations are located in the watershed.

Station Name	Station Number	Latitude	Longitude	Watershed Area A (mi2)	Years on Record
Cobb Creek Near Eakly	07325800	35.29055	98.59389	132.0	43
Lake Creek Near Sickles	07325840	35.39167	98.5175	19.1	9
Lake Creek Near Eakly	07325850	35.29083	98.52889	52.5	19
Willow Creek near Albert	07325860	35.23333	98.46583	28.2	16

Flood Frequency Analysis: PeakFQ calculated floods for return years 2, 5, 10, 25, 50, and 100 for each of the chosen USGS gage stations

	Floods for Various Return Years (cfs)					
Station Number	Q_2	Q_5	Q_{10}	Q_{25}	Q_{50}	Q_{100}
07325800	1888	4246	6473	10130	13520	17520
07325840	635.8	1223	1669	2273	2741	3218
07325850	892.7	2539	4300	7431	10500	14250
07325860	525	1811	3535	7335	11860	18390

Flood Frequency Analysis: Flood to index flood rations for each of chosen USGS gage stations and median rations for each return period

	USGS Station Number				
	07325800	07325840	07325850	07325860	Median
Q_{100}/Q_2	9.28	5.06	15.96	35.03	12.62
Q_{50}/Q_2	7.16	4.31	11.76	22.59	9.46
Q_{25}/Q_2	5.37	3.58	8.32	13.97	6.84
Q_{10}/Q_2	3.43	2.63	4.82	6.73	4.12
Q_5/Q_2	2.25	1.92	2.84	3.45	2.55
Q_2/Q_2	1	1	1	1	1

Flood Frequency Analysis: Regional Flood Curve

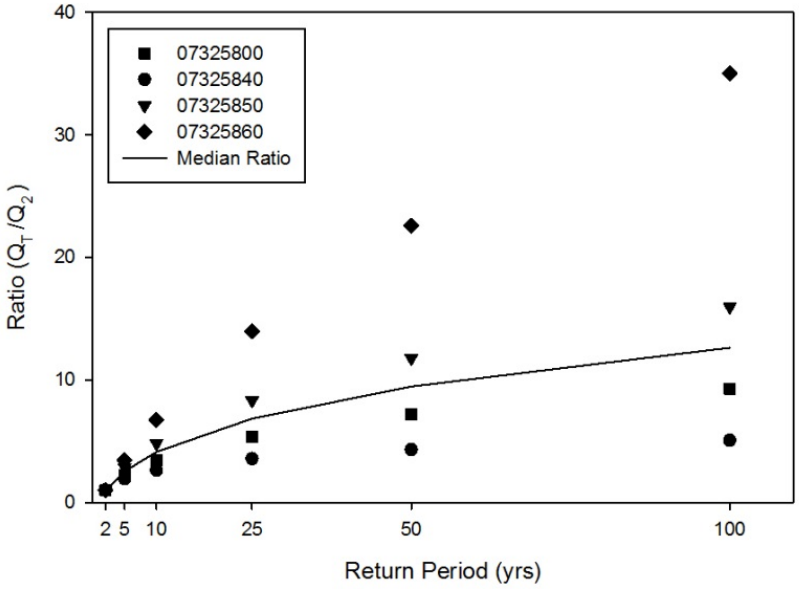

Flood Frequency Analysis: USGS gage station data of watershed area (*A*) vs PeakFQ determined index flood (Q_2) and determined linear fit equation. R^2 and NOF of fit equation were 0.98 and 0.11 respectively.

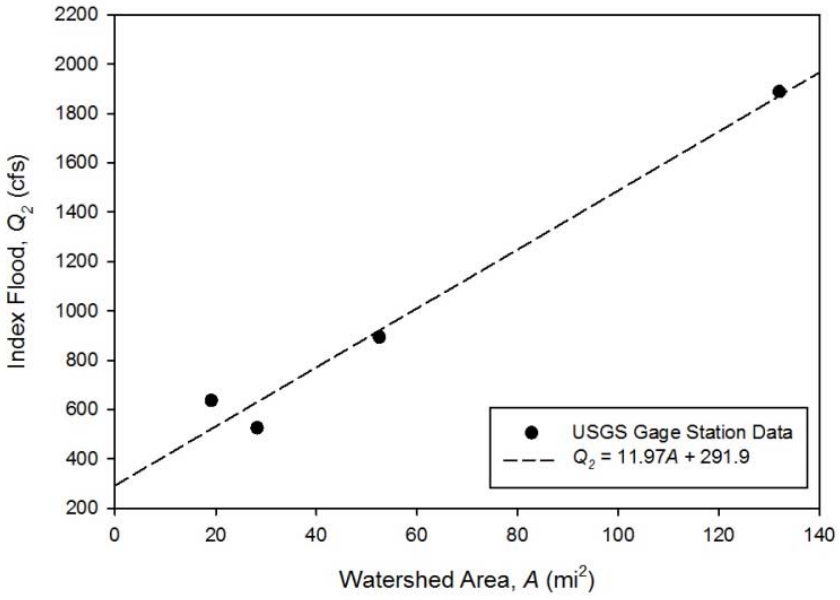

Flood Frequency Analysis: Monitoring sites watershed area and calculated 2, 5, 10, 25, 50, and 100 year return period floods.

Monitoring Site	Watershed Area (mi^2)	Q_2 (cfs)	Q_5 (cfs)	Q_{10} (cfs)	Q_{25} (cfs)	Q_{50} (cfs)	Q_{100} (cfs)
FM1	24.3	583	1485	2404	3992	5518	7360
FM2	25.0	591	1505	2436	4044	5591	7458
FM3	35.7	719	1832	2966	4924	6807	9080
FM4	36.9	733	1867	3022	5017	6935	9251
FM5	42.8	804	2047	3313	5501	7604	10144
WC1	2.0	316	806	1305	2166	2994	3994
WC2	16.3	486	1239	2006	3330	4603	6140
Not Used	23.0	567	1443	2337	3880	5363	7154
WC3	25.3	594	1514	2450	4068	5623	7501

Flood Frequency Analysis: PeakFQ Annual Exceedance Probability Plots for USGS gage station 07325800

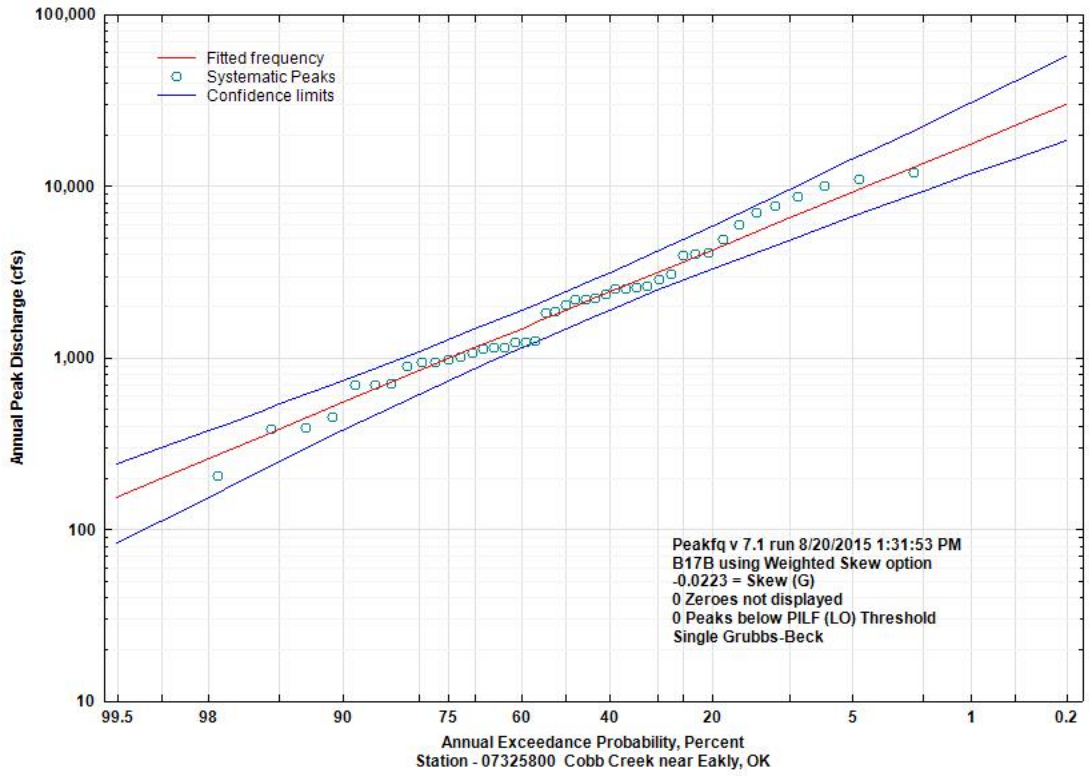

Flood Frequency Analysis: PeakFQ Annual Exceedance Probability Plots for USGS gage station 07325840

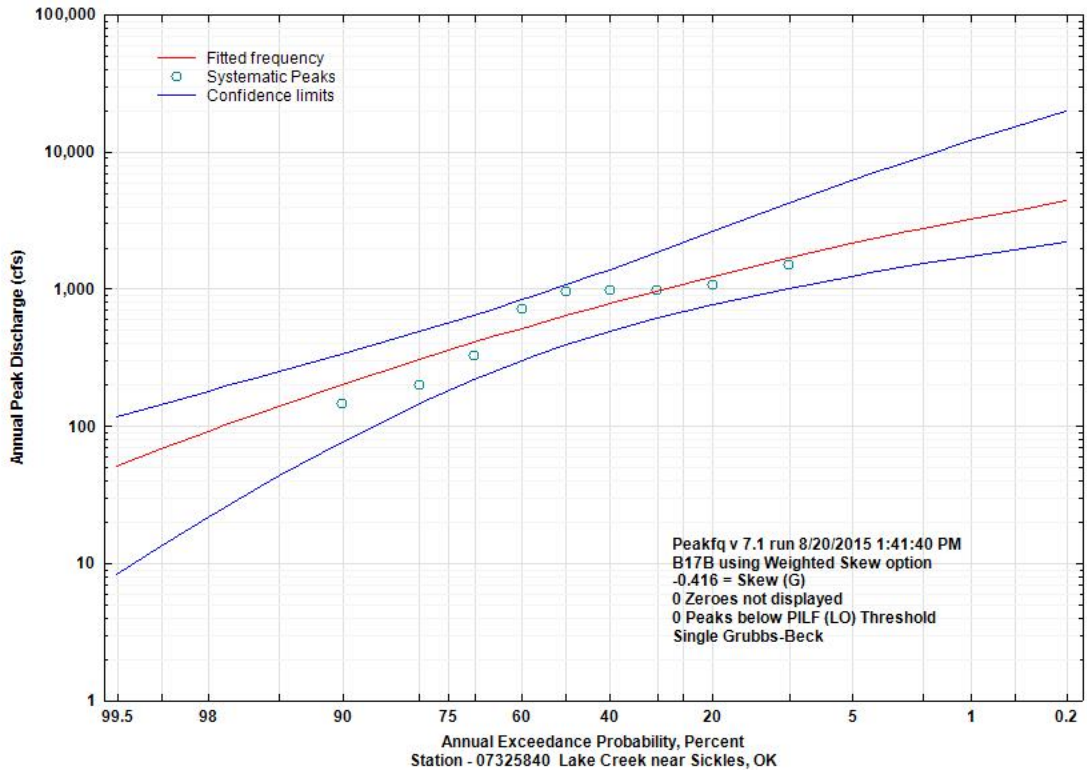

Flood Frequency Analysis: PeakFQ Annual Exceedance Probability Plots for USGS gage station 07325850

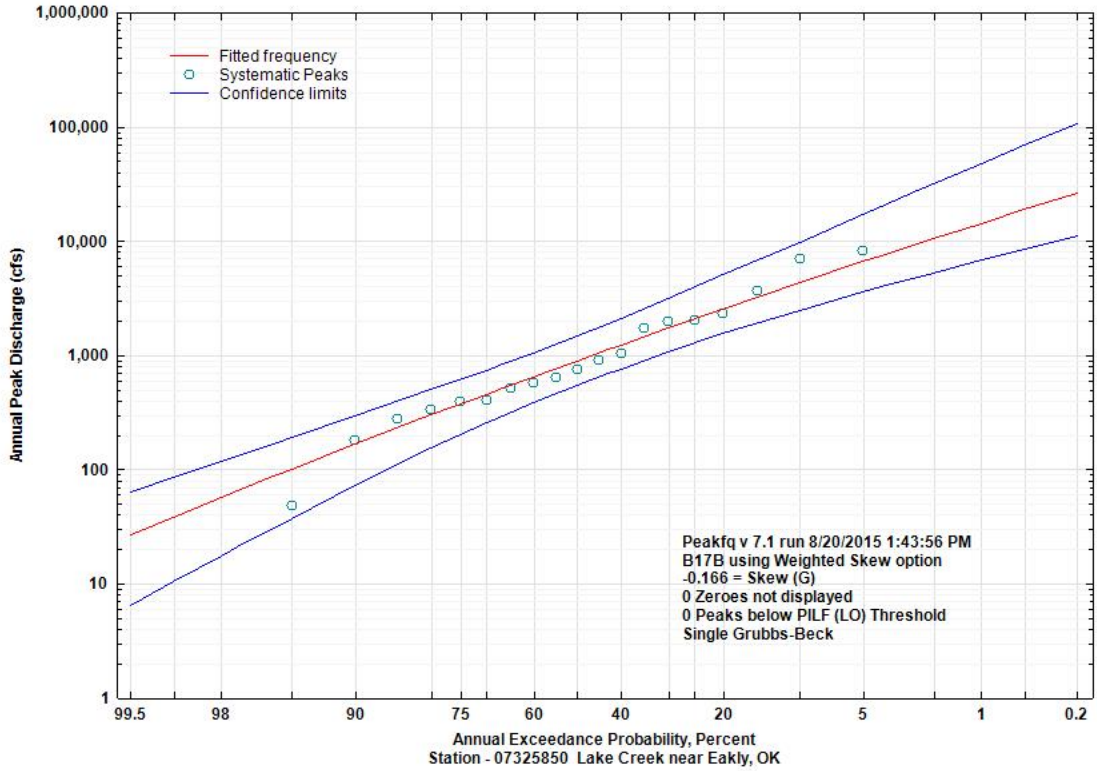

Flood Frequency Analysis: PeakFQ Annual Exceedance Probability Plots for USGS gage station 07325860

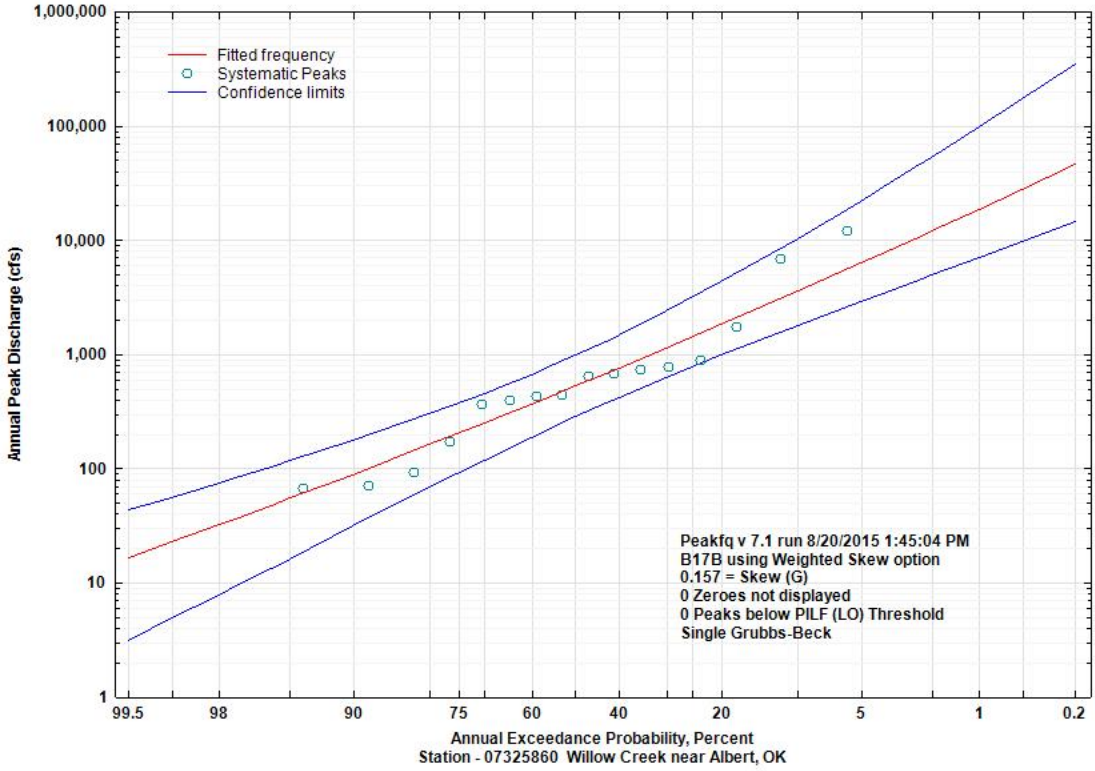

VITA

Kate Riis Klavon

Candidate for the Degree of

Master of Science

Thesis: ADVANCES IN MODELING COHESIVE SEDIMENT DETACHMENT AND A PROCESS-BASED METHOD FOR STREAM RESTORATION TO DETERMINE SEDIMENT LOADS

Major Field: Biosystems and Agricultural Engineering

Biographical:

Education:

Completed the requirements for the Master of Science in Biosystems and Agricultural Engineering at Oklahoma State University, Stillwater, Oklahoma in May, 2016.

Completed the requirements for the Bachelor of Science in Agricultural Engineering at Iowa State University, Ames, Iowa in 2014.

Experience:

Graduate Research Assistant | Stillwater, Oklahoma Aug '14-Present
Oklahoma State University: Department of Biosystems and Agricultural Engineering

Fluid Mechanics Teaching Assistant | Stillwater, Oklahoma Jan-May '15
Oklahoma State University: College of Engineering

Water Resources Intern | Ames, Iowa May '13-July '14
United States Department of Agriculture: Agricultural Research Service

Undergraduate Research Assistant | Ames, Iowa Jan '11-Aug '12
Iowa State University: Department of Agricultural and Biosystems Engineering

Professional Memberships:

American Society of Agricultural and Biological Engineers
American Society of Civil Engineers
Engineer in Training